CONVERSION OF POLYOLEFIN WASTE INTO FUELS AND OTHER VALUABLE PRODUCTS BY HYDROTHERMAL PROCESSING

by

Kai Jin

A Dissertation

Submitted to the Faculty of Purdue University

In Partial Fulfillment of the Requirements for the degree of

Doctor of Philosophy

School of Engineering Technology

West Lafayette, Indiana

May 2021

THE PURDUE UNIVERSITY GRADUATE SCHOOL
STATEMENT OF COMMITTEE APPROVAL

Dr. Gozdem Kilaz, Chair

School of Engineering Technology

Dr. Nien-Hwa Linda Wang

Davidson School of Chemical Engineering

Dr. Jason Ostanek

School of Engineering Technology

Dr. John Sheffield

School of Engineering Technology

Approved by:

Dr. Kathryne A. Newton

Dedicated to my family.

ACKNOWLEDGMENTS

I would like to first deeply thank my advisor, Dr. Gozdem Kilaz, for supporting me and guiding me in my study at Purdue. She strongly supported me so I can work on what I really enjoyed. I would like to also deeply thank my co-advisor, Dr. Nien-Hwa Linda Wang. I can never reach this stage without any part of my advisors' help. Their insights and critical thinking lighted my way. I would also like to express my thanks to Dr. Jason Ostanek and Dr. John Sheffield for serving on my committee. Furthermore, I would like to thank my group members in FLORE, Dr. Petr Vozka, Mr. Brent Modereger, Mr. Louis Edwards Caceres Martinez, and Mr. Jacob Guthrie, and my group members in Wang's Lab, Dr. Wan-Ting Grace Chen, Dr. Hoon Choi, Dr. David Harvey, Mr. Yi Ding, Mr. Clayton Gentilcore, and Mr. Che-Yu Chou. I am also grateful to my collaborator, Dr. Yang Xiao, for his help and guidance.

I would much appreciate the support from my family as always.

I am very thankful for my funding sources, the School of Engineering Technology at Purdue University, Davidson School of Chemical Engineering at Purdue University, and Trask Innovation Fund from the Purdue Research Foundation.

TABLE OF CONTENTS

LIST OF TABLES

LIST OF FIGURES

LIST OF ABBREVIATIONS

ASTM	American Society for Testing and Materials
DSC	Differential Scanning Calorimetry
EDS	Energy-Dispersive X-ray Spectroscopy
FT-IR	Fourier-Transform Infrared Spectroscopy
GC×GC-FID	Two-Dimensional Gas Chromatography with a Flame Ionization Detector
GC×GC-MS	Two-Dimensional Gas Chromatography with Mass Spectrometry
GHG	Greenhouse Gas
HTP	Hydrothermal Processing
ICP	Inductively Coupled Plasma
LP-HTP	Low-Pressure Hydrothermal Processing
MS	Mass Spectrometry
OES	Optical Emission Spectroscopy
PE	Polyethylene
PP	Polypropylene
SEM	Scanning Electron Microscope
SWL	Supercritical Water Liquefaction
TGA	Thermalgravimetric Analysis
TOF	Time of Flight

ABSTRACT

Plastic waste is accumulated in landfills and the environment at an exponentially increasing rate. Currently, about 350 million tons of plastic waste is generated annually while only 9% is recycled. Plastic waste and its degradation products, microplastics, pose a severe threat to the ecosystem and eventually human health. Polyolefin (Polyethylene (PE) and Polypropylene (PP)) waste is 63% of the total plastic waste. Converting polyolefin waste into useful products including clean gasoline, diesel, wax, and monomers, via hydrothermal processing (HTP) can help reduce the plastic waste accumulation. In this study, sorted PE waste was converted via supercritical water liquefaction (SWL) into gasoline blendstock, No.1 ultra-low-sulfur diesel, and clean waxes with high yields and high purities. Comprehensive reaction pathways for PE conversion were proposed based on detailed GC×GC analyses. Furthermore, a new low-pressure (~2 MPa) hydrothermal processing (LP-HTP) method was developed to convert mixed polyolefin waste. This new LP-HTP method can save 90% of the capital cost and energy compared to SWL. The oil products were distilled into clean gasoline and No.1 ultra-low-sulfur diesel. The reaction pathways of PE and PP were independent while the synergistic effects improved the fuel qualities. With this LP-HTP method, polyolefin waste can be converted into up to 190 million tons of fuels globally, while 92% of the energy and 71% of the GHG emissions can be saved compared to conventional methods for producing fuels. Overall, this method is robust, flexible, energy-efficient, and environmental-friendly. It has a great potential for reducing the polyolefin waste accumulation in the environment and associated risks to human health.

CHAPTER 1 INTRODUCTION

1.1 Background

1.1.1 Plastic Waste

Plastic products are becoming inseparable from people's lives. They are widely used as packing materials, construction materials, and disposable containers. Plastic products derived from petroleum are cheap, versatile, and endurable. The great demand for plastic products drives an exponential increase in plastic production and waste generation. The plastic waste generated in the last 15 years was more than that in the past 100 years before 2005 (Geyer, Jambeck, & Law, 2017a). More than 350 million tons of plastic waste was generated as of 2017 and around 8 billion tons of plastic waste has been accumulated on earth.

Currently, only 9% of plastic waste is recycled, and 12% incinerated. The rest, 79%, was landfilled or released to lands and oceans, Figure 1.1 (Geyer et al., 2017a). A floating plastic waste gyre named "Great Pacific Garbage Patch" was found in the Pacific Ocean with the same size as Texas (Lavers & Bond, 2017). If the current trend of plastic waste generation continues, there will be more than 30 billion tons of plastic waste by 2050 and more plastic waste than fish in oceans (Laville & Taylor, 2017).

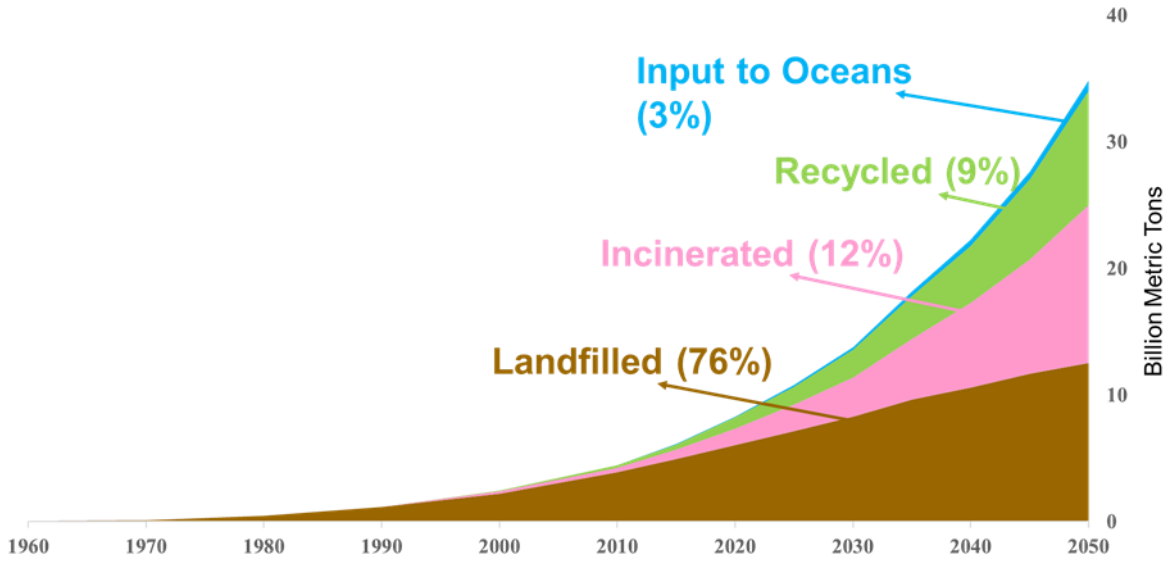

Figure 1. 1 The global plastic waste accumulation/disposal and projection

Plastics have a long degradation time in natural environments, ranging from 100 to 1,000 years (Horton, Walton, Spurgeon, Lahive, & Svendsen, 2017). The existence of plastic waste has caused multiple environmental problems. More than 267 species of animals were found dead because of entanglement and ingestion of plastic waste (Guern, 2018). Millions of birds and fish were killed by plastic debris annually (Guern, 2018). The degradation of plastic waste releases microplastics and toxic chemicals in the environment causing pollutions to lands, surface- and ground-water, and oceans (Horton et al., 2017; Smith, Love, Rochman, & Neff, 2018). Microplastics were found all over the world, in the beaches in the Pacific islands, the snow in the Alps, the Arctic ice, and Mariana Trench (Bergmann et al., 2019; Chiba et al., 2018a; "Great Pacific Garbage Patch | National Geographic Society," n.d.; Souza Machado et al., 2019). Microplastics cannot be digested and are transported along the food chain. Eventually, they will accumulate in human bodies (Cole, Lindeque, Halsband, & Galloway, 2011). Recent studies showed that microplastics can also be adsorbed via human inhalation and skins, posing risks of particle toxicity, oxidative stress, inflammation, translocation, and cancer (Prata, da Costa, Lopes, Duarte, & Rocha-Santos, 2020; Schwabl et al., 2019).

To sum, plastic waste accumulation has become a severe global problem that poses great hazards to ecosystems and human health.

1.1.2 Sherwood Plot

Landfills currently take the majority of plastic waste. However, landfilling is only accumulating the waste and other recycling methods are still needed. Furthermore, it will not be economical to re-collect plastic waste from landfills for further processing. Here, a Sherwood plot was used to predict the cost of a product with a known concentration in the feed, Figure 1.2 (Jin, Vozka, Kilaz, Chen, & Wang, 2020; Sherwood, 1959). The estimated cost for re-collecting plastic waste from landfills is \$0.5-1.0/kg and removing all current plastic waste will cost four trillion US dollars.

The plastic waste in oceans is in a worse situation. The most advanced technology to purify ocean water from plastic waste and other toxic chemicals will cost \$0.003/gallon and there are 3.5×10^{20} gallons of water in the oceans (Copeland & Tiemann, 2013; Mihelcic et al., 2017). The total cost will be about $\$10^{18}$, which is 10,000 times the global gross domestic product (GDP). Apparently, this cost is beyond the affordability of any country or organization.

In short, it will not be economical to re-collect plastic waste from landfills or oceans for further processing. Plastic waste needs to be collected and treated before it spreads into the environment.

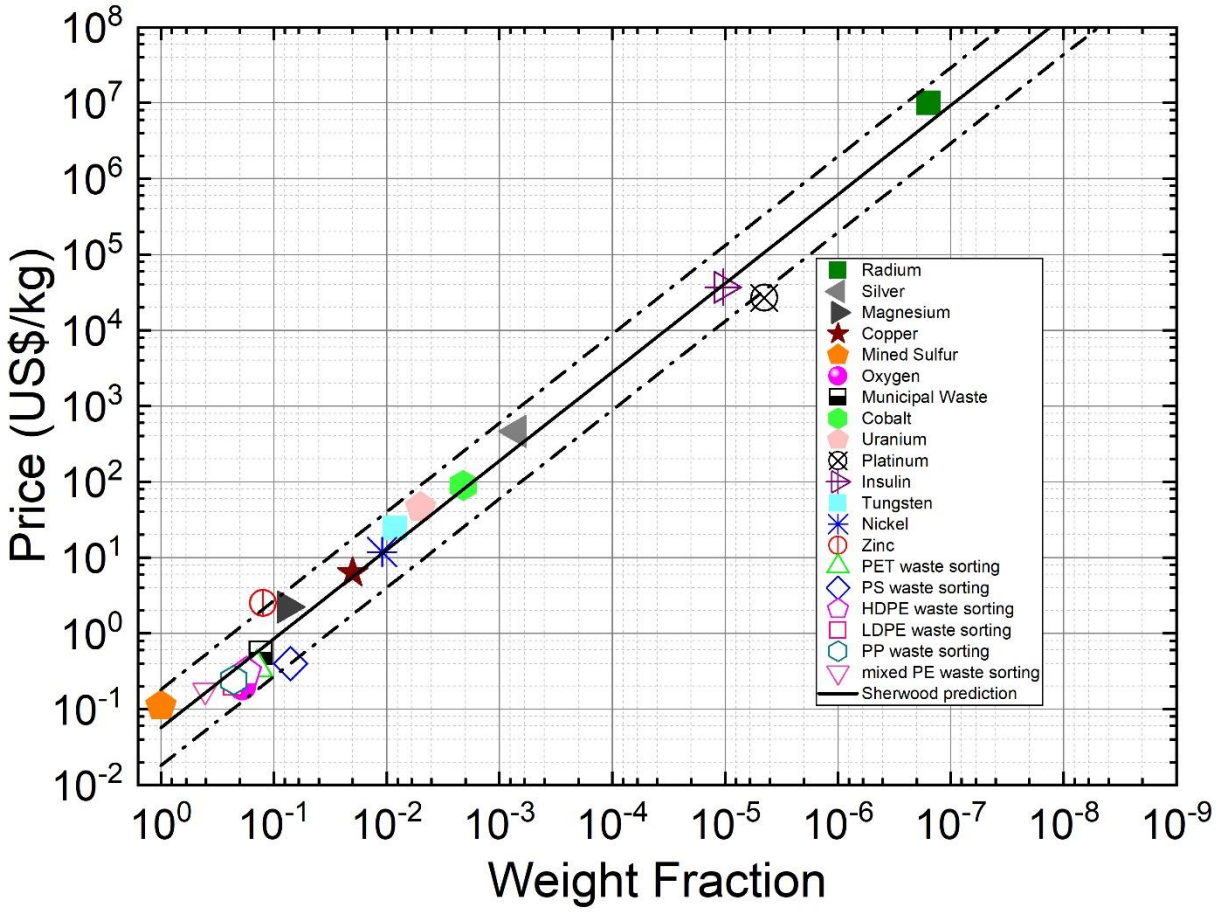

Figure 1. 2 The Sherwood plot predicting product costs/prices based on its concentration in the raw materials.

1.1.3 Current Recycling Methods

Existing methods for reducing plastic waste accumulation include incineration, mechanical recycling, pyrolysis, gasification, and biodegradation. However, these methods are not efficient to solve the plastic waste problem. Incineration recovers heat energy by the combustion of plastic waste. It has a low energy efficiency, less than 25%, and high GHG and other toxic gas emissions (Ni, Lu, Mo, & Zeng, 2016; Tyskeng & Finnveden, 2010). Therefore, “Tipping fees” are needed

from material recycling facilities to maintain the operations of incinerators. Mechanical recycling utilizes mechanical processes such as washing, melting, and re-molding to convert plastic waste into other plastic products. However, degradation occurs, and plastics cannot be mechanically recycled more than ten times (Plinke, Wenk, Wloff, Castiglione, & Palmark, 2020; Ragaert, Delva, & Van Geem, 2017). Furthermore, additives such as colorant cannot be mechanically separated and different types of plastics are immiscible. As a result, mechanical recycling can only downgrade sorted plastic waste with limited applications (Ragaert et al., 2017). Pyrolysis is a thermal degradation method converting mixed plastic waste into oils. However, oil yields and qualities are low and upgrading in refineries are required. A significant char formation up to 40% can be commonly observed, especially in fast pyrolysis (Akubo, Nahil, & Williams, 2019; Park, Jeong, & Kim, 2019). Expensive catalysts are also needed (Akubo et al., 2019). Gasification produces CO, CO_2, and H_2 by cracking plastic waste at a temperature up to 1,000 °C (Ahmed, Nipattummakul, & Gupta, 2011; Janajreh, Adeyemi, & Elagroudy, 2020; Kannan, Al Shoaibi, & Srinivasakannan, 2013). The energy consumption is high, twice as that of pyrolysis, and no embodied energy in polymers is preserved. Furthermore, gas products are more difficult to transport than oils. Researchers are also investigating biodegradation. However, it is still in a research stage.

In short, existing recycling methods have not been efficient in solving the plastic waste accumulation problem. New efficient and economical methods are needed.

1.1.4 Polyolefins

Different types of plastic have varied chemical compositions and structures. It is impractical to expect a single method can efficiently convert all types of plastic waste. For instance, Polyvinyl chloride (PVC) contains chloride and is not suitable for producing fuels.

In this study, we focused on the conversion of polyolefin waste. Polyolefins include type 2, high-density polyethylene (HDPE), type 4, low-density polyethylene (LDPE), and type 5 polypropylene (PP), Figure 1.3. Polyolefins are widely used as disposable packing materials, grocery bags, films, and containers. Polyolefin waste accounts for 63% of the total plastic waste. The amount of polyolefin waste is further increasing in the COVID period, as gowns, surgery masks, and take-out containers are all made of polyolefins. The recycling ratio of polyolefin waste is lower, 5-10%, compared to other types of plastic waste such as PET bottles. In summary,

polyolefin waste is the majority of the total plastic waste and was chosen to be studied in this research.

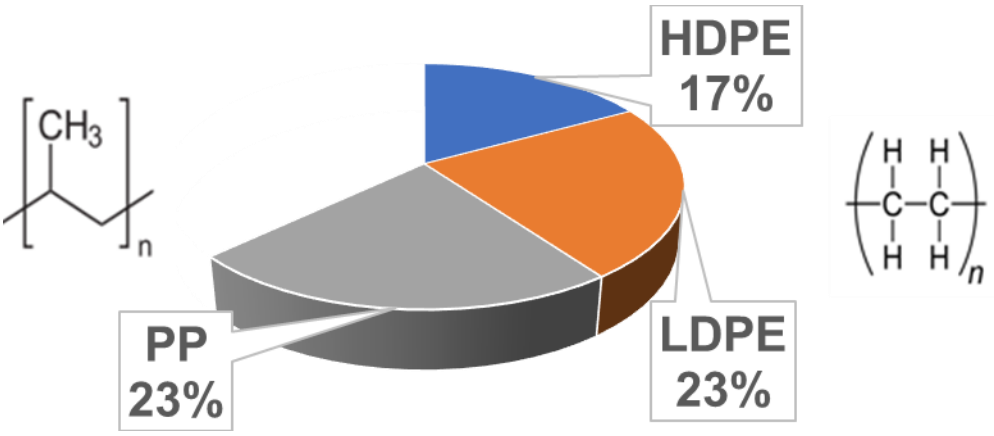

Figure 1. 3 Polyolefins and their chemical structures

1.1.5 Hydrothermal Processing

Hydrothermal processing (HTP) has the potential to efficiently convert plastic waste into useful products. HTP is a thermochemical depolymerization process that can convert organic feedstocks such as biomass or plastics into gas, oil, and solid (Brown, Duan, & Savage, 2010). An illustration of HTP is shown in Figure 1.4. The organic feed and sub-/supercritical water are loaded into an enclosed reactor. The reaction temperature is between 250-500°C and the reaction pressure between 1-30 MPa. HTP has been successfully used for converting biomass material into bio-crude oils and hydrolyzing condensation polymers such as polyethylene terephthalate (PET) and polycarbonate (PC) (Funazukuri, 2015; Pedersen et al., 2016; Savage, Gopalan, Mizan, Martino, & Brock, 1995).

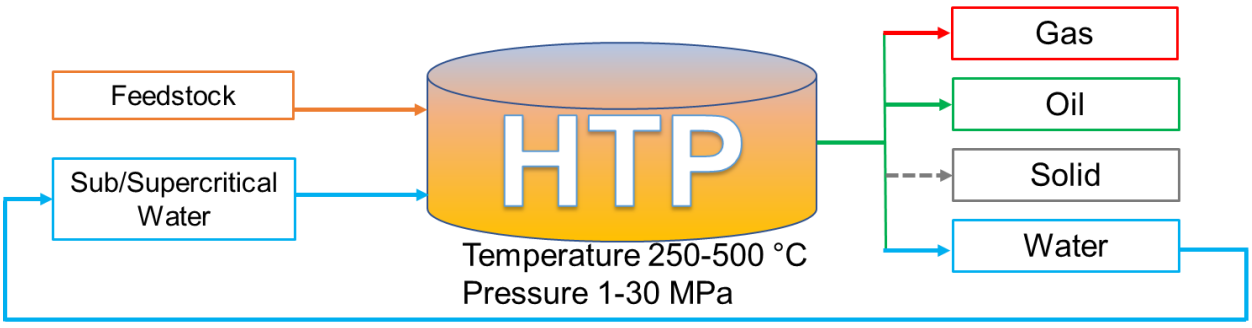

Figure 1. 4 The illustration of hydrothermal processing

Water plays a critical role in HTP. It can serve as a solvent, reactant, and catalyst. When approaching and exceeding the critical point, water's properties change significantly, Figure 1.5. The dielectric constant is a parameter indicating the polarity. At room temperature, water has a dielectric constant of 80 indicating a strong polarity. However, at a higher temperature above 200°C, the dielectric constant of water is reduced to about 5, indicating water has become a non-polar solvent which will have good solubility for dissolving polymers. With increased temperature, the ion product (K_w) of water also changes significantly, which shows different reactions based on ions and free radicals can occur in HTP. In sum, HTP is a flexible process producing varied products via different reaction pathways. One can manipulate the reaction conditions to selectively produce desired products.

Literature has reported some preliminary research of HTP on polyolefin polymers using supercritical water (Funazukuri, 2015; Moriya & Enomoto, 1999; Williams & Slaney, 2007). However, more work is needed to construct the reaction pathways, to explore the product applications, to evaluate HTP for energy efficiency, environmental impacts, and economical potentials, and to develop HTP as a technically and economically feasible method for polyolefin waste.

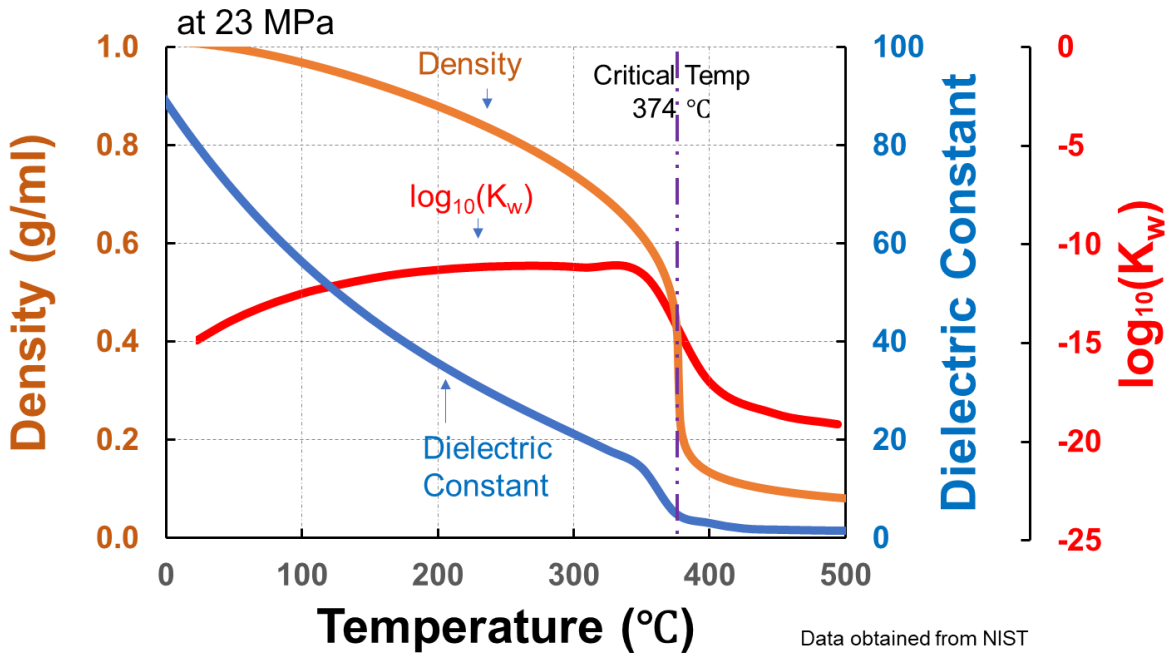

Figure 1. 5 The relation between the density, dielectric constant, and ion product of water versus temperature

1.2 The Problem

The problem addressed in this study is the lack of fundamental knowledge, engineering design, and product application verification for developing HTP as an efficient and economical solution for plastic waste.

1.3 Research Questions

The key research questions answered in this study include:

1. What are the chemical compositions of the HTP products from different types of plastic waste?
2. What are the reaction pathways for different types of plastic in HTP?
3. How will reaction temperature, time, and pressure affect the reaction pathways and product compositions?
4. What are the applications of the products derived from different types of plastic waste?
5. Are polyethylene (PE) and polypropylene (PP) waste feasible for producing clean gasoline and diesel via HTP and are there any synergistic effects on reaction mechanisms, product yields, and qualities in the co-processing?
6. How is HTP compared to other plastic recycling methods (incineration, mechanical recycling, pyrolysis, and gasification) in terms of energy efficiency, greenhouse gas (GHG) emissions, and economical feasibility?

1.4 Research Objectives

The long-term objective of this study is to develop hydrothermal processing as an efficient and economical method for plastic waste. The detailed objectives are as following:

1. Understand the conversions of PE, PP, and their mixtures with different mass ratios.
2. Construct the reaction pathways for PE, PP, and their mixtures.
3. Determine the effects of reaction conditions on the reaction pathways and product compositions.
4. Test and qualify the products as clean gasoline, diesel, and waxes.
5. Apply the optimal reaction conditions to actual plastic waste to prove the technical feasibility of HTP.

6. Evaluate HTP and compare it to other recycling methods in terms of process energy consumptions, GHG emissions, and economical potentials.

The deliverables of this study are two peer-reviewed publications (Jin, Vozka, Gentilcore, Kilaz, & Wang, 2021; Jin et al., 2020).

1.5 Significance

The development of HTP on plastic waste is with great potentials for reducing plastic waste accumulation by converting the waste into useful products. With the methods developed in this study, 220 million tons of polyolefin waste can be converted into 190 million tons of clean fuels annually, while saving 1.5 billion barrels of crude-oil-equivalent energy and reducing associated GHG emissions. A circular economy can also be achieved by producing waxes and other monomers using HTP. This study built a solid basis for HTP and sighted the technical and economic feasibility for the conversion of plastic waste into useful products via HTP.

1.6 Assumptions

The following assumptions were made during the research:

1. The oil product yields were calculated based on mass differences and verified with collected oil weight.
2. The gas product yields were calculated based on the gas pressure and gas chemical compositions using the ideal gas law.
3. The diesel fraction yields were calculated based on the chemical compositions.
4. The octane number and cetane number were predicted by the FT-IR fuel analyzer based on the FT-IR spectra.
5. The potential profits of HTP were calculated based on the average price of gasoline and diesel between 2015-2020.

1.7 Delimitations

The delimitations of this research were:

1. This study focused on the conversion for producing oils and waxes. Conversion for gases was not considered.
2. This study focused on the conversion of PE, PP, and their mixtures. Other types of plastic such as polyethylene terephthalate (PET) and polyvinyl chloride (PVC) were not considered as the feedstock.
3. For oil products, this study focused on producing clean gasoline and diesel. Other oil products such as crudes or heavy oils were not considered as the main product.
4. Biomass waste such as food residue was not considered or tested in the experiments. The effect of biomass waste in the feed was not determined.

1.8 Limitations

The limitations of this research were as following:

1. Cycloparaffins and olefins were grouped because GC×GC-FID cannot distinguish them in the chromatogram.
2. The experiments were conducted in a batch reactor. No continuous reactor was used in this study.
3. Engine tests for gasoline and diesel were not conducted because the required sample amounts were beyond the production capability of this study.

1.9 Summary

In this chapter, the background was first introduced in Section 1.1, followed by the statement of the problem and research questions in Sections 1.2 and 1.3, respectively. The research objectives were introduced in Section 1.4. The significance, assumption, delimitations, and limitations were discussed in Sections 1.5, 1.6, 1.7, and 1.8, respectively.

CHAPTER 2 REVIEW OF LITERATURE

2.1 Hydrothermal processing

HTP was first studied on the conversions of biomass materials. Water was found to process significantly different properties near and above the critical point. Many applications were then explored including biomass fuel production, waste treatment, and material synthesis (Savage, 1999; Savage et al., 1995). For example, a study was reported for converting aspen woods and glycerol at 400°C and 30 MPa. The oil product had a higher heating value (HHV) of 34 MJ/kg (Pedersen et al., 2016). Swine manure and algal biomass were also studied in HTP and the oil product was with a HHV of 28 MJ/kg (Chen et al., 2016).

HTP was further studied for the conversion of different types of plastics. Funazukuri et al. studied the hydrolysis of condensation polymers including polyethylene terephthalate (PET) and polycarbonate (PC) in HTP (Funazukuri, 2015). Valuable monomers were obtained from HTP and following purifications.

Several studies reported the use of HTP on polyolefins. A literature map was plotted accordingly, Figure 10. Watanabe et al. conducted HTP experiments for LDPE and compared the results to that of pyrolysis (Watanabe, Hirakoso, Sawamoto, Tadafumi Adschiri, & Arai, 1998). It was found that the HTP oil has a higher olefins/paraffins ratio than the one of pyrolysis. The reason was believed because of different reaction phases. Moriya et al. and Su et al. reported similar results as that of Watanabe et al. (Moriya & Enomoto, 1999; L. Su et al., 2005). Zhao et al. studied HTP at a lower reaction temperature, 250-350°C, and solid fuels were the main product while the oil yield was only 10-30% (X. Zhao, Zhan, Xie, & Gao, 2018).

One recent article reported the conversions of four types of common plastic (PE, PP, PET, and PC) into oil and solid products via HTP (Seshasayee & Savage, 2020). Two different reaction temperatures and reaction times were tested. The yields of the products were measured by weight calculation. The chemical compositions of the products were analyzed using nuclear magnetic resonance (NMR), gas chromatography-mass spectrometry (GC-MS), Fourier-transform infrared spectroscopy (FT-IR), elemental analysis, and thermogravimetric analysis (TGA). This article explored how the plastic feed type, reaction temperature, and reaction time affect the oil yields, chemical compositions, and some physical properties. In the end, the authors also commented on

the potential values of the products as monomers and crude oils (Seshasayee & Savage, 2020) However, this article did not provide new knowledge on purposing the reaction pathways nor qualifying the products for any practical use. Only rough descriptions were used for the reaction pathways. The products were believed to be monomers and crude oil but were without any qualifications being done to support the statements.

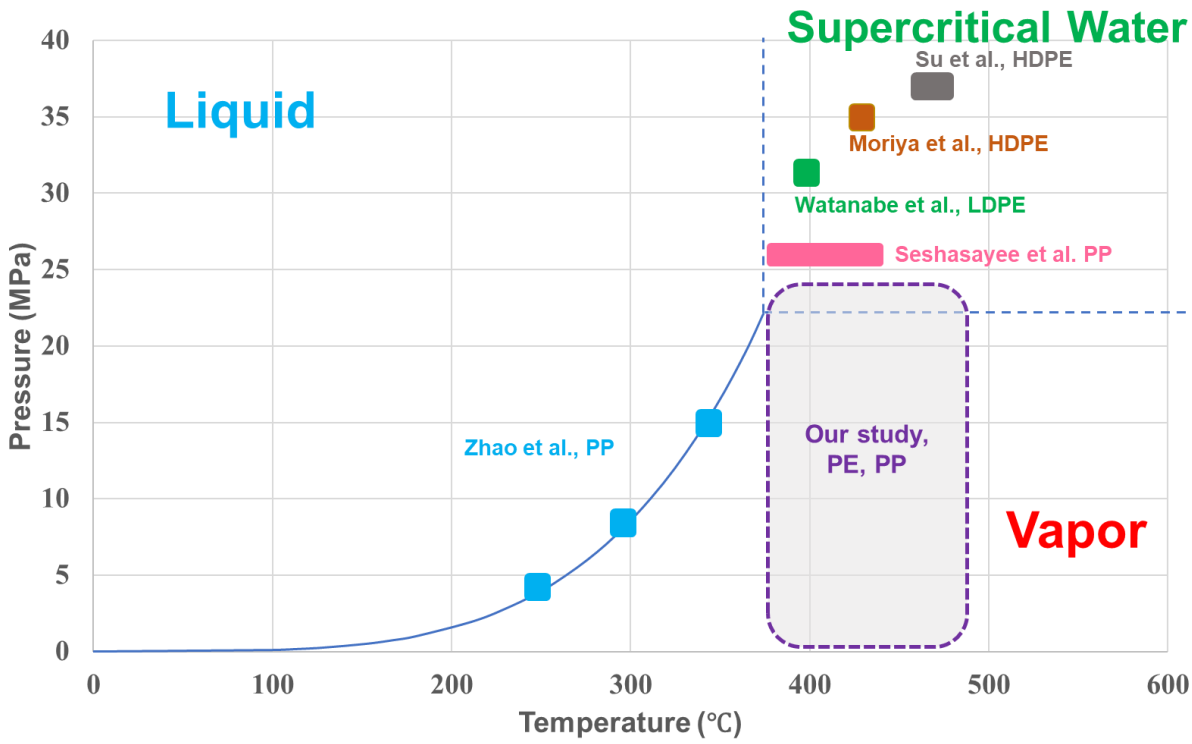

Figure 2. 1 Literature review map on HTP for plastic waste

The article by Zhao et al. studied the use of HTP for converting six types of plastics, including PC, high impact polystyrene (HIPS), acrylonitrile butadiene styrene (ABS), PP, and polyamide 6 (PA6) (X. Zhao et al., 2018). Oils and solid residues were observed after reactions. The oils were analyzed for chemical compositions using gas chromatography-mass spectrometry (GC-MS). Bisphenol A was found in the PC oils while alkane-aromatics were the major compounds in the HIPS and ABS oils. PP-oil was rich in alkanes and caprolactam was found in PA6 oils. The solid residues were analyzed using thermogravimetric analysis (TGA) and differential scanning calorimeter (DSC). Based on the TGA and DSC results, the authors concluded the solids to be potential solid fuels. The authors also commented that hydrothermal

methods can be a novel waste-to-energy technique. One limitation of this article is that the authors did not investigate the intrinsic reactions and no new reaction mechanism was proposed.

Though many studies reported the use of HTP to convert polyolefin waste, no comprehensive reaction pathways have been proposed. The products were also not tested as commercial fuels or waxes. There are still knowledge gaps before HTP can become a practical solution for the polyolefin waste accumulation problem.

Furthermore, current studies on HTP focused on using subcritical- or supercritical water, and no study was found using steam for the conversion of polyolefin waste. Steam near or above critical point possesses similar properties as supercritical water such as the dielectric constant. Therefore, it has the potential to reduce the process capital cost and energy demand as the use of steam requires a lower pressure.

2.2 Co-processing of PE and PP Waste

Currently, most of the plastic waste was collected in mixtures. A further separation into sorted plastic waste will add up to the total processing cost. It is also possible for different types of plastics to interact during the co-processing to improve product yields and qualities. Therefore, co-processing of different plastic waste becomes an attractive research field.

Mixed polyolefins have been studied as the feedstock in pyrolysis. A recent study reported the conversion of mixed PE and PP waste into fuels via catalytic pyrolysis (Kassargy, Awad, Burnens, Kahine, & Tazerout, 2018). The reaction temperature was 500°C and zeolite catalyst was used at a 1:10 mass ratio for the catalyst to plastic feedstock. An oil yield between 75-80% was achieved and three fractions were obtained, including a gasoline fraction, a diesel fraction, and an intermediate oil fraction. Only one mixing ratio (50%:50% for PE:PP) was reported for fuel properties, and the gasoline fraction was not qualified as the octane number was lower than required. The researchers concluded that no interaction between PE and PP was found. The limitation of this study was that only a single mixing ratio was tested, and the flexibility of co-processing was not explored.

A recent study reported the co-processing of LLDPE and PP in SWL (P. Zhao et al., 2021). Different mixing ratios of LLDPE and PP between 1:3 and 3:1 were tested at 400 °C and 1 hr. The researchers compared the experimental results with mathematic calculation and concluded the existence of synergistic effects. They also found that the oil was shifting to the light end when

more PP was in the feedstock. However, only one reaction temperature and reaction time were tested in this study and it is unclear whether the synergistic effects will vary with different reaction conditions. Furthermore, the oil fractions were not tested for any applications.

No study was reported on the co-processing of mixed polyolefins in HTP using steam. Our study was the first one reporting the synergistic effects of PE and PP in LP-HTP.

2.3 Fuel property requirements

For oils to be qualified as commercial gasoline and diesel, a set of properties is required. The requirements for commercial gasoline and diesel are shown in Table 2.1 and 2.2, respectively.

Octane number is a key parameter in evaluating gasoline quality. It measures the resistance of the fuel against compression in gasoline engines. Anti-knocking index (AKI), the averaged octane number of two types of test engines, is required to be 87 or higher. Gasoline with a too low AKI will result in engine knocking and associated damages to engine gears.

Kinematic viscosity is also vital for fuels. A too high viscosity will result in an insufficient blending of fuels and air and will cause partial combustion with less power generated. Fuel density also needs to be in a reasonable range, as suggested by ASTM D4052.

T_{10}, T_{50}, T_{90}, $T_{final,}$ and distillation residue are obtained from distillation separations. They provide information on the boiling point distributions. Based on these values, the drivability index (DI), an important measure of the gasoline performance in different conditions, can be calculated.

Reid vapor pressure is a measure of the volatility of gasoline. A high Reid vapor pressure indicates high levels of vaporization, which will help car-starting in cold seasons. However, it will result in vapor-lock in hot seasons. Therefore, an appropriate range of Reid vapor pressure is needed according to ASTM D5191.

Lead and sulfur in traditional petroleum-derived gasoline produce toxins and pollution gases such as SO_2. A concentration limit is requested by ASTM D4814.

The presence of aromatics in gasoline can help improve the octane number but will also likely increase the amount of multi-ring aromatics in the exhaust gas. Benzene, as commonly seen in aromatic mixtures, is toxic. Therefore, the concentrations of aromatics and benzene are required to be below a specific value.

Similar to the octane number for gasoline, diesel has an important parameter, cetane number, for indicating the combustion rate and the compression needed for ignition. A cetane number between 40 and 60 is required for diesel fuels.

Flashpoint is a measure of the temperature at which diesel can be ignited. It is a key property for fuel storage safety. ASTM requires the flashpoint to be at least 38 °C for No.1 diesel.

Water and sediment are impurities in fuels. They can cause incomplete combustion and engine plugging. ASTM requires the water and sediment content to be no more than 0.05%.

In sum, several property measurements are needed to qualify oil products as commercial gasoline and diesel, and the measurements were considered in this study.

Table 2. 1 Gasoline properties, ASTM requirements and measurements

Gasoline properties	ASTM requirements and measurements
Anti-knocking index (AKI)	D4814
Kinematic Viscosity (mm2/s)	D7042
Density (g/cm3)	D4052
T_{10}, T_{50}, T_{90}, and T_{final} (°C)	D86
Distillation residue (wt.%)	D86
Drivability index (DI(°C))	D4814
Reid vapor pressure (psi)	D5191
Lead (ppm)	D4814
Sulfur (ppm)	D4814
Benzene (wt.%)	N/A
Aromatics (wt.%)	D4814
Hydrogen content (wt.%)	N/A
Gross calorific value (MJ/kg)	N/A

Table 2. 2 Diesel properties, ASTM requirements and measurements

Diesel properties	ASTM requirements and measurements
Cetane number	D975
Flash point (°C)	D56
Kinematic viscosity (mm2/s)	D7042
Cloud point (°C)	N/A
T_{90} (°C)	D86
Sulfur (ppm)	D975
Water and sediments (ppm)	D6304
Aromatics (wt%)	D975
Hydrogen content (wt%)	N/A
Gross heating value (MJ/kg)	N/A

2.4 Summary

In this chapter, the use of HTP for converting plastic waste was introduced in Section 2.1, followed by the co-processing of plastic waste in Section 2.2. The review on fuel property requirements were summarized in Section 2.3.

CHAPTER 3 METHODOLOGY

3.1 Materials

3.1.1 Plastic feedstock

Standard polyolefin polymers and actual waste were used as feedstock in this study. Standard PE ($\overline{Mw}$ = 180,000 g/mol) and PP ($\overline{Mw}$ = 250,000 g/mol) pellets were purchased from Sigma Aldrich (St. Louis, MO). EREMA pellets (EREMA North America, Ipswich, MA), made from post-consumer PE grocery bags, were used as PE actual waste in tests. Similarly, Berry shredded flakes (Berry Global, Evansville, IN), made from post-industry PP containers and lids, were used as PP actual waste. The pictures of the plastic feedstock are shown in Figure 3.1.

Figure 3. 1 Standard PP polymer pellets, standard PE polymer pellets, pelletized PE waste, and shredded PP waste (from left to right)

3.1.2 Other materials

The water used in experiments was obtained from a Milli-Q water purification system and was degassed for 30 mins before use.

Commercial gasoline and diesel were tested for fuel property comparisons. The commercial gasoline and diesel samples were obtained from local gas stations (West Lafayette, IN) including BP, ExxonMobil, Family Express, GoLo, Marathon, Meijer, Shell, and Speedway.

A commercial paraffin wax was purchased from VWR (Radnor, PA) and used as reference material.

The *n*-Eicosane and *n*-Tetracontane which were used as references in GC×GC-MS, were purchased from Sigma Aldrich (St. Louis, MO).

The activated carbon used for wax purification was CAL 12X40 with a mean particle diameter of 1.0 ± 0.1 mm, and was purchased from Calgon Carbon Corporation (Pittsburgh, PA).

3.2 Instrumentation

3.2.1 Reaction

The experiments were conducted using a 500ml batch high-temperature high-pressure reactor, Parr Type 4570 (Parr Instrument Company, Moline, IL), Figure 3.2. This reactor system was composed of a 500ml reactor cylinder (2.5” ID and 6.6” inside depth) and a reactor head, a magnetic drive (0-600 RPM), a pressure gauge (0-34.5 MPa), a safety rupture disc, a gas inlet, an outlet valve, a liquid sampling valve, cooling coils, and a thermowell with a Type J thermocouple. The cylinder, head, and internal parts were made of Alloy C276 and the valves and external fittings were made of stainless steel. An electric heater assembly (110V) is used for heating.

Figure 3. 2 Parr type 4570 high-temperature high-pressure batch reactor (www.parrinst.com)

3.2.2 Separation

The glassware used for filtrations and liquid-liquid separations were purchased from Fisher Scientific (Hampton, NH).

Oil products were separated into different fractions by distillation. The distillation apparatus was assembled according to ASTM D86 method. An illustration is shown as Figure 3.3.

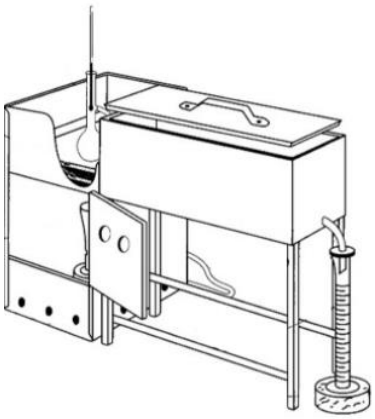

Figure 3. 3 Distillation apparatus (https://engineering.purdue.edu/FLORE)

3.2.3 Chemical composition analysis of gas products

The chemical compositions of the gas products were obtained via gas chromatography with a flame ionization detector (GC-FID). The details are shown in Table 3.1.

Table 3. 1 Parameters for GC-FID analysis of gas products

Parameter	Description
Column	J&W GS-CarbonPLOT GC Column, 30 m, 0.32 mm, 3.00 μm, 7 inch cage (FID: Front Detector, 20 Hz Data Rate, 0.01 min Minimum Peak Width)
Gas Flow Rates	2.5 mL/min He (12.03 psi, 40 cm/s avg. velocity), 45.0 mL/min H_2, 400 mL/min Air
Oven Temperature	Hold at 50 °C for 1 min, ramp from 50 °C to 350 °C at rate of 10 °C/min, hold at 350 °C for 5 min
Temperatures	Inlet: 275 °C; Detector: 275 °C
Pressure & Split Ratio	Inlet: constant pressure of 12.0 psi, 107 mL/min total flow (Split Ratio of 19.2, Split Flow of 99.2 mL/min)
Sample Injections (Manual Injection)	C_1-C_6 Paraffins (1000 molar ppm each, in He): 1 mL C_2-C_6 Olefins (100 molar ppm each, in He): 2 mL Gas samples: 1 mL

3.2.4 Chemical composition analysis of oil products

The chemical compositions of the oil products were obtained by comprehensive two-dimensional gas chromatography with a flame ionization detector (GC×GC-FID) using a gas chromatograph Agilent 7890B system (Agilent, Santa Clara, CA) with a 30 m mid-polar primary column DB-17ms (Agilent, Santa Clara, CA) and 0.8 m nonpolar secondary column DB-1ms (Agilent, Santa Clara, CA) (Petr Vozka & Kilaz, 2019a). The details are shown in Table 3.2.

Table 3. 2 Chromatographic conditions for GC×GC-FID

Parameter	Description
Analytical column	Primary: DB-17ms Agilent (30 m × 0.25 mm × 0.25 μm) Secondary: DB-1ms Agilent (0.8 m × 0.25 mm × 0.25 μm)
Carrier gas	UHP helium, 1.5 mL/min
Oven temperature	Isothermal 40 °C for 0.2 min, followed by a linear gradient of 3 °C/min to a temperature 260 °C being held isothermally for 20 min
Modulation period	2.5 s with 0.42 s hot pulse time
Offsets	Secondary oven: 50 °C Modulator: 15 °C
Temperatures	Inlet: 280 °C FID: 300 °C

3.2.5 Wax yield and chemical composition analysis

The thermogravimetric analysis (TGA) of wax products was conducted using a TGA Q50 analyzer manufactured by TA Instrument (Columbus, OH).

The chemical compositions of the wax products were obtained via comprehensive two-dimensional gas chromatography with a mass spectrometry detector (GC×GC-MS). The details are shown in Table 3.3.

Table 3. 3 Chromatographic conditions for GC×GC-TOF/MS

Parameter	Description
Analytical column	Primary: ZB-35HT Phonomenex (60 m × 0.25 mm × 0.25 μm) Secondary: ZB-1HT Phenomenex (1.9 m × 0.25 mm × 0.25 μm)
Carrier gas	UHP helium, 1.25 mL/min
Oven temperature	Isothermal 40 °C for 0.2 min, followed by a linear gradient of 3 °C/min to a temperature 300 °C being held isothermally for 20 min
Modulation period	3.0 s with 0.50 s hot pulse time
Offsets	Secondary oven: 10 °C Modulator: 70 °C
Temperatures	Inlet: 280 °C Transfer line: 300 °C

The purity of the wax products was analyzed by using Fourier-Transform Infrared Spectroscopy (FT-IR). A Thermo-Nicolet Nexus 470 FT-IR with an ultra-high performance, versatile Attenuated Total Reflectance (ATR) sampling accessory was used in this study. The resolution for this FT-IR instrument was 4 cm^{-1} and the spectral range was 800-4500 cm^{-1}. Hardware configuration and data collection were achieved by using OMNIC software (version 8.3).

3.2.6 Chemical composition analysis of solids

The chemical compositions of the solid products were analyzed using Energy Dispersive X-Ray Spectroscopy (EDS) with a JCM-6000PLUS instrument manufactured by JEOL (Tokyo, Japan).

3.2.7 Fuel property measurement

For the fuel property measurements, ASTM standard equipment was utilized. The density and kinematic viscosity were measured using a SVM 3001 Stabinger viscometer following ASTM D4052 and D7042, respectively. The flashpoint was measured via a Tag 4 flash point tester following ASTM D56. The cloud point was measured via a manual cloud point apparatus (Koehler Instrument Co., New York, NY) following ASTM D2500. The heating value was measured using a 6200 Isoperibol calorimeter (Parr Instrument Company, Moline, IL) following ASTM D4809. The octane number and cetane number were obtained by testing samples with an Eraspec FT-IR fuel analyzer. The Reid vapor pressure was obtained by testing samples using an Eraspec vapor pressure tester following ASTM D5191. The lead and sulfur content were obtained via inductively coupled plasma-optical emission spectrometry (ICP-OES) using a Perkin-Elmer Optima 8300 instrument. The hydrogen content, benzene content, and aromaticity were calculated based on the chemical compositions obtained from the GC×GC-FID chromatograms.

3.3 Methods

3.3.1 Reaction

For each reaction experiment, the plastic feed and DI water were first weighted, then mixed, and loaded into the reactor. In each test, 40 g of plastic feed was used. Different amount of water was added to reach the target pressure, 70 g of water for SWL at 23 MPa, and 0-17 g for LP-HTP at 0.25-10.25 MPa.

The reactor was sealed subsequently and purged with nitrogen three times to remove any residue air. A nitrogen gas blanket was added at 0.62 MPa to build an inert atmosphere. The heating was turned on and it took 1 hr to reach the target temperature, 425-450°C. The reaction time started once the target temperature was reached. After reactions, the reactor was cooled with forced air convection and it took 1 hr to cool down to room temperature. The gas pressures before and after reaction were measured at room temperature to calculate the gas yields. Stirring at 300 RPM was used through the whole process including heating, reaction, and cooling.

3.3.2 Product separation

After the reactor was cooled to room temperature, the gas pressure was first recorded and then the reactor was dissembled. The gas product was sampled for GC-FID analysis, using a Tedlar bag and the rest gas product was released in a fume hood.

The solids were separated from the water-oil-solid mixture via filtration, then washed three times using acetone, dried in a furnace overnight, and weighed. For tests using actual polyolefin waste, the solid consisted of char and inorganic additives. The solid was heat-treated in furnace at 500 °C for 1 hr to burn off char, and the residue, which was the inorganic additives, was weighted again.

The oil and water were separated by using a separation funnel and weighted separately.

The wax products obtained from PE waste were purified before analysis. The crude wax product was first sampled about 5 g, and then mixed with 50 ml toluene in a 100 ml flask. The flask was heated at 50 °C for 1 hr with a stir bar in it. Filtration was then conducted to separate the insoluble materials. The solution was collected, mixed with about 2.5 g of activated carbon, stirred for 2 hr at 50 °C. Centrifugation was conducted to separate out the activated carbon. The solution

was placed in a refrigerator at -18 °C to precipitate the wax products. At the end, the wax was collected via centrifugation at -18 °C.

3.3.3 Yield calculation

Gas product yields were calculated using the ideal gas law, based on gas pressure and gas chemical compositions. Solid yields were calculated based on dry mass. Oil product yields were calculated by subtracting the gas and solid yields from 100 wt.% and were confirmed by comparing them to the collected oil masses.

3.3.4 Oil distillation

Oil distillations in this study were conducted using an in-house one-stage batch distillation unit following ASTM D86 method. Oils were separated into three fractions, including gasoline fraction, diesel fraction, and heavy oil fraction. Oils from multiple runs at the same condition were combined and distilled. The gasoline fraction was collected at the boiling point range of 20-170 °C. The diesel fraction was collected at the range of 170-300 °C. The remainder was collected as the heavy oil fraction. All fractions were weighted at room temperature. The diesel yield based on distillation was lower than that based on chemical compositions because of the limited separation efficiency of the one-stage batch distillation unit. The efficiency will be optimized in the future. From distillation experiments, the values for T_{10}, T_{50}, T_{90}, T_{final}, and distillation residue were obtained as well, where T_x refers to the temperature at which x vol% of the sample evaporated.

3.3.5 Chemical composition analysis of gas products

The chemical compositions of gas products were obtained using GC-FID. Details were shown in Table 3.1.

3.3.6 Chemical composition analysis of oil products

The chemical compositions of oil products were obtained from GC×GC-FID analyses. Two different gas chromatography columns (DB-17 as the primary column and DB-1 as the secondary column) were used in tandem in the GC×GC system, Figure 3.3. A modulator was used to connect the two columns. Because the two columns have varied stationary phases, the separation

mechanisms were different, which enhanced the separation efficiency of complex hydrocarbon mixtures such as gasoline and diesel.

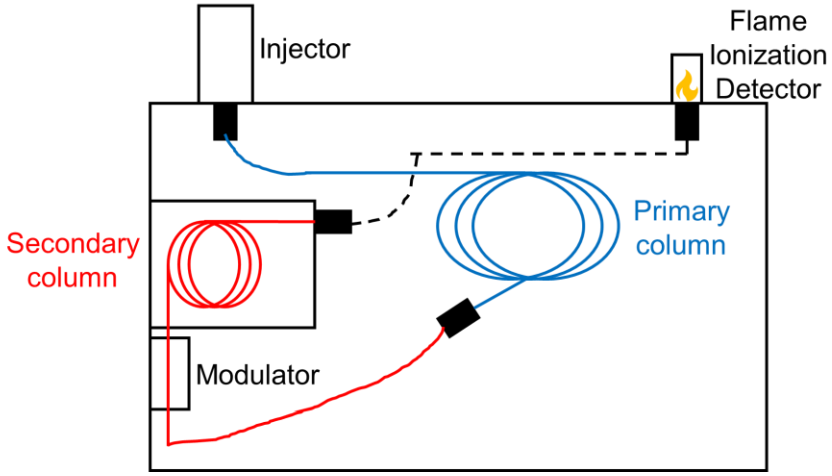

Figure 3. 4 The illustration of GC×GC-FID

FID was used to detect the organic chemicals in the oil samples. FID can provide quantitative information on the detected peaks in the chromatogram, Figure 3.4. Unlike a mass spectrometry detector, FID itself cannot identify the chemical structure information of a peak. Therefore, classifications were developed for the identification of chromatograms. In this study, a mixture of 24 standard compounds were first injected and tested in GC×GC-FID to develop the classification. After that, the chromatogram was divided into fractions based on carbon number from C_5 to C_{31}, and chemical category, including *n*-paraffins, isoparaffins, olefins, monocycloparaffins, dicycloparaffins, tricycloparaffins, alkylbenzenes, cycloaromatics, naphthalenes, biphenyls, anthracenes and phenanthrenes, and pyrenes. Furthermore, the olefins monocycloparaffins, dicycloparaffins and tricycloparaffins were grouped to reduce the analysis difficulty. In a similar way, alkylbenzenes, cycloaromatics, naphthalenes, biphenyls, anthracenes and phenanthrenes, and pyrenes were grouped as aromatics. An example of the chromatogram with classification is shown in Figure 3.5. The development of the classification can also be found in a previous study (Petr Vozka & Kilaz, 2019a).

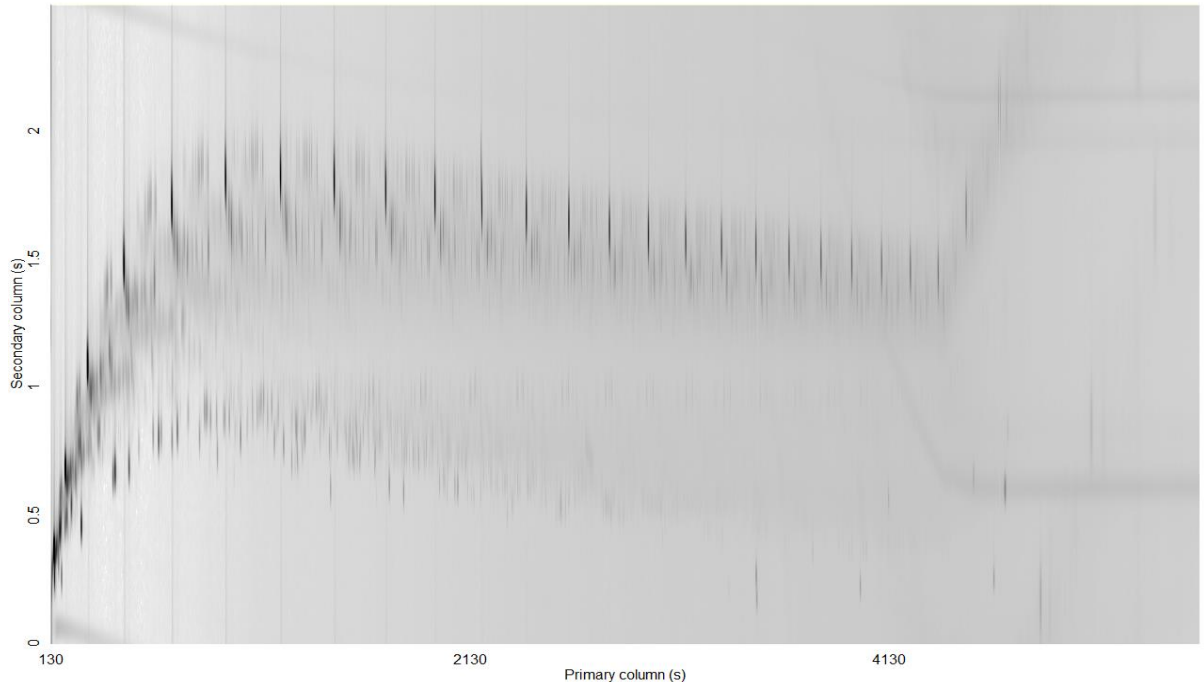

Figure 3. 5 GC×GC-FID chromatogram projection

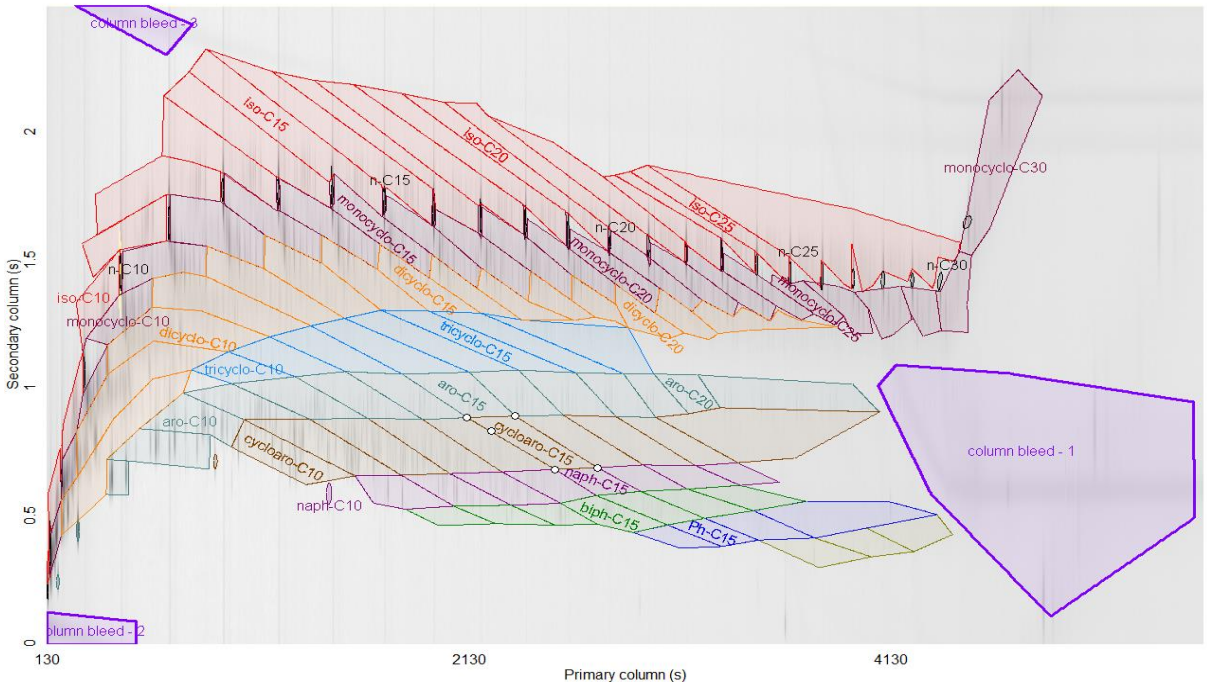

Figure 3. 6 GC×GC-FID chromatogram projection with classification

3.3.7 Chemical composition analysis of wax products

The wax yield was calculated based on the wax weight obtained from TGA. Each time around 50 mg of the wax sample was heated from 20 °C to 550 °C at 10 °C/min under nitrogen. The change of weight was recorded by the TGA analyzer and compared to those of standard chemicals, *n*-icosane (*n*-C_{20}) and *n*-tetracontane (*n*-C_{40}).

The wax products were analyzed using FT-IR for chemical structure information. The details were mentioned in Section 3.2.5.

For GC×GC-MS analysis, the hydrocarbon classification was achieved by testing three *n*-paraffin standard chemicals (*n*-C22, *n*-C25, and *n*-C28). Dilution in toluene was conducted for each sample. The injection split ratio was set as 20:1. A 70 eV EI was used for ionization. The acquisition rate of mass spectra was 200 Hz, and the detector gain is 1,750 V. Data collection, processing, and analysis were conducted using the ChromaTOF software (Version 1.90.60.0.43266).

3.3.8 Chemical compositions analysis of solid residues

The solid residue was analyzed using SEM-EDS as introduced in Section 3.2.3. Each time around 2 g of sample was tested.

3.3.9 Fuel property measurement of gasoline and diesel products

For fuel property measurements, ASTM standard procedures were followed. The details are shown in Table 3.4.

Table 3. 4 The fuel properties and the ASTM standard methods

Properties	Product categories	ASTM methods
Density	Gasoline & Diesel	D4052
Kinematic viscosity	Gasoline & Diesel	D7042
Flash point	Diesel	D56
Cloud point	Diesel	D2500
Heating value	Gasoline & Diesel	D4809
Water content	Diesel	D6304
Reid vapor pressure	Gasoline	D5191
T_{10}, T_{50}, and T_{90}	Gasoline & Diesel	D86
Drivability index	Gasoline	D4814

3.4 Summary

In this chapter, the materials used in this study was introduced in Section 3.1, followed by instrumentation in Section 3.2, and methods in Section 3.3.

CHAPTER 4 CONVERSION OF POLYETHYLENE WASTE INTO CLEAN FUELS AND WAXES VIA HYDROTHERMAL PROCESSING (HTP)

4.1 Introduction

Over the past few decades, people have developed a dependency on single-use plastic products in their daily lives. The amount of plastic waste generated over the past 15 years exceeded the total amount of plastic waste generated over the past 100 years before 2005 (Geyer, Jambeck, & Law, 2017b). Globally, less than 14% of the plastic waste is collected, and less than 9% is recycled and reused (*MacArthur, E., Beyond plastic waste. In American Association for the Advancement of Science: 2017.*, n.d.), resulting in a rapid accumulation of the plastics in the environment, where they degrade slowly into microplastics and release toxic chemicals into the groundwater, rivers, and oceans (Geyer et al., 2017b; Rochman et al., 2013). Microplastics were found everywhere, in the beaches in the Pacific islands, the snow in the Alps, the Arctic ice, and the Mariana Trench (Bergmann et al., 2019; Chiba et al., 2018b; "Great Pacific Garbage Patch | National Geographic Society," n.d.). Moreover, recent studies reported finding microplastics in human stool, indicating the presence and potential accumulation of microplastics in the human digestive systems (Schwabl et al., 2019). Biologists have begun studying the impact of microplastics on animal health (Cole et al., 2011). It may take decades for scientists to fully understand the impact of plastic pollution on ecosystems and human health (Wright & Kelly, 2017).

By 2050, the planet will have 30 billion tons of plastics waste, mostly in landfills (MacArthur, 2017). According to the Sherwood analysis, Figure A.1, it may take about $0.8 to retrieve 1 kg of plastic waste from landfills (Sherwood, 1959). Processing the plastic waste into useful products will incur additional costs. Virgin plastics can also be produced from crude oil at a lower cost. Thus, it would not be economical to retrieve plastic waste from landfills for further processing.

Existing methods for reducing plastic waste accumulation have been ineffective. Incineration is an option for reducing the accumulation of complex plastic waste, which is usually mixed with trash or other contaminants. However, it requires control of the generated toxic gases, such as dioxins and polybrominated diphenyl ethers (Ni et al., 2016). The energy recovery is also

low (Eriksson & Finnveden, 2017). For these reasons, tipping fees are needed to offset the processing costs (Eco.cycle, 2011). Mechanical recycling works well for sorted, relatively clean plastic waste, such as clear PET waste (Type 1) (Garcia & Robertson, 2017), which can be mechanically recycled up to 10 times. However, since the polymers degrade during the repeated cycles, the final waste has to be landfilled or incinerated. This method does not work well for mixed plastic waste because of the immiscibility of the various polymers. Moreover, colored plastic waste can only be converted into dark-colored products, which have limited uses (Hopewell, Dvorak, & Kosior, 2009). Pyrolysis can convert mixed plastic waste into crude oil but has relatively low yields without the use of catalysts, and the oil needs to be upgraded and refined for use as fuels (Baytekin, Baytekin, & Grzybowski, 2013; Wang & Zhang, 2012). The potential profits of pyrolysis are uncertain, because of high processing costs and fluctuations in crude oil prices.

Hydrothermal Processing (HTP) is a thermal-chemical depolymerization method in which subcritical or supercritical water is used in an enclosed reactor. Water serves as a solvent, and possibly as a catalyst or a reactant (Peterson et al., 2008). HTP can be used for converting plastic waste into various products, including solid fuels, liquid fuels, specialty chemicals, solvents, or monomers (Funazukuri, 2015; Moriya & Enomoto, 1999; X. Su, Zhao, Zhang, & Bi, 2004; Watanabe et al., 1998; Williams & Slaney, 2007; X. Zhao et al., 2018). HTP requires lower temperatures (280-450 °C) and higher pressures (7-30 MPa) than pyrolysis. When liquid water is heated at a high pressure to form supercritical water, there is no phase change from the liquid to steam, resulting in a low energy requirement for this process. As the reaction conditions approach the critical point, the water properties such as density, dielectric constant, ionic strength, viscosity, and heat/mass transport coefficients change rapidly (Peterson et al., 2008). Water is transformed from a polar, highly H-bonded solvent to a non-polar solvent, which has similar solvent properties as an organic solvent like hexane at room temperature. These significant changes enable the sub- or supercritical water to allow the dissolution of non-polar solutes and a wide range of fast, selective, and efficient reactions. HTP can be used to convert sorted polypropylene (PP, Type 5) waste into clean gasoline-like fuels (Chen, Jin, & Linda Wang, 2019). High oil yields, up to 91 wt. %, were reported at 425 °C, 2-4 h or 450 °C, 0.5-1 h. The oils had a similar boiling point range as gasoline and a high heating value (48−49 MJ/kg). The pathways for converting PP via HTP were also reported (Chen et al., 2019).

Most plastic waste (40%) is polyethylene (PE), either high-density (HDPE) or low-density (LDPE). Previous HTP studies of model PE conversion showed that PE was cracked into short hydrocarbons, mainly paraffins and olefins at 400-550 °C (Moriya & Enomoto, 1999; X. Su et al., 2004; Watanabe et al., 1998). The effects of the reaction temperature, reaction time, and polymer feed-to-water ratio on oil yields and oil compositions were reported, but no comprehensive reaction pathways for PE conversion were proposed. Furthermore, the oils were not evaluated for specific fuel applications.

The objectives of this study are to (1) understand the reaction pathways of a model PE in HTP; (2) find the optimal conditions for converting sorted HDPE (Type 2) and LDPE (Type 4) waste or a mixture of the two into valuable products; and (3) test the product qualities for fuels or wax applications. Comprehensive reaction pathways were inferred from two-dimensional gas chromatography (GC×GC) data of the intermediate reaction products. The pathways helped identify reaction conditions for improving the yields and properties of the desired products. The chemical compositions of the oil and wax products were obtained via GC×GC. The wax products were also analyzed using Fourier-transform infrared spectroscopy (FTIR) and thermogravimetric analysis (TGA). The properties of the oil products, density, viscosity, flash point, cloud point, water and sediment content, sulfur content, cetane number (CN), octane number (ON), and the net heat of combustion were evaluated for potential uses as liquid transportation fuels. The results showed that PE waste can be converted into clean waxes or high cetane number ultra-low sulfur diesel. Preliminary analyses indicated that the HTP method is more energy-efficient than incineration and pyrolysis and may have lower greenhouse gas (GHG) emissions.

4.2 Experimental

4.2.1 Feedstocks

Four feedstocks were tested: (1) model HDPE polymer pellets with a weight-average molecular weight of 180,000 g/mol (Sigma Aldrich, St. Louis, MO), (2) EREMA pellets, made from supermarket customer drop-off shopping bags containing both LDPE and HDPE (EREMA North America, Ipswich, MA), (3) HDPE milk jugs, and (4) HDPE grocery bags. The milk jugs and grocery bags were obtained from local grocery stores (West Lafayette, IN). Deionized (DI)

water was obtained from a Milli-Q water purification system and was degassed for 30 min before use.

4.2.2 Commercial samples

Gasoline and diesel samples were obtained from local gas stations and were tested for comparison purposes (West Lafayette, IN). Three gasoline samples were obtained from ExxonMobil, Shell, and GoLo, respectively. Five diesel samples were obtained from Family Express (two different gas stations), Speedway, Meijer, and Marathon. The commercial paraffin wax used as reference material was purchased from VWR (Radnor, PA). *n*-Icosane and *n*-Tetracontane standards were obtained from Sigma Aldrich (St. Louis, MO). Activated carbon CAL 12X40 with a mean particle diameter of 1.0 ± 0.1 mm used for wax purification was purchased from Calgon Carbon Corporation (Pittsburgh, PA).

4.2.3 HTP reactor

A 500 mL high-pressure high-temperature reactor was used, with 63.5 mm ID and 167.64 mm inside depth (Type 4570). It was purchased from Parr Instrument Company (Moline, IL). It was equipped with a magnetic drive (0-600 RPM), a pressure gauge, a safety rupture disc, gas inlet, and outlet valves, a liquid sampling valve, a cooling coil, and a thermowell with a Type J thermocouple. The reactor can operate at pressures up to 34.5 MPa and temperatures up to 500 °C.

4.2.4 HTP experiments and product separation

HTP experiments were conducted at 400-450 °C for 0.5-4 h. In each test, 40 g polymer was used and 70 ml of DI water was added to ensure that the water reached a supercritical state. After loading the feed, the reactor was assembled and purged twice with nitrogen to remove any residual air. Nitrogen gas was then added to increase the gauge pressure to 0.62 MPa. It took about 60 minutes to reach 425 °C or 65 minutes to reach 450 °C. The reaction time reported did not include the heating time. The initial and final gas pressures in the reactor were recorded. The stirring rate was 300 RPM throughout the heating, reaction, and cooling stages. Once the reaction was completed, the reactor was air-cooled. It took 10 min for the temperature to decrease from 425 to 300 °C, and additional 60 min to cool down to room temperature. No conversion of PE to wax

or oil was observed at temperatures below 300 °C. After the reactor was cooled to room temperature, the gas pressure was measured, and the gas (referred to as the "HTP gas") was sampled.

The mixture of the produced oil, water, and solids (if any) was transferred into a glass flask and weighed. The solids (referred to as the "HTP solid") were removed from the liquid phases using filtration, dried, and weighed. Water was separated from the oil (referred to as the "HTP oil") with a separatory funnel, and both were then weighed. Because some of the HTP oil (up to 3 g) could remain on the reactor inner surface, 20 ml of toluene was used to dissolve the oil and the amount was estimated from the weight increase.

The HTP solid yield (wt. %) was calculated from the dry mass of the solid and the initial polymer mass. The HTP gas yield was calculated from the gas pressure after the reaction via the ideal gas law as reported in a previous study (Chen et al., 2019). The HTP oil yield was calculated with two methods: (1) from the total mass of the collected HTP oil and the mass of the feedstock, and (2) by subtracting the HTP solid yield and the HTP gas yield from 100 wt. %. The oil yields obtained from the two methods were the same within experimental error, Figure A.2.

At short reaction times, 30 and 40 min, most of the HTP oil was embedded in the HTP solid and thus could not be separated by filtration. For this reason, the yields of the HTP oil and the HTP solid were calculated from TGA data.

4.2.5 Analyses of HTP gas

Analyses of the gas products were done with an HP 6890 gas chromatograph equipped with a flame ionization detector (FID) for C_1–C_6 hydrocarbons, Table A.1.

4.2.6 Analyses of HTP oil

4.2.6.1 Chemical composition analysis

The HTP oil was analyzed using a comprehensive two-dimensional gas chromatography system with a flame ionization detector (GC×GC-FID). An Agilent chromatograph 7890B GC system with a non-moving quad-jet dual stage thermal modulator and liquid nitrogen cooling was used. The samples were injected with no dilution. The injection split ratio was 300:1. The relative amounts of the following hydrocarbons for carbon numbers between C_6 and C_{31} were determined

as reported previously (Petr Vozka & Kilaz, 2019b): *n*-paraffins, isoparaffins, monocycloparaffins, dicycloparaffins, tricycloparaffins, alkylbenzenes, cycloaromatics (indans, tetralins, etc.), naphthalenes, biphenyls, anthracenes and phenanthrenes, and pyrenes. Since olefins co-eluted with cycloparaffins with the same carbon number, they were lumped together in the weight percent results. More chromatography details can be found in Table A.2. ChromaTOF software (version 4.71 optimized for GC×GC-FID) was used to collect and process the data, with a collection rate of 200 MHz and a signal-to-noise ratio of 50.

4.2.6.2 Other properties

The sulfur content of the HTP products was measured with a TS-100 Trace Sulfur Analyzer (Mitsubishi Chemical Corporation). Each sample was combusted in an argon atmosphere under controlled oxygen content in a pyrolysis furnace at 800-1000 °C. The flue gases were then analyzed with a sulfur detector (chemiluminescence detection) following ASTM D1552. The water content in oils was measured with a K20 Karl Fischer coulometric titrator (Mettler Toledo) via ASTM D6304. An SVM 3001 Stabinger viscometer (Anton Paar) was used to measure density and viscosity at 40 °C via ASTM D4052 and ASTM D7042, respectively. The flash point was measured using a Tag 4 flash point tester (Anton Paar) via ASTM D56. The cloud point was measured with a manual cloud point apparatus (Koehler) via ASTM D2500. The gross heat of combustion was measured with 6200 Isoperibol calorimeter (Parr Instrument Company) via ASTM D4809. The net heat of combustion was calculated from the gross heat of combustion and the hydrogen content, which was calculated from GC×GC-FID results as done previously (P. Vozka, Mo, Šimáček, & Kilaz, 2018). Standard octane number (ON) and cetane number (CN) tests require samples over one liter, which were not available. Instead, the ON for the gasoline fractions and the CN for the diesel fractions were estimated from the FTIR spectra with an Eraspec (Eralytics) fuel analyzer (Eralytics, n.d.). The fractions were obtained using batch distillation following the ASTM standard D86.

4.2.7 Analyses of HTP solids

4.2.7.1 HTP wax analysis

In order to measure the yield of HTP oil in HTP solid, TGA was done using a TGA Q50 manufactured by TA Instrument (Columbus, OH). Approximately 50 mg of the sample was heated in a nitrogen environment from 20 °C to 550 °C at 10 °C/min. The mass changes with increasing temperature were compared to those observed with two standards, *n*-icosane (*n*-C_{20}) and *n*-tetracontane (*n*-C_{40}).

The wax products from PE waste were purified as follows. Crude HTP wax, ca. 5 g, was weighed in a 100 ml flask. Then, 50 ml toluene was added to the flask, with a stirring bar placed inside. The flask was then sealed and placed for 1 h in a water bath at 50 °C with stirring. The dispersion was filtered to separate the insoluble materials. About 2.5 g of activated carbon was then added into the solution, and the mixture was stirred for 2 h at 50 °C, to remove colored impurities from the samples. The activated carbon was then separated from the solution after centrifugation at 50 °C. The solution was cooled to -18 °C for the wax to precipitate. Finally, the dispersion was centrifuged to collect the wax particles at -18 °C.

Chemical structure information of the HTP wax was obtained from FTIR spectroscopy and GC×GC with a time-of-flight mass spectrometry (TOF/MS). A Thermo-Nicolet Nexus 470 FTIR with an ultra-high performance, versatile Attenuated Total Reflectance sampling accessory was used. The resolution was 4 cm^{-1}, and the spectral range was 800-4500 cm^{-1}. OMNIC software (version 8.3) was used for hardware configuration and data collection. GC×GC-TOF/MS results were obtained using LECO's Pegasus GC-HRT^{+} 4D high resolution TOFMS composed of an Agilent 7890B GC system with a non-moving quad-jet dual stage thermal modulator and liquid nitrogen cooling. Instead of using the NIST database, the hydrocarbon classification was based on three *n*-paraffin standards (*n*-C_{22}, *n*-C_{25}, and *n*-C_{28}). Each wax sample was diluted in toluene (99.9% pure; Sigma-Aldrich). The injection split ratio was 20:1. Ionization was achieved using 70 eV EI. The acquisition rate of the mass spectra was 200 Hz with a detector gain voltage of 1750 V. ChromaTOF software (Version 1.90.60.0.43266) was used for data collection (with an m/z of 45–550), processing, and analysis, Table A.3.

4.2.7.2 Inorganic residue analysis

Inorganic residues were found after the HTP of post-consumer PE wastes. The inorganic residues (ca. 2 g) were prepared by heating the HTP solid in the muffle furnace at 550 °C for 1 h or longer to ensure complete removal of the organic residues. The elements in the inorganic residue were identified by Scanning Electron Microscopy – Energy Dispersive X-ray Spectroscopy (SEM-EDS) analysis, by using a JCM-6000PLUS instrument manufactured by JEOL (Tokyo, Japan).

4.3 Results and discussion

The product yields and the chemical compositions of the HTP products from model PE as a function of time are discussed in Section 4.3.1. From these results, the potential HTP reaction pathways of PE were derived in Section 4.3.2. To test the feasibility of HTP conversion, post-consumer plastic wastes (EREMA pellets, chopped HDPE milk jugs, and chopped HDPE grocery bags) were tested in Section 4.3.3. The HTP oils produced from the EREMA pellets were evaluated as potential liquid transportation fuels in Section 4.3.4. The HTP solids from the EREMA pellets were evaluated as potential wax products in Section 4.3.5. The net energy ratio, GHG emissions, and potential profits of HTP were compared with those of other recycling methods in Section 4.3.6. The PE and PP conversions via HTP were compared in Section 4.3.7.

4.3.1 Yields and compositions of HTP products from model PE

For 400 °C, no oil was produced from model PE for reaction times up to 3 h. The yields of the solid, oil, and gas products at 425 °C for a reaction time from 1 to 4 h are shown in Figure 4.1. For reaction times less than 40 min, only solid products were obtained, and no gas was generated. The solid consisted mostly of waxes and a small amount of oil that was embedded in the solid. The solid at reaction times of 30 and 40 min consisted mostly of *n*-paraffins and olefins, Figure A.3. The solid product yield decreased, and the oil product yield increased with increasing reaction times up to 2.5 h. Further increases in reaction time resulted in higher gas yields and slightly lower oil yields, Figure. 4.1. At all tested conditions, no char was found.

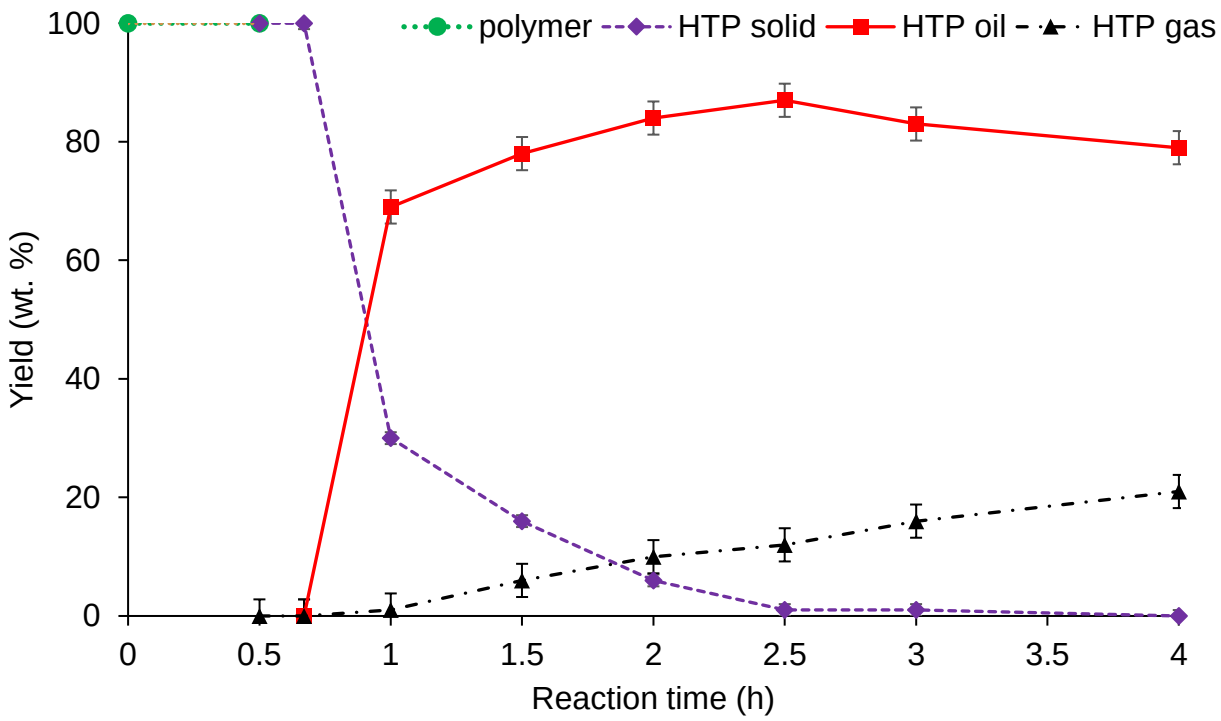

Figure 4. 1 Yields of solid, oil, and gas products at different reaction times at 425 °C.

Products from model HDPE at 425 °C, 1-4 h are divided into five groups, Figure 4.2. The solid and heavy hydrocarbon yields decreased with time, as expected from continuous cracking of the solids and the heavy hydrocarbons (C_{21+}) into shorter hydrocarbons and gas. The diesel-like fraction (C_{10}-C_{20}) increased with time from 32 wt.% at 1 h to 45 wt.% at 2.5 h. The gasoline-like fraction (C_6-C_9) increased from 12 wt.% at 1 h to 30 wt.% at 4 h. Similar trends have been reported elsewhere (Moriya & Enomoto, 1999). The maximum yield of the diesel-like fraction was observed at 2.5 h.

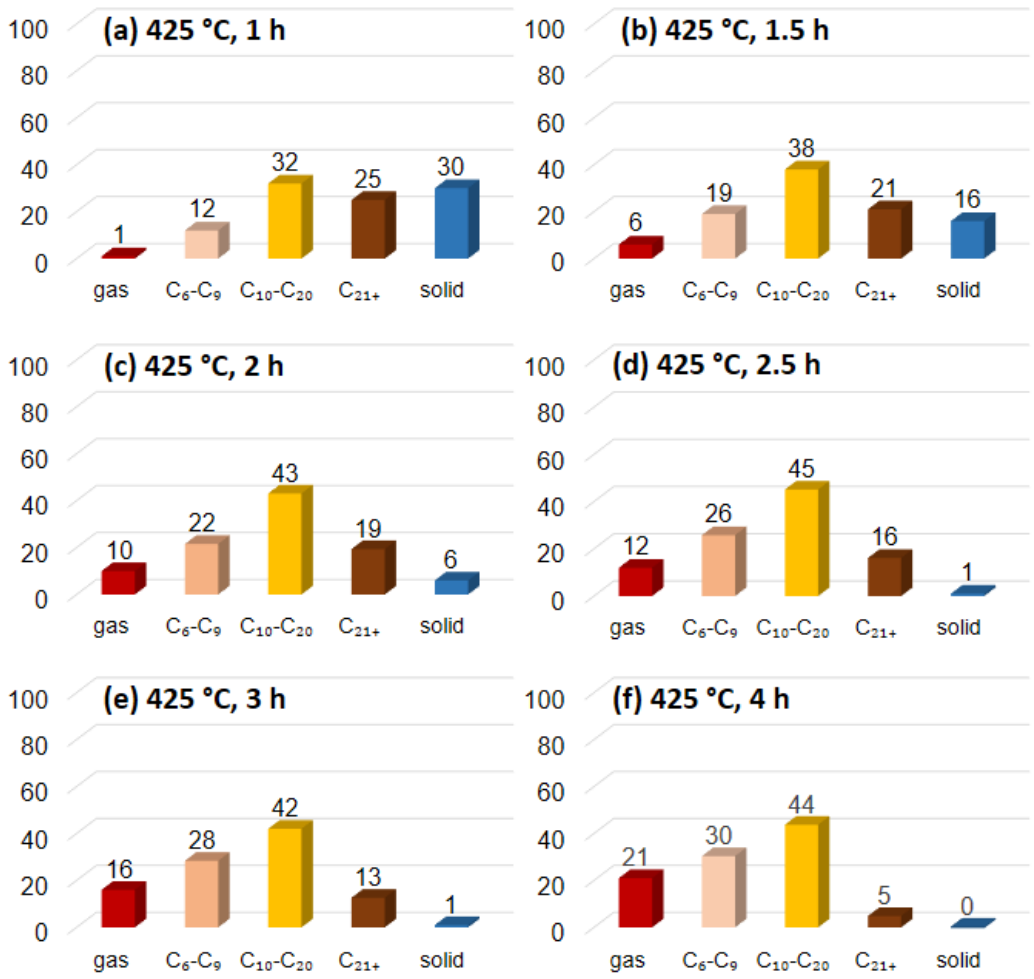

Figure 4. 2 HTP yields (wt. %) of products obtained from model HDPE at 425 °C and from 1 to 4 h. The oil is listed as three fractions, C_6-C_9 ("gasoline"), C_{10}-C_{20} ("diesel"), and C_{21+} ("heavy hydrocarbons"). The yields of the oil fractions were calculated from GC×GC-FID data.

Detailed composition data for four hydrocarbon classes and various carbon numbers at 425 °C and 0.5-4 h were determined with GC×GC-FID, Figure 4.3(a). The yields of *n*-paraffins and cycloparaffins first increased with time from 40 min to 1 h and then peaked at ca. 1.5-2 h. The results indicated a significant conversion of the longer hydrocarbons to shorter *n*-paraffins, cycloparaffins, and olefins. When the reaction time was increased from 2 to 4 h, the *n*-paraffins yield did not change significantly. The cycloparaffins and olefins yields decreased, and the aromatics yields increased, indicating the conversion of cycloparaffins and olefins to aromatics. The yields of aromatics and isoparaffins were quite low and increased slightly with time.

A solid product of long-chain *n*-paraffins and olefins were present from 1 to 3 h, Figure 4.2. It was converted to HTP oil over longer times, 1-4 h. The HTP oils were analyzed with GC×GC-FID to determine the carbon number distribution for each hydrocarbon class as a function of time, Figure 4.3(b). With increasing reaction times, the carbon number distribution curves shifted from heavier to lighter hydrocarbons, indicating that longer hydrocarbons broke down to shorter hydrocarbons. For each carbon number group, the percentage of aromatics and isoparaffins increased with increasing reaction time, indicating that some of cycloparaffins and olefins were converted to aromatics, and some of the *n*-paraffins were converted to isoparaffins, Figure 3(b). No significant amounts of oxygenated compounds were found in either the solid or the oil products under all conditions tested. No water was lost during the HTP experiments.

Similar trends in the yields of solid, oil, and gas and similar variations in hydrocarbon class distributions were found at 450 °C, Figures A.4 and A.5, indicating that at higher temperatures, the reactions followed the same reaction pathways but were faster. The results at 450 °C were followed only up to 1 h because then the pressure reached the reactor pressure limit. Again, no char was found.

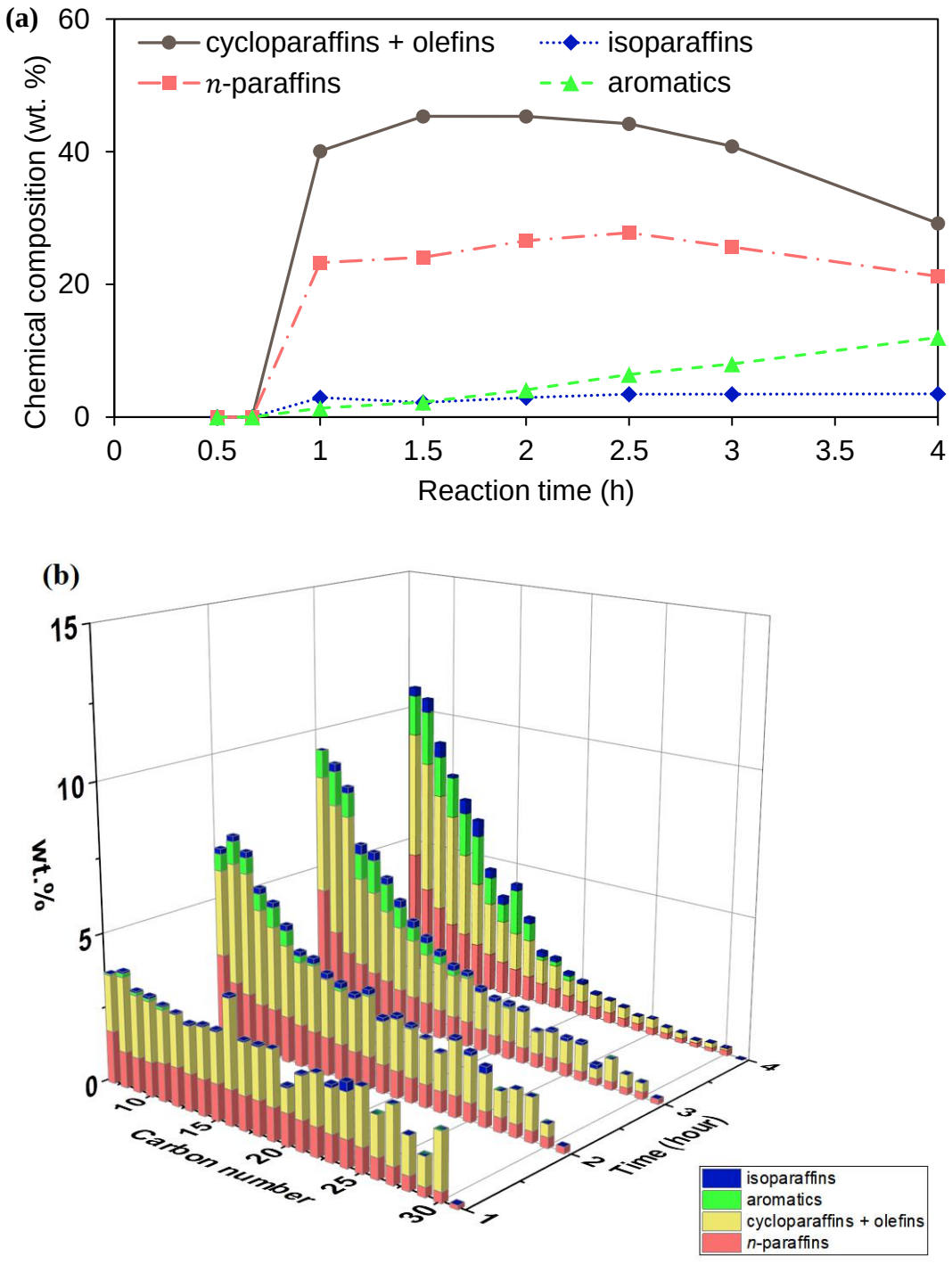

Figure 4. 3 Chemical compositions of the oils produced at 425 °C from 1 to 4 hr. (a) wt. % of four hydrocarbon classes; and (b) wt. % of the hydrocarbons of a given carbon number in each class.

4.3.2 Reaction pathways for HTP of PE

Based on the product yields and the chemical compositions of the products as a function of time, Figures 4.1-4.3, some possible reaction pathways of PE were postulated, Figure 4.4. At 425 °C or higher and a pressure of 23 MPa, the conversion begins with depolymerization of PE, which is initiated by free radical dissociation. Since the C-C bond energy (348 kJ/mol) is lower than the C-H bond energy (413 kJ/mol), the dissociation results in the breaking of C-C bonds and in generating long-chain hydrocarbons. At times from 0 to 1 h, long-chain *n*-paraffins are converted into α-olefins and shorter-chain *n*-paraffins via β-scission and hydrogen abstraction, respectively. The α-olefins generate additional free radicals by different dissociation reactions and are converted into cycloparaffins via cyclization. From 1 to 4 h, the cycloparaffins are dehydrogenated first to alkylbenzenes and then to multi-ring aromatics. A small fraction of isoparaffins is produced from *n*-paraffin radicals via isomerization. Gases are formed from olefins, *n*-paraffins, and isoparaffins by further thermal cracking or by recombination of short-chain free radicals. More details and reaction equations are shown in Figure A.6. At higher temperatures (450 °C), the reaction pathways are evidently the same, but the reactions are faster. LDPE, which has the same chemical structure ($-CH_2-CH_2-$) as HDPE, is expected to follow the same reaction pathways.

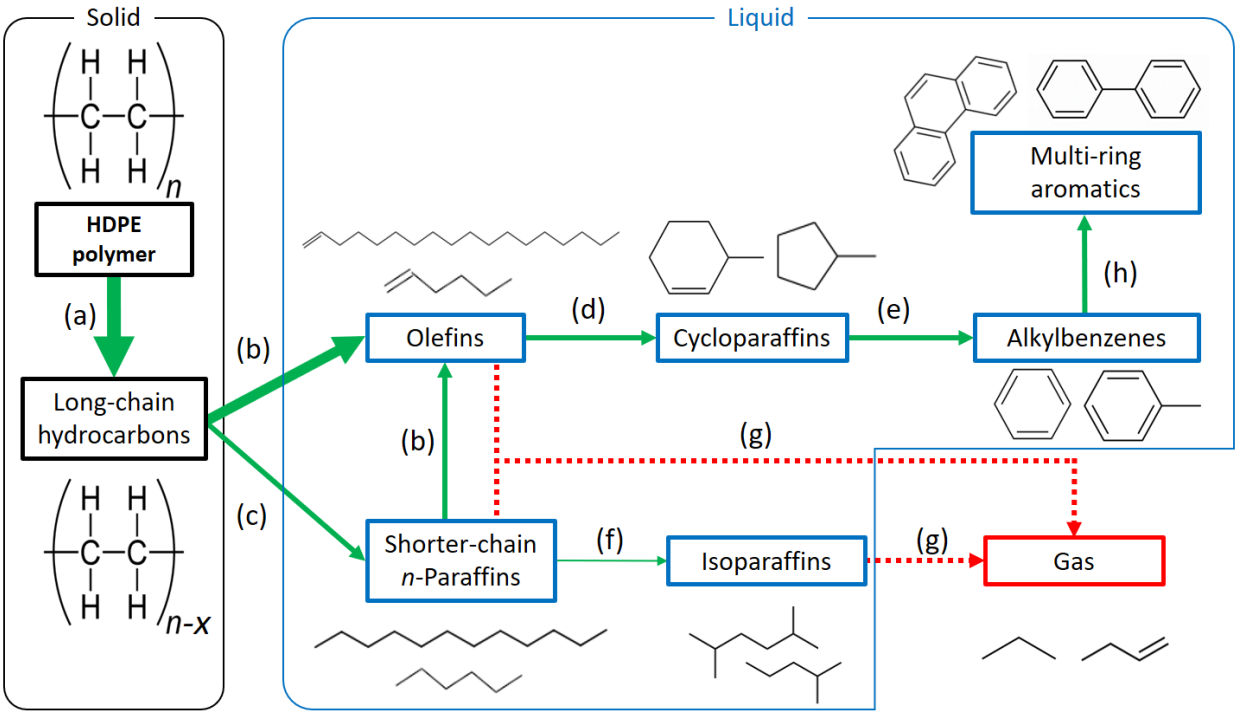

Figure 4. 4 Potential reaction pathways for PE under HTP. (a) depolymerization, (b) β-scission, (c) hydrogen abstraction, (d) cyclization, (e) dehydrogenation, (f) isomerization, (g) further cracking to gas, and (h) formation of multi-ring aromatics. The thickness of the arrows indicates the relative amounts of products.

4.3.3 HTP for post-consumer PE waste

To test the feasibility of HTP conversion of post-consumer plastic wastes, three types of wastes, EREMA pellets, chopped HDPE milk jugs, and chopped HDPE grocery bags were tested under the same condition for the model HDPE, at 425 °C and 2.5 h. The oil yield of the HDPE milk jugs was similar to that of model HDPE, 87 wt. %. The oil yields of the HDPE grocery bags and the EREMA pellets were lower, probably because of the presence of inorganic additives in the wastes, Figure 4.5. The SEM-EDS results and the elemental compositions of the inorganic residues obtained from EREMA waste are reported in Figure A.7 and Table A.4. For the EREMA waste, the amount of inorganic residue was ca. 5 wt. %. The solid residue was found to contain mostly calcium, oxygen, carbon, silicon, chlorine, and titanium. These elements came primarily from the pigments and fillers in the products. The HTP gas consisted of mainly *n*-paraffins, isoparaffins, and olefins from C_1 to C_5. The gas can be combusted for energy recovery, Table A.5.

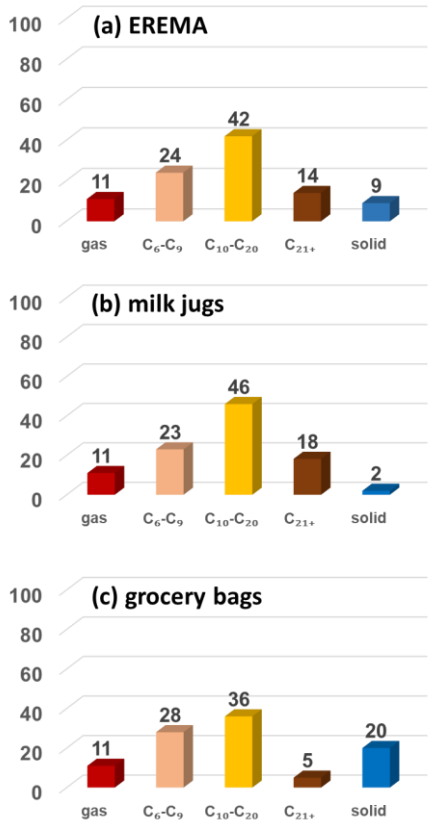

Figure 4. 5 HTP yields (wt. %) of products obtained from (a) EREMA pellets, (b) HDPE milk jugs, and (c) HDPE grocery bags, at 425 °C and 2.5 hr.

The chemical compositions of the HTP oils for the three cases were quite similar, Figure 4.6 and Table A.6. The products from the EREMA pellets were evaluated for commercial applications: (1) HTP oil as potential liquid transportation fuels and (2) HTP solid as a potential wax product.

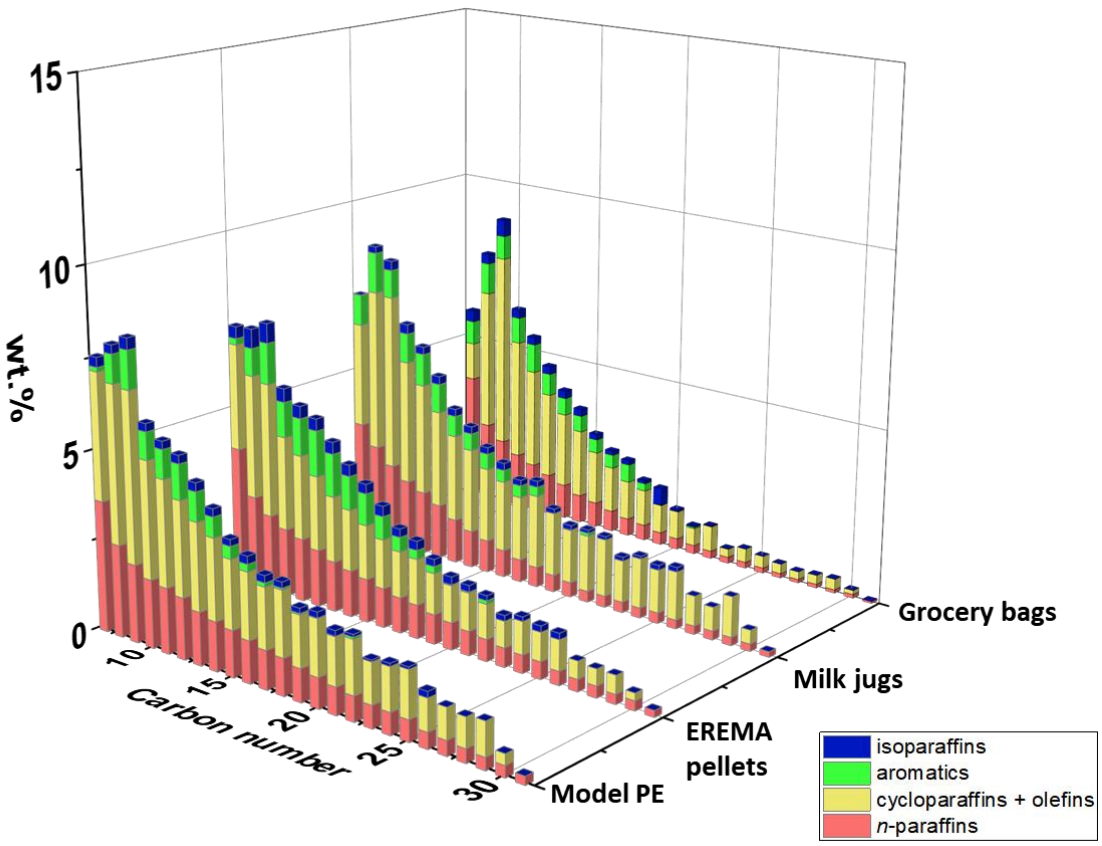

Figure 4. 6 Chemical composition of HTP oils obtained from model PE, EREMA pellets, milk jugs, and grocery bags at 425 °C and 2.5 hr.

4.3.4 HTP conversion of PE waste into liquid transportation fuels

For 425 °C and 2.5-3 h or 450 °C and 45 min, the oil yields were high, 87 wt. %. The oil products contained large fractions of hydrocarbons in the diesel fuel range (C_{10}-C_{20}). The oil produced at 425 °C and 2.5 h from PE waste (EREMA) was considered for possible use as a liquid transportation fuel. Since the oil had a wide carbon number distribution from C_6 to C_{31}, the oil was distilled to produce a gasoline-like fraction with b.p. ≤ 170 °C, a diesel-like fraction with b.p. 170-300 °C, and a heavy oil fraction with b.p. ≥ 300 °C. The distillation yields of these fractions were 27.7, 46.2, and 26.1 wt. %, respectively. The distillation process could be improved further for scale-up to increase the product yields or to improve the product quality.

The HTP heavy oil had a similar carbon distribution as a base oil (C_{18}-C_{40}), which can be a feedstock for lubricants, specialty solvents, or other chemicals. It can also be recycled and further

cracked into lighter hydrocarbons using HTP. Further studies or evaluations of the heavy oil are beyond the scope of this study.

The gasoline-like fraction (referred to as the "HTP gasoline") looks similar to a commercial gasoline, Figure 4.7(a). The diesel-like fraction (referred to as the "HTP diesel") also looks similar to a commercial No. 2 diesel, Figure 4.7(b). The GC×GC-FID chromatogram of HTP diesel was less complex than that of the commercial diesel, Figures 4.7(c) and 4.7(d). The detailed compositions of HTP gasoline, HTP diesel, commercial gasoline, and commercial diesel are shown in Figure 4.8 and Tables A.7 and A.8. The HTP gasoline had similar carbon number distribution as the commercial gasoline, but different hydrocarbon class distributions. The HTP gasoline had more *n*-paraffins and cycloparaffins and less isoparaffins and aromatics than the commercial gasoline. The HTP gasoline contained less benzene (0.41 wt. %) than the commercial gasoline samples (0.53-0.91 wt. %), Table A.7. The HTP gasoline was evaluated as a potential gasoline blendstock in Section 4.3.4.1.

The HTP diesel had a similar carbon number range as the commercial No. 2 diesel, but the distribution was slightly positively skewed, Figure 4.8. The HTP diesel had more *n*-paraffins and cycloparaffins and fewer isoparaffins and aromatics than the commercial diesel samples, Table A.8. The HTP diesel was evaluated as a potential No. 1 diesel and as a potential blendstock for No. 2 diesel as described in Section 4.3.4.2.

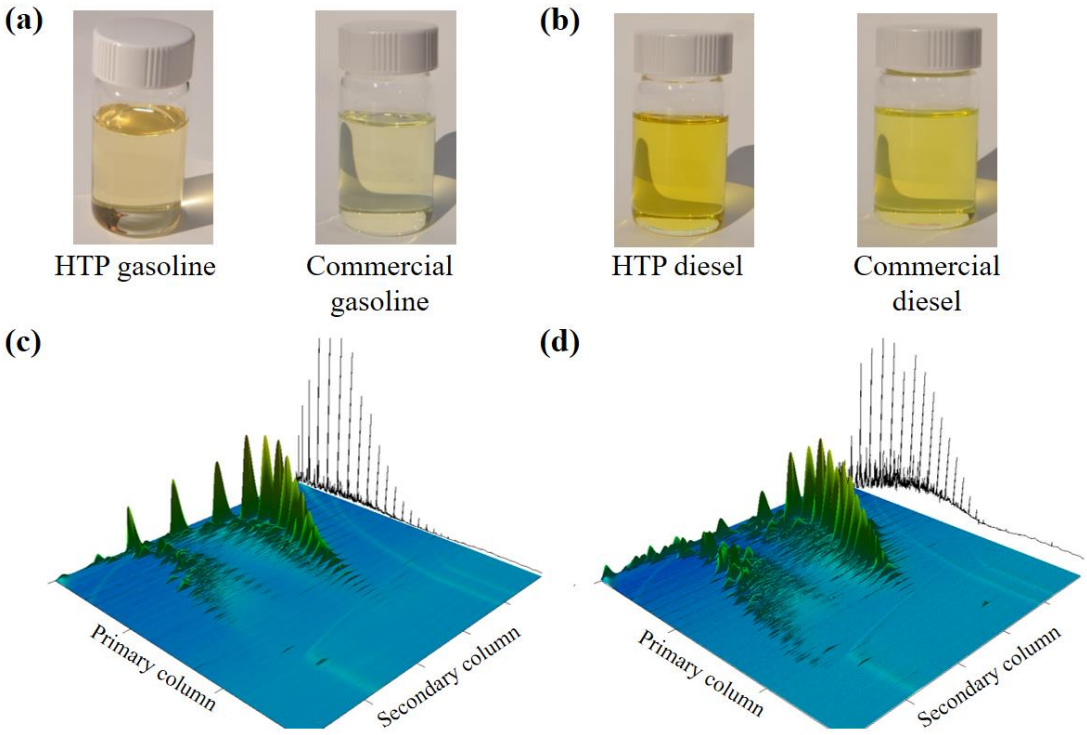

Figure 4. 7 The HTP oils and their characterization. (a) Photographs of HTP gasoline and commercial gasoline. (b) Photographs of HTP diesel and commercial diesel. Two-dimensional GC×GC-FID spectra for (c) HTP diesel and (d) commercial diesel (Speedway).

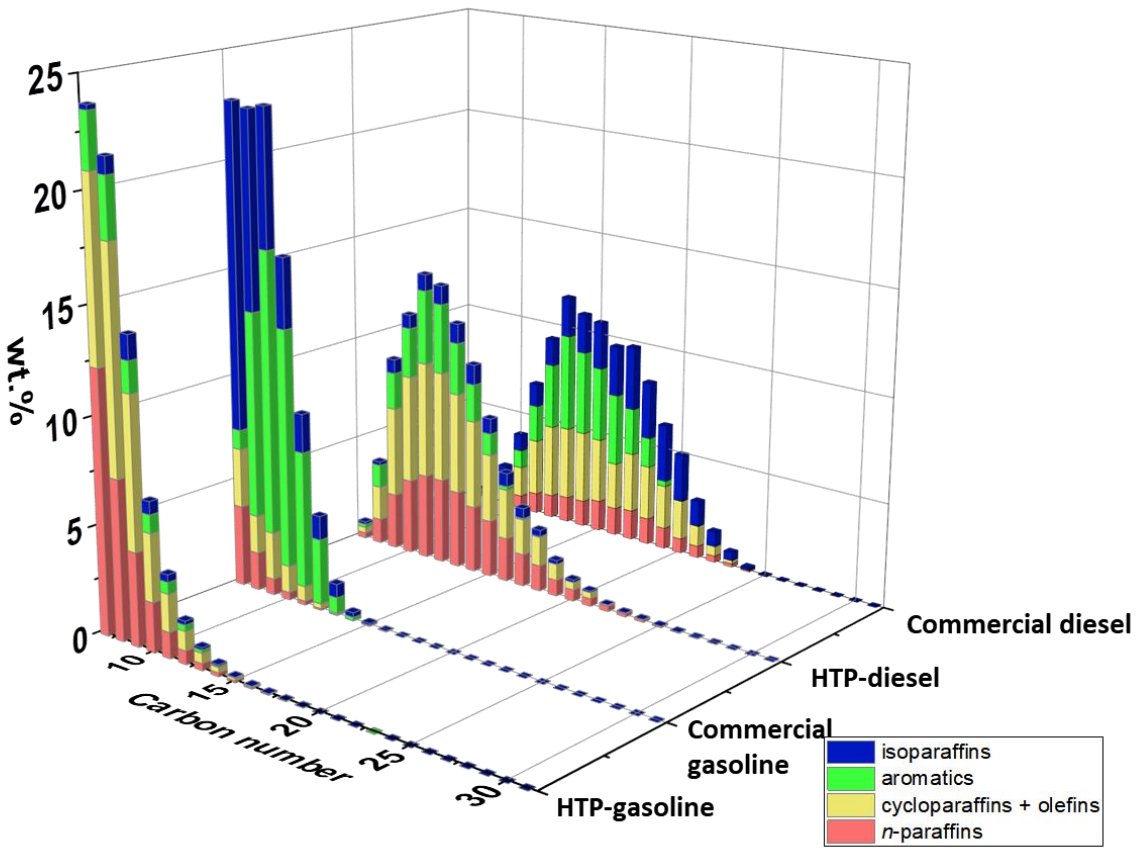

Figure 4. 8 Comparison of the chemical compositions of HTP gasoline with commercial gasoline and HTP diesel with commercial diesel.

4.3.4.1 Evaluation of the HTP gasoline as a potential gasoline

The HTP gasoline fuel properties are compared to those of three commercial gasoline samples in Table 4.1. As expected from the chemical composition results in Figure 4.8, the octane number (ON) of the HTP gasoline was lower than that of the GoLo gasoline. This was confirmed by the values of the research octane number (RON), the motor octane number (MON), and the anti-knocking index (AKI, the average of RON and MON) estimated from FTIR spectra using Eraspec. The density of the HTP gasoline was similar to those of the commercial gasolines. The kinematic viscosity of the HTP gasoline was slightly higher.

Since the HTP gasoline had low ON, it probably cannot be used as “road-ready” gasoline. Hence, it was evaluated as a potential gasoline blendstock. Two blends of HTP gasoline and GoLo gasoline were produced, one with 10 vol. % of HTP gasoline, HTP-10G, and one with 50 vol. %

of HTP gasoline, HTP-50G. The properties of the two blends are shown in Table 4.1. The ON of the blends was higher than that of the HTP gasoline but still lower than that of the commercial gasoline. This result indicates that the HTP gasoline could be blended with gasolines with a higher AKI (e.g., 92) and yield an acceptable product. The HTP gasoline could also be used as a feedstock for producing gasoline via an isomerization process (Naqvi et al., 2018).

Table 4. 1 Fuel property results for, HTP gasoline, HTP gasoline blends (HTP-10G and HTP-50G) with GoLo gasoline, and commercial gasoline samples.

Property	HTP gas.	HTP-10G	HTP-50G	ExxonMobil gas.	Shell gas.	GoLo gas.
Water and sediment (vol. %)	<0.05	<0.05	<0.05	<0.05	<0.05	<0.05
Density at 15 °C (g/cm^3)	0.7495	0.7428	0.7459	0.7465	0.7540	0.7367
Kin. viscosity at 15 °C (mm^2/s)	0.771	0.601	0.662	0.614	0.617	0.568
Sulfur (ppm)	<15	<15	<15	<15	<15	<15
Research Octane Number	76	90	84	-	-	92
Motor Octane Number	72	81	77	-	-	83
Anti-knocking index	74	86	81	87	87	87

4.3.4.2 Evaluation of the HTP diesel as a potential fuel

Several properties of the HTP diesel were measured and compared to the requirements of ASTM D975 for ultra-low-sulfur, No. 1 or No. 2 diesel, Table 4.2. The key requirements are: (1) 90 vol. % boils at a temperature below 288 °C for No. 1 diesel and between 282 and 338 °C for No. 2 diesel; (2) sulfur content is less than 15 ppm, and (3) cetane number (CN) higher than 40 (ASTM International, 2019). The HTP diesel contained 8.5 ppm of sulfur and met all the requirements for ultra-low-sulfur No. 1 diesel, Table 4.2. The CN of the HTP diesel was 61, which was higher than the CN 46 for the commercial diesel. The higher CN was due to the higher *n*-paraffin content and the lower isoparaffin content, Figure 4.8 and Table A.8. The HTP diesel also had a higher net heat of combustion, because it had fewer aromatics. The high CN makes HTP diesel a great blendstock (CN booster) for diesel with low CN.

Because of the boiling point range selected for collecting the distillation fractions, the HTP diesel had a slightly lower density, viscosity, and flash point than that of the commercial No. 2

diesel (Table 4.2). The HTP diesel was tested for its potential as a blendstock for No. 2-D diesel. Two blends of Speedway diesel and HTP diesel were produced, HTP 10D and HTP 50-D, with 10 and 50 vol. % HTP diesel, respectively. The CN values of the diesel blends were higher than that of the Speedway diesel.

The HTP-10D blend met all the other requirements for No. 2-D diesel. The HTP-50D blend met all the other requirements except the flash point (50 °C), which is slightly lower than 52 °C, the minimum required for No. 2-D diesel. The flash point is a safety-related property and defines the minimum temperature at ambient pressure at which a vapor-air mixture can be ignited in a closed space (Schemme, Samsun, Peters, & Stolten, 2017). The flash point reported here was measured via the ASTM D56 method, which is slightly different than the ASTM D93 method for diesel fuels. In general, D56 gives lower flash point values than the D93 (ASTM International, 2016, 2018; MIL-DTL-5624W, 2016). Thus, the flash point value of 50 °C for the HTP-50D measured by the D56 method may still qualify as No. 2-D diesel.

Table 4. 2 ASTM D975 requirements for ultra-low sulfur No. 1-D, No. 2-D, and properties of HTP diesel, HTP-10D, and HTP-50D, which are blends of the HTP diesel with Speedway No. 2 diesel.

Property	ASTM No.1-D S15	ASTM No. 2-D S15	Speedway No. 2 diesel	HTP diesel	HTP-10D	HTP-50D
Distillation temperature (°C) for 90 % recovered	<288	282-338	317	286	-	-
Flash Point (°C)	>38	>52	58*	46*	57*	50*
Water and Sediment (vol. %)	<0.05	<0.05	<0.05	0.01	<0.05	<0.05
Density at 40 °C (g/cm^3)	-	-	0.828	0.798	0.813	0.825
Kinematic Viscosity at 40 °C (mm^2/s)	1.3-2.4	1.9-4.1	2.685	1.650	2.549	2.070
Sulfur (ppm)	<15	<15	<15	8.5	<15	<15
Cetane number	>40	>40	46	61	48	55
Aromaticity (vol. %)	<35	<35	30	18	28	24
Cloud Point (°C)	(-7)-(-22)		-11	-7	-10	-9
Hydrogen content (wt. %)	-	-	13.89	14.04	13.91	13.96
Net heat of combustion (MJ/kg)	-	-	42.62	42.94	42.66	42.79

*ASTM D56 was used instead of ASTM D93

As discussed in Section 4.3.2, at a higher temperature, 450 °C, the reactions followed the same pathways. For this reason, the compositions of the HTP oils obtained at 425 °C, 2.5 h and 450 °C, 30 min, were similar. The HTP oils at 425 °C, 3 h and 450 °C, 45 min were also similar, Figure 4.9. The reaction rates at 450 °C were approximately four to five times faster than at 425 °C. At these reaction conditions, the oil yields were high, 86-87 % and the oil products contained large fractions (50-75%) of hydrocarbons in the diesel fuel range (C_{10}-C_{20}).

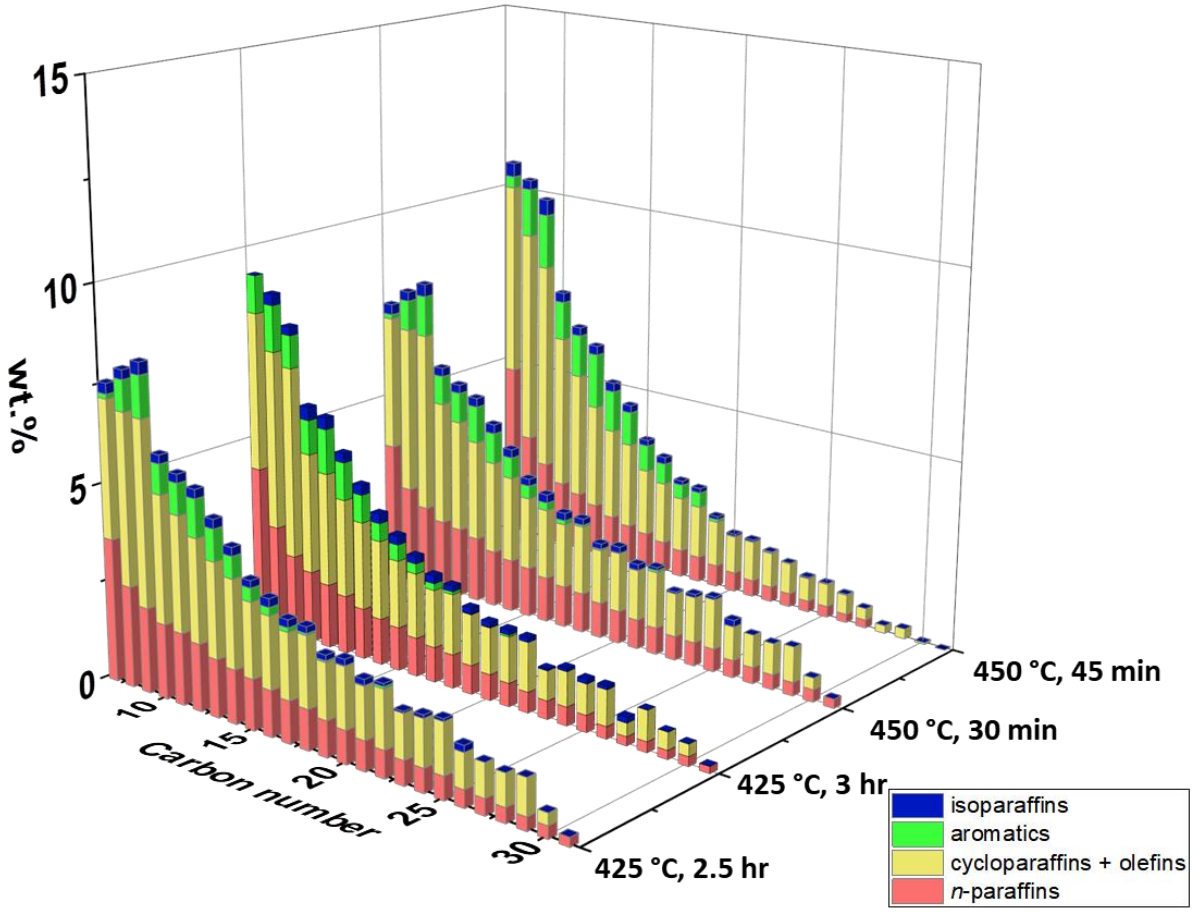

Figure 4. 9 Comparison of the carbon number distributions and chemical compositions of the HTP oils produced at 425 and 450 °C for various reaction times.

4.3.5 HTP conversion of PE waste (EREMA pellets) into waxes

The highest HTP solid yields from the model HDPE were obtained at 425 °C and 30 and 40 min. No gas was produced under these conditions. These conditions were tested for converting the EREMA waste into solid products. The compositions and the yields of the solids and the

potential of the solids as wax products were evaluated by using TGA, Figure 4.10, FTIR, and GCxGC-TOF/MS, Figure 4.11.

TGA was done to probe the amount of oil embedded in the solid and the solid composition. The mass loss below 150 °C (at which *n*-C_{20} starts to evaporate in TGA) was taken to be the mass of the oil with a carbon number less than 20 (referred to as "Fraction 1"). The mass loss between 150 and 375 °C was taken to be the wax fraction with carbon numbers between 20 and 40 (referred to as "Fraction 2") since C_{40} is known to evaporate fully at 375 °C. The mass loss above 375 °C with a carbon number above 40 was taken as the heavy wax fraction (referred to as "Fraction 3") (Table 4.3). The sum of Fractions 2 and 3, with carbon numbers greater than 20, was defined as the HTP wax. The yields were 42-57 wt. % for Fraction 2 and 55- 39 wt. % for Fraction 3, and the overall wax yields were quite high, ca. 97%.

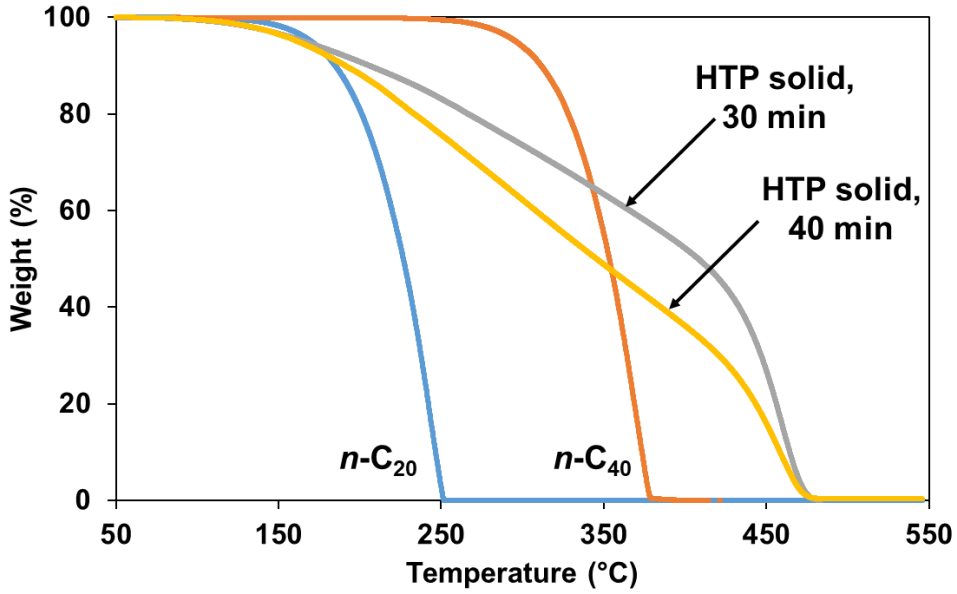

Figure 4. 10 TGA analysis of HTP solids at 30 and 40 min and compared with *n*-C_{20} and *n*-C_{40} standards.

Table 4. 3 Yields of HTP materials produced at 425 °C, 30 or 40 min.

Fraction	Carbon Number	Yield (wt. %)	
		30 min	40 min
(1)	< 20	3.4	3.5
(2)	20 – 40	42.0	57.5
(3)	> 40	54.6	39.0
HTP wax = (2) + (3)	≥20	96.6	96.5

The HTP wax from EREMA pellets was transparent at room temperature, Figure 4.11(a). The FTIR spectra of the HTP wax and commercial paraffin wax are quite similar, Figure 4.11(b). The two peaks at 2920 cm^{-1} and 2850 cm^{-1} are assigned to the asymmetrical stretching vibration and the symmetrical stretching vibration of -CH_2-, respectively. The 1460 cm^{-1} peak arises from the bending vibration of -CH_2-. The two peaks at 2960 cm^{-1} and 1380 cm^{-1} are from the stretching vibration and the bending vibration of -CH_3. The peak at 910 cm^{-1} is from the C=CH_2 bonds and indicates the presence of vinyl groups. Qualitative GC×GC-TOF/MS results, Figure 4.11(c) showed that the fraction of the HTP wax with carbon numbers between 20 and 40 consisted of ca. 80 wt. % of *n*-paraffins and 20 wt. % of α-olefins, Table A.9.

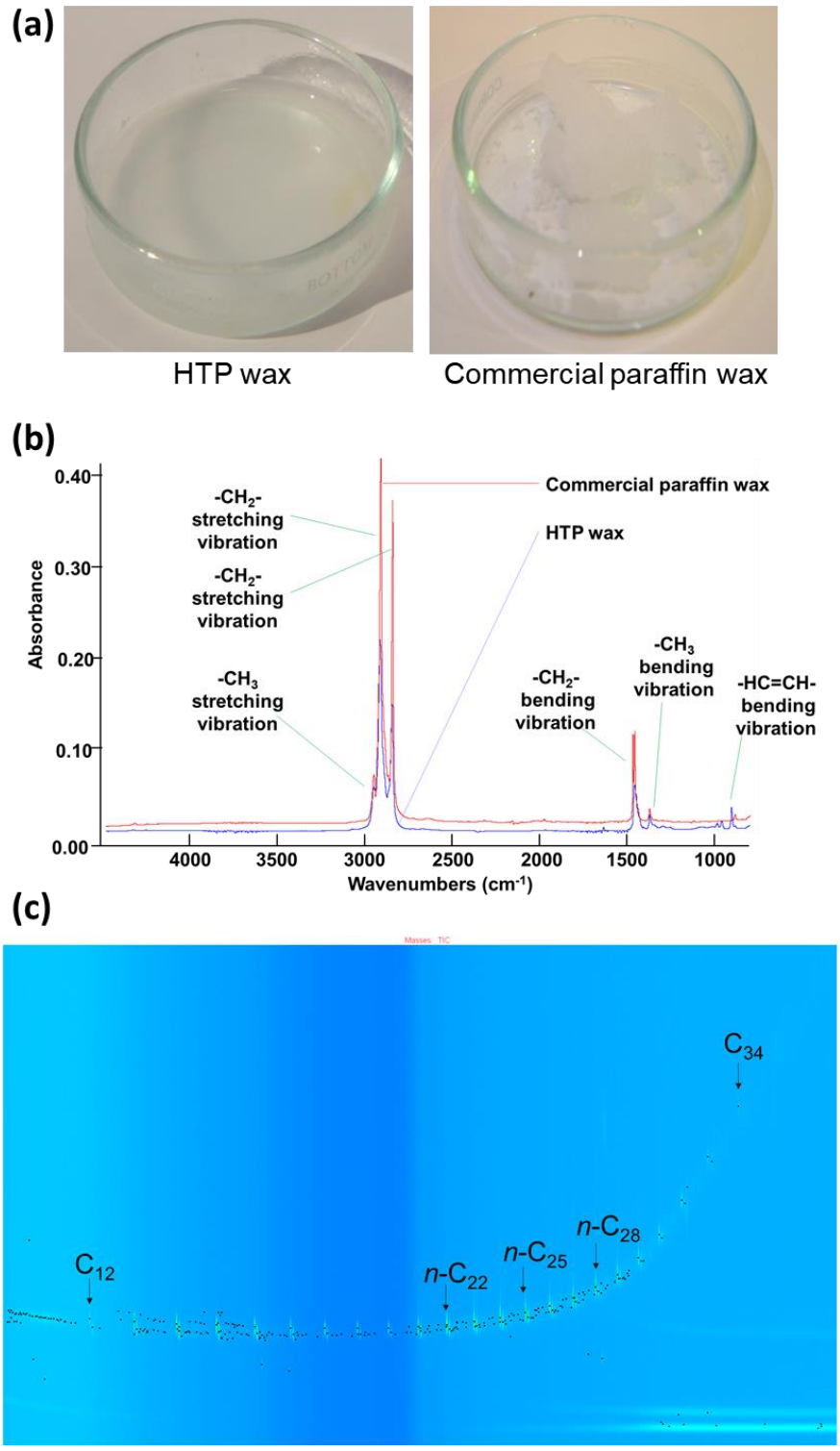

Figure 4. 11 HTP wax and characterization. (a) Photographs of HTP wax and commercial paraffin wax. (b) Comparison of FTIR spectra of HTP wax and commercial paraffin wax. (c) GC×GC-TOF/MS chromatograms of HTP wax with designated carbon numbers and three standards used for classification.

4.3.6 Comparison of PE and PP conversion via HTP

Polypropylene (PP) waste can also be converted into oils and gases at temperatures between 380 and 450 °C (Chen et al., 2019). At 425 °C, the oil yield from PP was 91 wt. % at 2 h, indicating a faster conversion than from PE. The oil from PP had more olefins and cycloparaffins (ca. 90 wt. %) and fewer paraffins (ca. 10 wt. %).

The differences in the reaction rates and the oil compositions are evidently caused by the different molecular structures of PE and PP. Since PP has two types of C-C bonds (Chen et al., 2019), a -CH_2-CH_2- bond (on the backbone) with a bond energy of 348 kJ/mol, and a C-CH_3 bond with lower bond energy (335 kJ/mol), it tends to break up faster. When the -CH_2-CH_2- bonds are broken, *n*-paraffins and α-olefins are produced via hydrogen abstraction and β-scission. By contrast, when the C-CH_3 bonds are broken in PP, only olefins are produced via β-scission. These differences evidently result in a higher percentage of olefins and cycloparaffins in the PP oil. Since PE only has the -CH_2-CH_2- bond on the backbone, more energy is required for depolymerization and more *n*-paraffins are produced.

4.3.7 Comparison of HTP to fuels or waxes with other plastic recycling methods

The HTP conversion of PE waste to fuels or waxes was compared to several other methods with respect to net energy ratio (energy available in products to energy used for conversion), GHG emissions, and potential profits, Figure 4.12. The data for HTP of PE waste were adapted from the data for biomass HTP processes (Zhu, Biddy, Jones, Elliott, & Schmidt, 2014).

The energy ratios for HTP to fuels or waxes were larger than those of pyrolysis to fuels, incineration, and HTP of biomass to fuels. The energy ratios were lower than those for mechanical recycling, which uses lower processing temperatures and does not involve depolymerization. Moreover, GHG emissions were estimated to be lower than those in pyrolysis and biomass HTP, and much lower than in incineration.

The potential profits were estimated as detailed in Tables A.10 and A.11. The profits for HTP conversion were $332 for fuels and $719 for waxes per ton of feedstock. They are higher than those for pyrolysis ($75/ton PE) or producing diesel from crude oil ($80/ton). Thus, HTP seems to be an economically feasible recycling method. The HTP conversion of biomass into biodiesel is not profitable currently because of low oil yields and the costs for necessary

hydrotreating (Zhu et al., 2014). Moreover, biodiesel has a lower heating value (39 MJ/kg) because it contains oxygenated compounds (Sivaramakrishnan & Ravikumar, 2011). The state-of-the-art HTP technologies can produce bio-diesels at $3.50 per gallon of gasoline-equivalent (GGE) (Zhu et al., 2014). This price is not competitive with current commercial diesel prices ($2.08/gallon or $2.36/GGE).

Although both HTP and pyrolysis can produce oils or fuels, pyrolysis reactions take place in viscous and highly concentrated polymer phases (Savage et al., 1995). At these conditions, second-order and higher-order reactions, such as polycondensation reactions, are significant and can eventually generate char (Savage, 2000). In supercritical water in HTP, since the polymer concentrations are lower, lower-order and unimolecular reactions, such as β-scission, are favored, and reactions with higher-orders are suppressed (Savage et al., 1995)(Akiya & Savage, 2002). Supercritical water serves as an effective solvent and reaction medium for polyolefins. Char did not form under all the conditions tested. Pyrolysis without added catalyst has average yields of 77 wt. % oil, 22 wt. % gas, and up to 0.2 wt. % char (Savage et al., 1995). The HTP method requires no added catalysts and has a higher oil yield (~87 wt.%) and a lower gas yield (~12 wt. %) than pyrolysis.

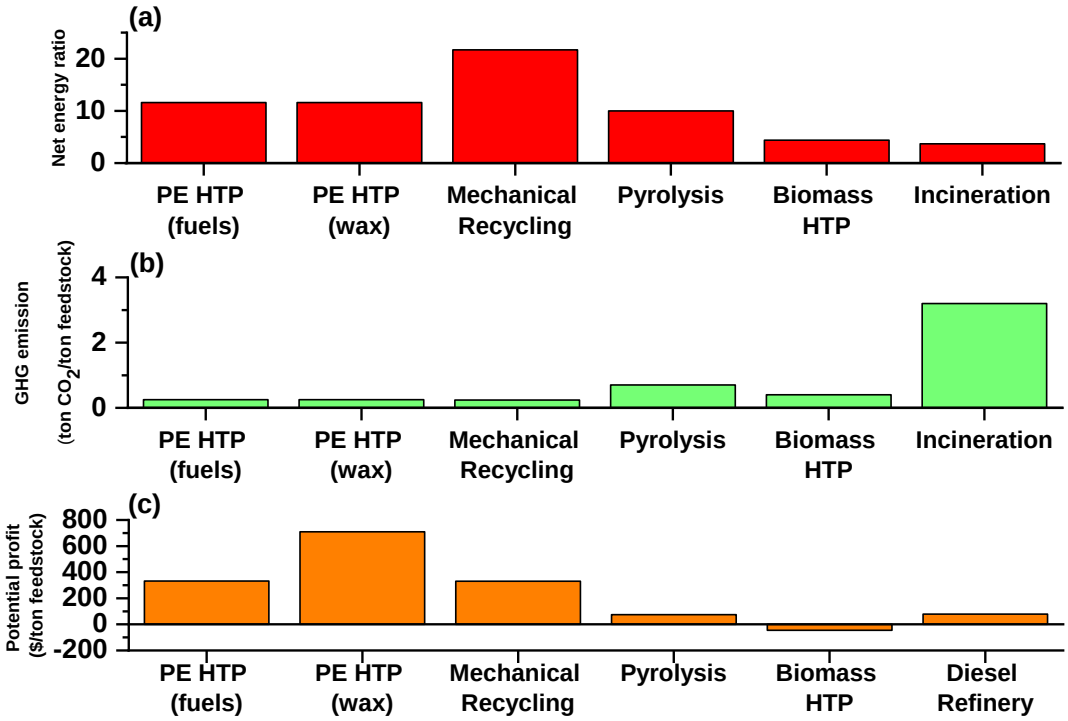

Figure 4. 12 Comparison of HTP for PE waste with other recycling methods and similar technologies. (a) Net energy ratio. (b) GHG emission (ton CO_2/ton feedstock). (c) Potential profit ($/ton feedstock).

4.4 Conclusions

HTP is a versatile upcycling method, which can convert post-consumer PE waste into fuels, waxes, gases, and monomers. Multiple reaction conditions were investigated, and reaction kinetic data for depolymerization of a model HDPE were obtained to probe the reaction mechanisms. Complete reaction pathways were postulated from detailed analyses of the chemical compositions of the intermediate products. The data and the pathways allowed identifying the reaction conditions for improving the yields, the chemical compositions, and the properties of the products. PE waste can be efficiently converted into valuable products, such as ultra-low sulfur gasoline, or diesel fuels, or clean waxes. Mixtures of paraffin and α-olefin waxes were obtained with high yields, 97 wt. % at 425 °C and 30 or 40 min. The highest oil yields for producing fuels, 86-87 wt. %, were obtained at 425 °C and 2.5 h or 450 °C and 45 min. No char was detected in all experiments. The HTP diesel-like fractions met all key specifications for No. 1-D ultra-low sulfur diesel and had a higher CN value of 61 than a commercial diesel, and a lower aromatic content, 18

vol. %. Blends of a commercial diesel with the diesel-like fraction, up to 50 vol. %, met all the specifications for No. 2-D ultra-low sulfur diesel. Overall, the HTP method is expected to be more energy-efficient than incineration or pyrolysis and have lower GHG emissions.

CHAPTER 5 LOW-PRESSURE HYDROTHERMAL PROCESSING OF MIXED POLYOLEFIN WASTES INTO CLEAN FUELS

5.1 Introduction

The amount of plastic waste has grown exponentially over the past 60 years and accelerated as COVID-19 spread (Adyel, 2020; Geyer et al., 2017a; Klemeš, Van Fan, Tan, & Jiang, 2020; Silva et al., 2020). Only 9% of the total plastic waste is recycled, and 12% is incinerated (Geyer et al., 2017a; MacArthur, 2017). The rest, about 6 billion tons, accumulates in landfills and oceans, where it degrades over decades into microplastics, releasing toxic chemicals into the environment, Figure 5.1 (Andrady, 2017; Geyer et al., 2017a; Lebreton, Egger, & Slat, 2019; Lebreton et al., 2018; Pabortsava & Lampitt, 2020; Rochman et al., 2013). Current technologies for removing plastic pollutants from water cost about $0.003 per gallon (Mihelcic et al., 2017; Tiemann, 2010). Cleaning up the oceans, containing 3.5×10^{18} gallons of water, could cost thousands of times the global GDP. Microplastics have been found in drinking water, plant roots, animals, and human organs (Choy et al., 2019; Cox et al., 2019; Li et al., 2020; Rochman & Hoellein, 2020). Their impact on ecosystems and human health is potentially devastating (Cox et al., 2019; Karbalaei, Hanachi, Walker, & Cole, 2018; Mitrano & Wohlleben, 2020; Ragusa et al., n.d.). This plastic pollution could be a more urgent threat to all life on land or below water than climate change.

Conventional methods, including incineration, mechanical recycling, and pyrolysis, are ineffective in reducing the plastic waste. Incineration releases greenhouse and toxic gases, has low energy recovery, and requires tipping fees ($20/ton) to be profitable (Eco.cycle, 2011; Eriksson & Finnveden, 2017; Lee, Benavides, & Wang, 2020). Mechanical recycling of mixed waste typically results in dark-colored, lower-value products. After several (<10) cycles, polymer properties degrade, and the wastes must be landfilled or incinerated (Garcia & Robertson, 2017; Hopewell et al., 2009; Schyns & Shaver, 2020). Pyrolysis can convert mixed plastic waste to oils with yields from 50 to 90%, but the oils have a wide carbon number distribution (Anuar Sharuddin, Abnisa, Wan Daud, & Aroua, 2016; Das & Tiwari, 2018; Kassargy, Awad, Burnens, Kahine, & Tazerout, 2017; Kassargy et al., 2018; Marcilla, Beltrán, & Navarro, 2009; Onwudili, Insura, & Williams,

2009; Santos, Almeida, Maria de Fatima, & Henriques, 2018). Fast catalytic pyrolysis generates significant amounts of polycyclic aromatic hydrocarbons and up to 40% char, resulting in catalyst deactivation (Akubo et al., 2019; Park et al., 2019). The oils from pyrolysis need extensive upgrading and separation to produce transportation fuels or other chemicals. Gasification converts mixed plastic waste into gases such as CH_4, H_2, CO and CO_2 (Ahmed et al., 2011; Janajreh et al., 2020; Kannan et al., 2013; Singh, Déparrois, Burra, Bhattacharya, & Gupta, 2019). Gasification has a high energy consumption as it requires a temperature between 500 and 800 °C. Embodied energy in plastic waste is lost because no polymer structure or carbon chain is preserved in gasification. The use of supercritical water in gasification can help reduce char formation, but the combination of high temperature and high pressure (≥23MPa) could result in a high capital cost (Bai, Wang, & Jin, 2020). Globally, more than 350 million tons of plastic waste is generated annually (Geyer et al., 2017a); 63% are polyolefins, polyethylene (PE) and polypropylene (PP), which have short lifetimes (<6 months) and low recycling rates (~5%) in the U.S (Environmental Protection Agency, 2020). Thus, almost all new polyolefin products are made from virgin feedstocks.

Supercritical water liquefaction (SWL) was shown to convert plastic waste into lower molecular-weight chemicals and the water serves as a solvent, reactant, or catalyst (Bai et al., 2019; Chen et al., 2019; Hatakeyama, Kojima, & Funazukuri, 2014; Ügdüler et al., 2020). Polyolefin waste was converted into oils with high yields (~90%) and no char using SWL. PP waste was converted mainly into naphtha; PE waste was converted into wax, clean gasoline blendstock, or diesel (Chen et al., 2019; Jin et al., 2020). Previous studies were limited to sorted polyolefin wastes, using high operating pressures (≥23 MPa) and requiring high capital and energy costs. Here, we developed efficient and economical low-pressure (~2 MPa) hydrothermal processing (LP-HTP) methods for converting polyolefin mixtures into clean fuels. The conversion pathways of PE, PP, and their mixtures at various pressures were found from comprehensive two-dimensional gas chromatography analysis of the products at different reaction times. Our new optimal LP-HTP methods produced oils with high yields (87%) and little char (<0.5%). The oils produced from the mixed wastes with 50% or more PP were distilled to produce qualified clean gasoline and ultra-low sulfur diesel fuels. With LP-HTP, 220 million tons of polyolefin wastes can be converted to 190 million tons of fuels annually, while saving 1.5 billion barrels of crude-oil-equivalent energy

and associated GHG emissions compared to conventional fuel production methods. The oils can also be used for producing other monomers to help achieve a circular economy, Figure 5.1.

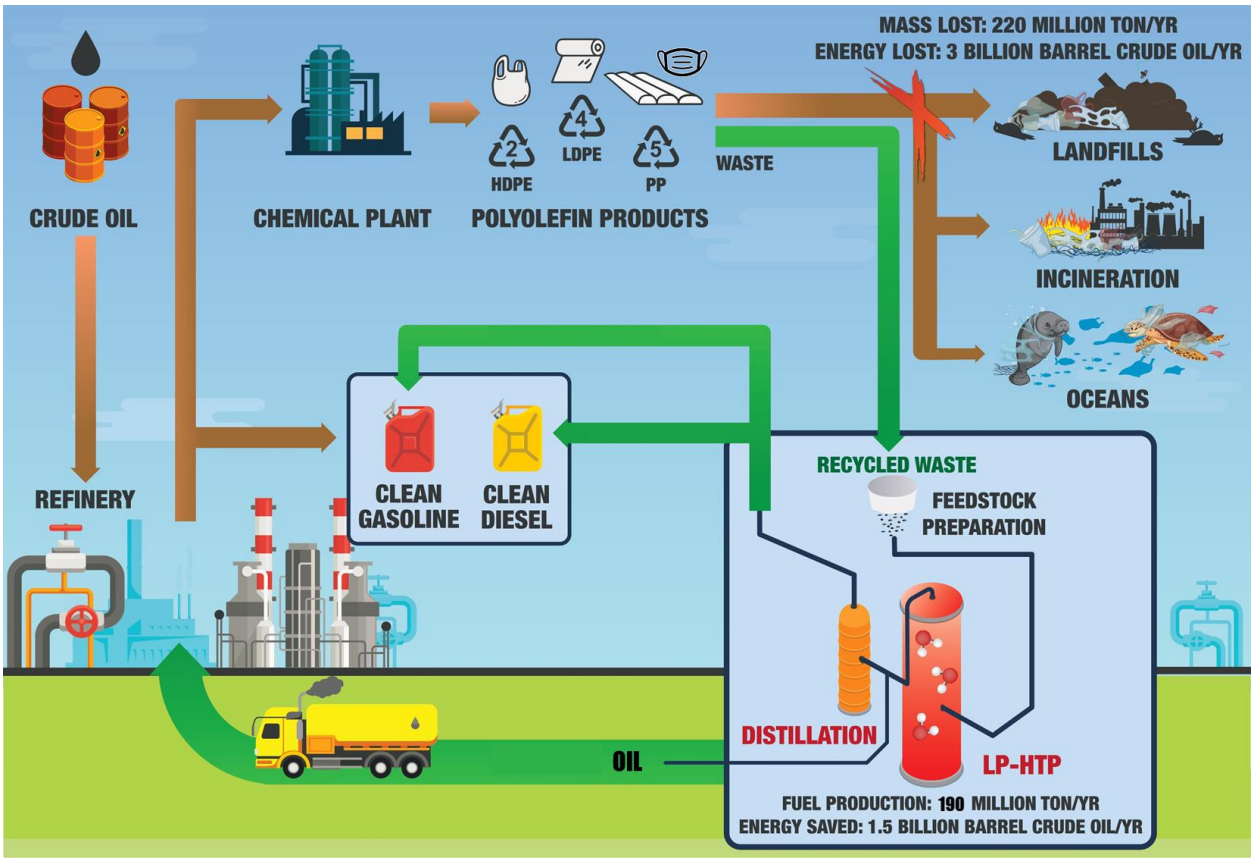

Figure 5. 1 Overview of LP-HTP for converting polyolefin waste into high-quality clean gasoline and diesel. LP-HTP has the potential to transform the current linear path from crude oils to polyolefin products and wastes into a more economical and sustainable circular path by producing clean gasoline and diesel fuels or by producing monomers that can be used to synthesize new polymers.

5.2 Experimental

5.2.1 Feedstocks

Four polyolefin feedstocks were used: (1) model HDPE pellets with a 180,000 g/mol weight-average molecular weight purchased from Sigma Aldrich (St. Louis, MO), (2) model PP pellets with a 250,000 g/mol weight-average molecular weight from Sigma Aldrich, (3) EREMA pellets, made from post-consumer PE grocery bags (EREMA North America, Ipswich, MA), and

(4) shredded post-industry PP waste (containers and lids) from Berry Plastics (Berry Global, Evansville, IN). The feed for co-processing tests was formed by mixing (1) and (2) or (3) and (4) based on mass ratio. The water used in LP-HTP and SWL tests was acquired from a Milli-Q water purification system and was degassed for 30 min before use. Commercial gasoline samples from ExxonMobil and BP and diesel samples from Speedway and Family Express, which were used as fuel property benchmarks, were purchased from local gas stations (West Lafayette, IN).

5.2.2 Reaction equipment and procedures

A 500 ml high-pressure high-temperature Parr batch reactor, Type 4570, was used for the experiments (Parr Instrument Company, Moline, IL). Reactions were conducted at 450 °C for 45-60 min. In each experiment, 40 g of polyolefin feed was used. Various amounts of water were added to the reactor to reach the target pressures at 450 °C, 70 g of water for SWL (23 MPa) and 0, 2, 5.5, and 17 g of water for LP-HTP at 0.25, 1.55, 3.75, and 10.25 MPa, respectively. After loading the feed mixture, the reactor was assembled and purged with N_2 three times to remove any residual air. The time for heating the reactor from room temperature to 450 °C for LP-HTP and SWL was 60 and 65 min, respectively. The reported reaction time did not include the heating time. After the reaction, air cooling with forced convection was utilized, and it took 10 min to cool down to 300 °C and another 50 min to cool down to room temperature. Stirring rate at 300 RPM was used through the heating, reaction, and cooling periods. After the reaction, the gas pressure was recorded at room temperature.

5.2.3 Separation of reaction products

A Tedlar bag was used for gas product sampling, and any remaining gas was released in a fume hood. The reactor was disassembled, and the mixture of oils, solids, and water was transferred to a glass flask. The solids were separated by filtration, washed three times using acetone, dried in an oven at 70 °C overnight, and weighed. The oils and water were separated by a glass funnel and weighted individually. For tests using polyolefin waste, the solid consisted of char and inorganic additives. The solid was treated in a muffle furnace at 500 °C for 1 hr to burn off char. The inorganic compounds (remaining residue) were weighed afterward and analyzed by SEM-EDS.

5.2.4 Yield calculation

The yields of solids were calculated based on dry mass. The gas yields were calculated using a method based on the gas chemical compositions (Chen et al., 2019; Jin et al., 2020). The oil yields were calculated by subtracting the yields of gas, char, and residual solid from 100 wt% and they were also verified with the collected oil masses, Figure B.1.

5.2.5 Oil distillation

An in-house one-stage batch distillation apparatus was built based on the ASTM D86 method and was used to separate oil products into gasoline fraction, diesel fraction, and heavy oil fraction. The oils from four runs at the same reaction conditions were combined and distilled. The gasoline fraction was collected for a boiling point from 25 to 170 ºC, and the diesel fraction was collected for a boiling point between 170 and 300 ºC, which corresponds to No. 1 diesel. The remainder was the heavy oil fraction. The diesel yield obtained from the distillation was lower than that calculated from the chemical composition due to the limited separation efficiency of the batch distillation method, which could be optimized for large scale production. The gasoline, diesel, and heavy oil fractions were weighed at room temperature. Distillation temperature values (T_{10}, T_{50}, T_{90}, T_{final}, and distillation residue) were also obtained from this batch distillation apparatus. Here, T_x refers to the temperature at which x vol% of the sample evaporated (A. International, 2020).

5.2.6 Chemical composition of the gas products

The chemical compositions of the gas samples were determined using gas chromatography coupled with flame ionization detection (GC-FID). Standard gases including C_1-C_6 paraffins and C_2-C_6 olefins were used for peak identification and response factor determination. An Agilent 6890 GC (GS-CarbonPLOT GC Column) coupled with G1701DA MSD ChemStation was utilized. The details are shown in Table B.1.

5.2.7 Chemical composition of the oil products

Detailed chemical compositions of all oil samples were obtained by comprehensive two-dimensional gas chromatography with a flame ionization detector (GC×GC-FID) using the method

described in previous study (Jin et al., 2020). Briefly, a gas chromatography Agilent 7890B system (Agilent, Santa Clara, CA) with a non-moving quad-jet dual-stage modulator (LECO Corporation, St. Joseph, MI), liquid nitrogen cooling, UHP He carrier gas, 30 m mid-polar primary column DB-17ms (Agilent, Santa Clara, CA) and 0.8 m nonpolar secondary column DB-1ms (Agilent, Santa Clara, CA) was used. The samples were injected without dilution into split/splitless inlet (Agilent, Santa Clara, CA) with a split ratio of 1:300. The oven temperature was set from 40 to 260 ºC with a 3 ºC/min temperature ramp rate. The secondary oven and modulator offsets were 50 and 15 ºC, respectively. The modulation period was 2.5 s with 0.42 s hot pulse time. The inlet and FID temperatures were 280 and 300 ºC, respectively. Data were collected and processed with a collection rate of 200 MHz and a signal-to-noise ratio of 50 using ChromaTOF software (version 4.71 optimized for GC×GC-FID). The classification of the compounds was developed following the procedure in the previous paper (Petr Vozka & Kilaz, 2019a). Each sample composition was reported as wt% for each carbon number (C_5 to C_{31}) from each hydrocarbon class (*n*-paraffins, isoparaffins, cycloparaffins (mono-, di-, tri-), and aromatics (alkylbenzenes, cycloaromatics, alkylnaphthalenes, and biphenyls)). Since this GC×GC-FID method cannot distinguish between olefins and cycloparaffins in the oil products, they were grouped and referred as "olefins and cycloparaffins". Hydrocarbon content was calculated from the GC×GC-FID data based on the procedure mentioned in the literature (P. Vozka et al., 2018).

5.2.8 Physical properties of the gasoline and diesel products

The fuel properties of the gasoline and diesel products were measured using the following methods. Density and kinematic viscosity were measured by an SVM 3001 Stabinger viscometer (Anton Paar) using ASTM methods D4052 and D7042, respectively. The flash point was measured using a Tag 4 flash point tester (Anton Paar) via ASTM D56. The cloud point was measured with a manual cloud point apparatus (Koehler Instrument Co., New York, NY) via ASTM D2500. The gross heating value was measured with a 6200 Isoperibol calorimeter (Parr Instrument Company, Moline, IL) via ASTM D4809. The water content in oils was measured with a K20 Karl Fischer coulometric titrator (Mettler Toledo, Columbus, OH) via ASTM D6304. Research octane numbers (RON), motor octane numbers (MON), anti-knocking indexes (AKI), and cetane numbers (CN) were estimated from FT-IR spectra using an Eraspec fuel analyzer ("ERASPEC Fuel analyzer - Spectral Fuel Analysis in Seconds," n.d.). Reid vapor pressure for gasoline products was measured

using an Eraspec vapor pressure tester following ASTM D5191 ("ERASPEC Fuel analyzer - Spectral Fuel Analysis in Seconds," n.d.). Drivability index was calculated based on T_{10}, T_{50}, and T_{90}, as described in ASTM D4814 (A. International, 2020). The sulfur and lead content in gasoline and diesel samples were measured via inductively coupled plasma-optical emission spectrometry (ICP-OES) using a Perkin-Elmer Optima 8300 instrument.

5.2.9 Analysis of the inorganic residue

The inorganic residue was analyzed using Scanning Electron Microscopy–Energy Dispersive X-ray Spectroscopy (SEM-EDS) with JCM-6000PLUS (JEOL, Tokyo, Japan).

5.3 Results and discussion

The compositions of products at different reaction times from model PE, model PP, and mixtures with various PE/PP ratios were analyzed to establish the reaction pathways for PE and PP mixtures at various pressures. The reaction pathways allowed optimization of reaction conditions (temperature, pressure, and time) and feedstock compositions to produce oils with a carbon number distribution from C_4 to C_{25}, which can be separated into gasoline (C_4-C_{12}) and diesel (C_8-C_{25}) fractions. The properties of the fractions obtained from PE and PP were evaluated for potential fuel applications. Furthermore, the energy efficiency and GHG emissions of LP-HTP were evaluated and compared with those of other fuel production and plastic recycling methods.

5.3.1 Tests of model PE and PP at various pressures and water content in the feed mixture

Our previous SWL studies of individual PE and PP showed that high oil yields were obtained at 23 MPa (64 wt% H_2O), 450 °C, and at reaction times between 45 and 60 min (Chen et al., 2019; Jin et al., 2020). Here, we determined the effects of pressure on the reaction pathways at 450 °C and 1 hr. The total pressure is related to the temperature and the amounts of water and nitrogen in the reactor (see Method and NIST Data(NIST, n.d.)). The lower pressure was achieved by having the water amount reduced from 64 wt% H_2O at 23 MPa (supercritical state) to subcritical states with 30, 12, 5, and 0 (only plastic) wt% H_2O, corresponding to pressures of 10.25, 3.75, 1.55, and 0.25 MPa, respectively. The effect of pressure and hence water content on gas and oil

yields were minimal, Figures. 5.2(a) and 5.2(b). Char formation (wt%) increased slightly as the water content decreased, with 0 wt% char from SWL, to ~0.4 wt% char at 5 wt% H_2O (1.55 MPa), and 1.5 wt% char for feedstock with no water. Less char was produced with more water in the feedstock mixture; apparently water molecules act as a solvent or a diluent, suppressing higher-order reactions for the formation of polyaromatic hydrocarbons, which are the precursors of char. The role of water as a solvent was confirmed in a previous study on SWL of PP (Chen et al., 2019). More importantly, the carbon number distribution and the chemical composition of the oils from model PE, Figure 5.2(c), or PP, Figure 5.2(d), were unaffected by the water content or the operating pressure. The results of Figure 5.2 on oil and gas yields and the chemical compositions of the reaction products indicate that the reaction pathways of PE and PP in LP-HTP (<23 MPa) are similar to those in SWL (23 MPa). Detailed reaction pathways of PE and PP in LP-HTP are discussed in the next section.

LP-HTP at a low pressure of 1.55 MPa is more economical than SWL for small-scale and industrial-scale applications, since one can save 90% of the capital costs and 80% of the energy, Table B.2 (Fivga & Dimitriou, 2018; Gracida-Alvarez, Winjobi, Sacramento-Rivero, & Shonnard, 2019; Zhu et al., 2014). Furthermore, this method with 5 wt% water in the feed mixture produced little char (<0.5 wt%), which is important for reducing maintenance costs for commercial production. For these reasons, the rest of the study was focused on the experiments with 5 wt% water, which were tested further for processing polyolefin mixtures with various PE/PP ratios.

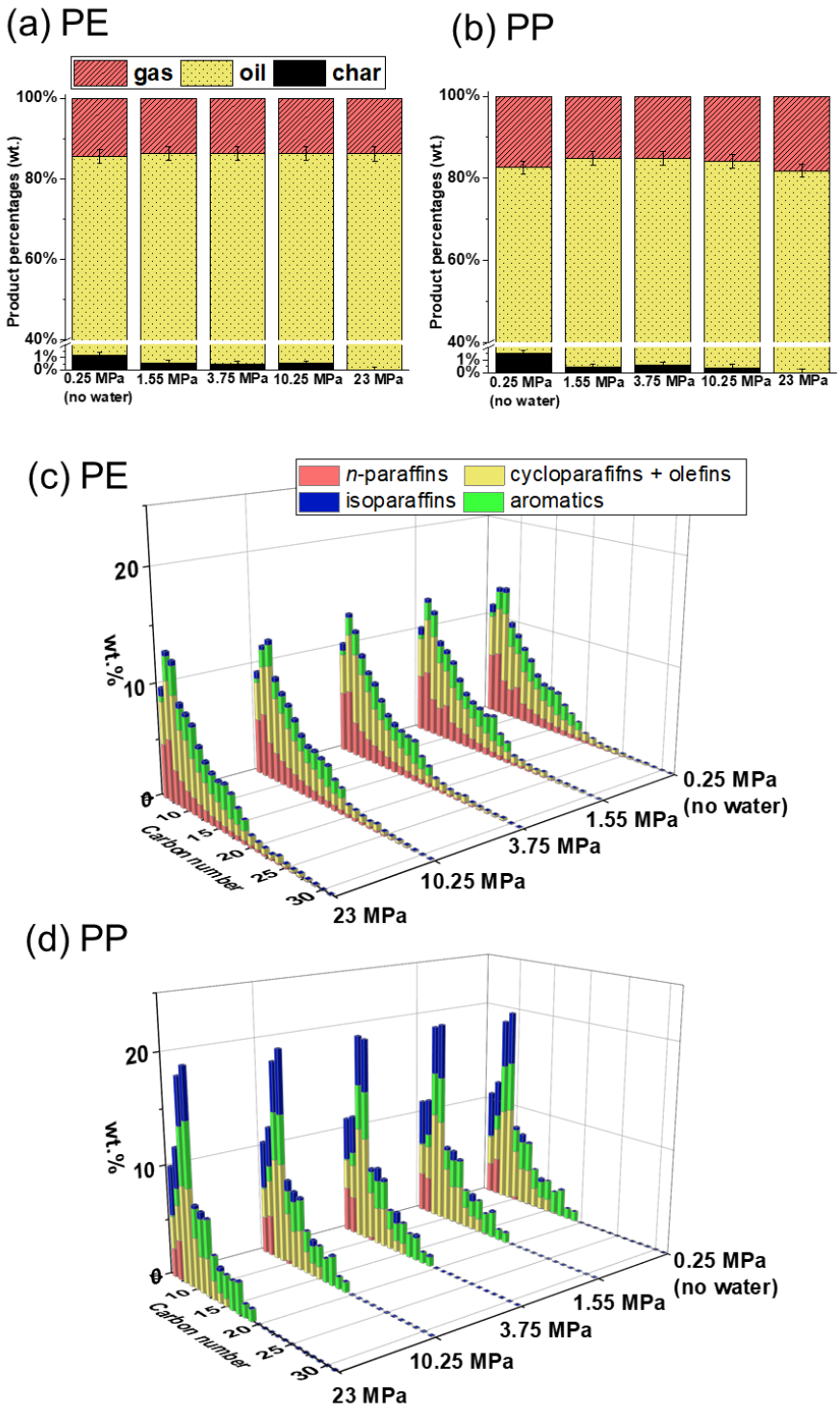

Figure 5. 2 Product yields and chemical compositions. Yields of solid, oil, and gas products at 450 °C, 1 hr reaction time, and different pressures from (a) model PE and (b) model PP. Chemical compositions of the oils produced from (c) model PE and (d) model PP (see Tables B.3 and B.4 for more details).

5.3.2 Individual reaction pathways of PE and PP in LP-HTP

The reaction pathways of PE and PP in LP-HTP, summarized in Figure 5.3, are developed based on detailed analysis of the products at different reaction times. Since the C-C bonds in the polymer chain have a lower energy (348 kJ/mol) than the C-H bonds (413 kJ/mol), the depolymerization of PE and PP is initiated primarily by breaking the C-C-bonds to start forming oligomers (Reaction A). The PE oligomers are further converted into olefins and *n*-paraffins via β-scission (Reaction B) and hydrogen abstraction (Reaction C), respectively (shown in green arrows). For PP oligomers, the reactions can occur in two ways (shown in blue arrows): by breaking the C-C bonds of the main chain and by breaking the C-CH_3 bonds (335 kJ/mol) of the branches. Breaking the C-C bonds, followed by β-scission (Reaction B) or hydrogen abstraction (Reaction C), generates olefins and isoparaffins, respectively. Breaking the C-CH_3 bonds followed by β-scission (Reaction B) generates only olefins. Since the C-CH_3 bonds have a lower bond energy than the C-C bonds, Reaction B is more favored. For this reason, PP depolymerization generates more olefins than isoparaffins.

For both PE and PP (shown in yellow arrows), the olefins are converted into cycloparaffins via cyclization (Reaction D), which are further dehydrogenated into single-ring aromatics (Reaction E), and then polycyclic aromatics (Reaction F). Some minor char formation was observed; it was caused apparently by further dehydrogenation of polycyclic aromatics. A small fraction of *n*-paraffins from PE depolymerization is converted into isoparaffins via isomerization (Reaction G). Similarly, in PP depolymerization, a small fraction of short *n*-paraffins (C_{6-7}) is produced from the isoparaffins (Reaction H). Gases are generated from further cracking of short *n*-paraffins, isoparaffins, and olefins (Reaction I).

As shown in Figure 5.4, increasing temperature from 425 to 450 °C resulted in a similar oil composition in a shorter time, indicating that the reactions in this temperature range follow the same pathways, while the reaction rates are higher at higher temperatures. The results of the individual reaction pathways indicated that the conditions of 450 °C, 45 min, and 1-23 MPa can achieve the highest oil yields with minimal char for conversion of both PE and PP.

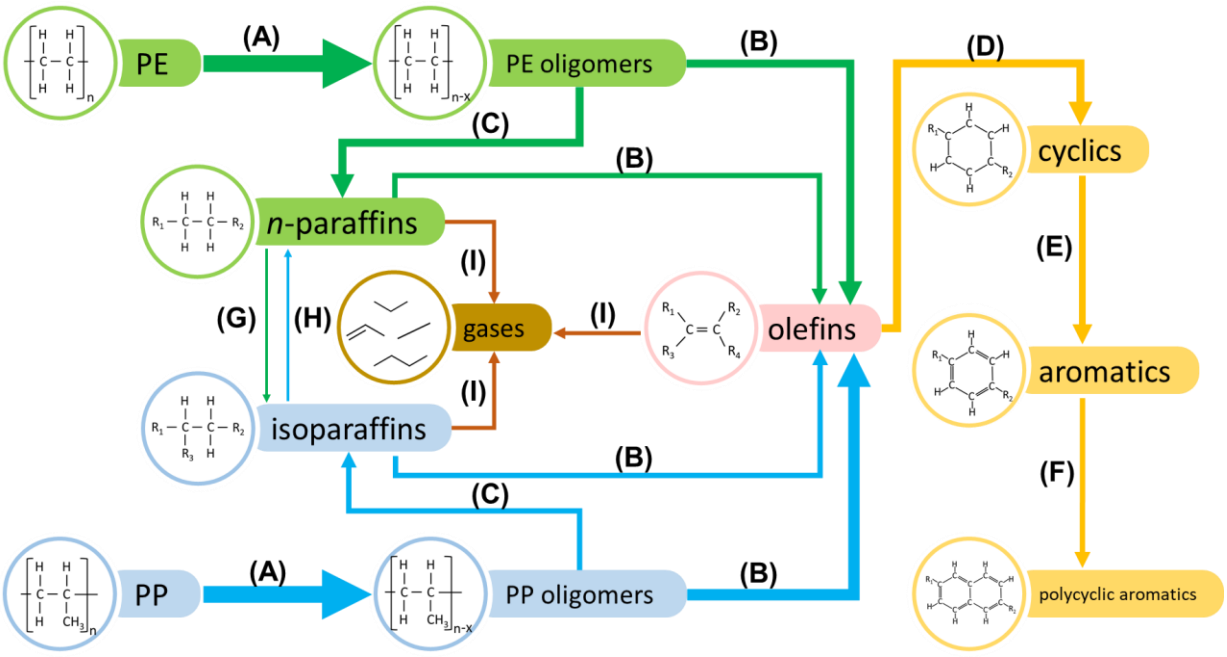

Figure 5. 3 Reaction pathways of PE and PP under LP-HTP. (A) Depolymerization, (B) β-scission, (C) hydrogen abstraction, (D) cyclization, (E) dehydrogenation, (F) formation of polycyclic aromatic hydrocarbon, (G) isomerization, (H) formation of short n-paraffins (C_{6-7}), (I) further cracking to gases. The thickness of the arrows indicates the relative amounts of products.

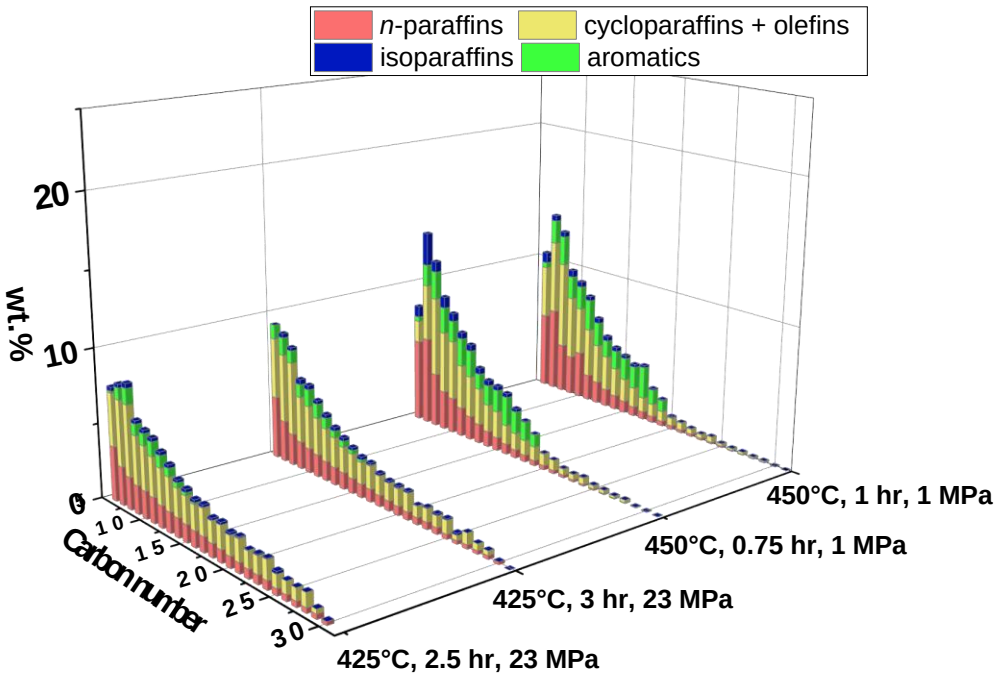

Figure 5. 4 Chemical compositions of oils obtained from model PE at 425-450 °C, 0.75-3 hr, and 1.55-23 MPa.

5.3.3 Reaction pathways of PE and PP mixtures in LP-HTP

Since most of the polyolefin wastes are mixtures of PE and PP, processing them together can reduce the feedstock cost. We examined the pathways of polyolefin mixtures with various weight ratios in LP-HTP. In Section 3.1, 60 min experiments were done to explore the effects of pressure. Figure 5.4 shows that at 450 °C, the oil compositions at 45 min and 60 min were similar. However, the oil yields at 45 min were higher than those at 60 min. For these reasons, subsequent experiments were conducted at 1.55 MPa, 450 °C, and 45 min. The feedstocks included PE and PP mixtures with the PE/PP ratios of 1:3, 1:1, and 3:1. The yields of gas (11-13 wt%), oil (86-87 wt%), and char (0.2-0.5 wt%) were similar for the model polyolefin mixtures with various PE/PP ratios, Figure 5.5(a).

The gas products consisted of C_1-C_6 hydrocarbons, Figure B.2. The chemical compositions of the oils from different feedstocks are shown in Figure 5.5(b). PP has C-CH_3 branches, which prefers to form isoparaffins, while PE requires isomerization of *n*-paraffins to form isoparaffins. For this reason, as PE in the feedstock increased from 0 to 100 wt%, the isoparaffin fraction (shown in blue) decreased. The aromatic fraction (shown in green) also decreased apparently because less olefins were generated in PE depolymerization, while the fractions of the reaction intermediates, olefins and cycloparaffins, decreased slightly. More olefins are generated in PP depolymerization because breaking the C-CH_3 bonds generated olefins, as mentioned in Section 3.2 and Figure 5.3. The pathways for the formation of olefins and gases were different for PP and PE, but the overall conversion rates were similar.

The fractions of the various types of hydrocarbons (*n*-paraffins, isoparaffins, olefins and cycloparaffins, and aromatics) are plotted versus the PE fraction in the feedstock, Figure 5.5(c). The four linear lines indicate that the pathways of PE and PP in the various mixtures are independent. Thus, the overall reaction pathways shown in Figure 5.3 are applicable for processing of polyolefin mixtures.

The reaction pathways were further validated using a 1:1 PE/PP waste mixture. The oil yield was lower for the waste mixture, which contained 6 wt% inorganic additives, primarily $CaCO_3$, $MgCO_3$, and TiO_2, as determined by EDS analysis, Table B.5 and Figure B.3. The oil yield based on the polymer content of the waste was similar to that of the model polyolefin mixture with the same PE/PP ratio. The chemical compositions and the carbon number distribution of the

oil from the waste mixture were also similar to those of the model polyolefin mixture. The presence of organic and inorganic additives apparently did not affect the reaction pathways.

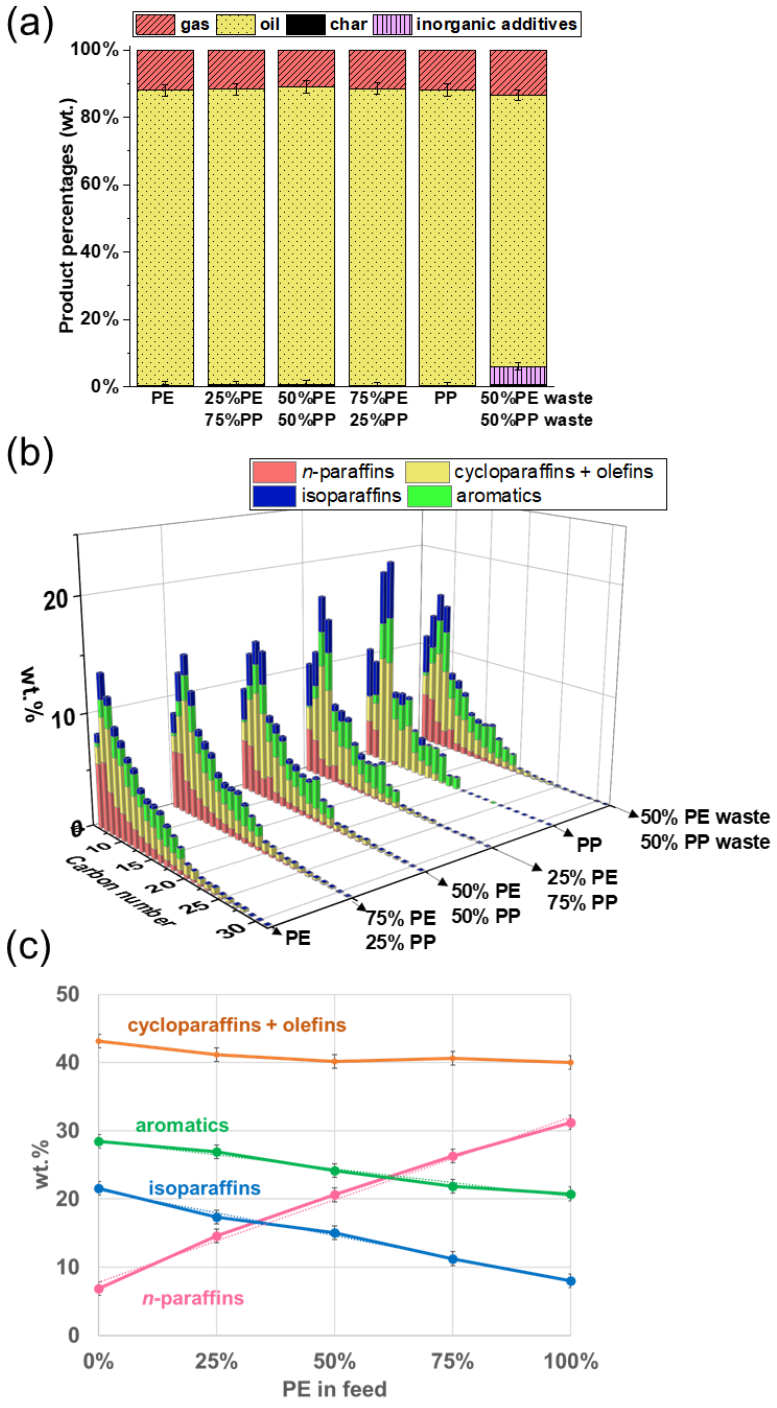

Figure 5. 5 Product yields and chemical compositions. (a) Yields of gas, oil, char, and inorganic additives, (b) oil chemical compositions of PE, PP, and PE/PP mixtures at 450 °C, 45 min, and 1.55 MPa, and (c) weight fractions of oil hydrocarbon classes versus PE weight fraction in feedstock.

5.3.4 Evaluation of the LP-HTP fractions from the oils derived from sorted PE and PP

The results of the pathways studies of PE and PP showed that among all the conditions tested, LP-HTP at 1.55 MPa, 450 ºC, and 45 min gave the highest oil yields with little char formation (< 0.5 wt%). The carbon number distribution and the chemical composition of the PE oil derived from LP-HTP were similar to those of the PE oil derived from SWL at 23 MPa, Figure 5.4. The PE oil from SWL was separated with distillation into two fractions. The heavy fraction was shown to have similar properties as No. 1 ultra-low sulfur diesel (Jin et al., 2020). The light fraction was low in isoparaffins and was qualified as a gasoline blendstock (Jin et al., 2020). Since the PE oils from LP-HTP had similar compositions as those from SWL, the distillation and the fuel property analyses were not repeated here.

In our previous study, PP was converted with SWL into naphtha-rich oils, which were not distilled into fractions or evaluated for fuel applications (Chen et al., 2019). Here, the LP-HTP PP oil obtained at 1.55 MPa, 450 ºC, and 45 min was separated with distillation to two fractions, which were evaluated as commercial gasoline and diesel fuels, respectively. The PP oil consisted of 64 wt% gasoline, 35 wt% diesel, and less than 1 wt% heavy oil, Figure B.4.

Since the gasoline fraction was obtained via distillation, the PP gasoline fraction, as expected, had a carbon number distribution similar to the average distribution of two commercial gasoline samples (see Methods). It had lower aromatic content and thus higher calorific value than the commercial gasoline, Figure 5.6(a). The PP diesel fraction had the same carbon number range (C_8-C_{25}) compared to commercial diesel but the distribution was centered at $C_{12,}$ instead of C_{15}.

The fuel properties of PP gasoline and diesel fractions were evaluated and compared with commercial fuels in Figure 5.6(c) and Figure 5.6(d), respectively. The most important properties for gasoline and diesel are the octane number and cetane number (CN), respectively. The anti-knocking index (AKI) is the average of the research octane number and the motor octane number. The AKI and CN are related to the chemical compositions; *n*-paraffins contribute to a high CN but a low AKI, whereas isoparaffins contribute to a high AKI but a low CN. As the PP oil was rich in isoparaffins, the AKI of the gasoline fraction (98) exceeded the ASTM requirement of 87, and the CN of the diesel fraction only met the minimum CN requirement (40). The PP gasoline and diesel fractions met all the other ASTM property requirements.

5.3.5 Evaluation of the LP-HTP fractions from the oils derived from mixed polyolefins

The oils derived from sorted PE were rich in *n*-paraffins. The heavy fraction from distillation qualified as high-quality diesel, but the light fraction, which was short of isoparaffins, could only qualify as gasoline blendstock. By contrast, the oils derived from sorted PP were rich in isoparaffins. The light fraction qualified as high-quality gasoline, and the heavy fraction qualified as marginal-quality diesel. The depolymerization pathways of PE and PP are independent, while the overall conversion rates in LP-HTP are similar. Therefore, co-processing of mixed polyolefins under the optimal conditions was expected to produce oils with a carbon number distribution in the C_4 to C_{25} range and rich in both *n*-paraffins and isoparaffins.

Mixed polyolefins with PP content from 25 to 75 wt% were converted to oils at 1.55 MPa, 450 °C, and 45 min. The oils were distilled into two fractions. As the PP wt% in the feedstock increased, the gasoline fraction increased from 49 to 58 wt%, and the diesel fraction decreased from 51 to 42 wt%. The gasoline and diesel fractions from the waste mixture were similar to those from model polyolefins with the same PP content. The details of the oil chemical compositions are shown in Figure B.4.

The carbon number distributions of the gasoline fractions from mixed polyolefins were similar to that of commercial gasoline, Figure 5.6(a). The numerical values can be found in Table B.6. As PP content in the feedstock increased, the gasoline fraction had more isoparaffins and a higher AKI, as shown in Figure 5.6(c). All the gasoline fractions derived from a feedstock with 50 wt% or more PP met the ASTM requirement of AKI (≥87). They had a lower aromatic content and a higher hydrogen content than commercial gasoline, and hence a higher gross calorific value. The benzene contents of the gasoline fractions were within the ASTM limit. The density values were similar to those reported by EPA from 1999 to 2019. Furthermore, the gasoline fractions met all other properties required by ASTM D4814 (A. International, 2020), including viscosity, T_{10}, T_{50}, T_{90}, T_{final}, distillation residue, drivability index, and Reid vapor pressure, Figure 5.6(c).

The gasoline fraction from the waste mixture was similar to that from model polyolefins with respect to chemical compositions and physical properties. It also contained little sulfur (7.7 ppm) and lead (0.4 ppm). All gasoline property values are reported in Table B.7. In summary, mixed polyolefins with 50 wt% or more PP can be used to produce clean (low lead, aromatic, benzene, and sulfur contents) gasoline fuels with high AKI and high calorific value.

All diesel fractions derived from mixed model polyolefins met the ASTM requirements for No. 1 diesel, including CN, flash point, viscosity, cloud point, T_{90}, water and sediment content, and sulfur content, Figures. 5.6(b) and 5.6(d). All diesel property values are reported in Tables B.8 and B.9. As the PE content in the feedstock increased, the diesel fraction had more *n*-paraffins and a higher CN. Moreover, the values of aromaticity, hydrogen content, and gross calorific value for the diesel fractions were similar to those of commercial diesel. The diesel fraction from the mixed waste had similar chemical compositions and fuel properties as those from model polyolefins. It also had a low sulfur content (6.5 ppm) and was qualified as No. 1 ultra-low sulfur diesel, which is the highest grade of diesel fuels. In summary, the diesel fractions derived from mixed polyolefins met or exceeded all the fuel properties required by ASTM D975 for No. 1 ultra-low sulfur diesel (ASTM International, 2020). For mixed polyolefins with 50 wt% or more PP, the oils obtained at 450 °C, 45 min, and 1.55 MPa can be separated with distillation into two fractions. The light fractions can be directly utilized as gasoline fuel and the heavy fractions as diesel fuel.

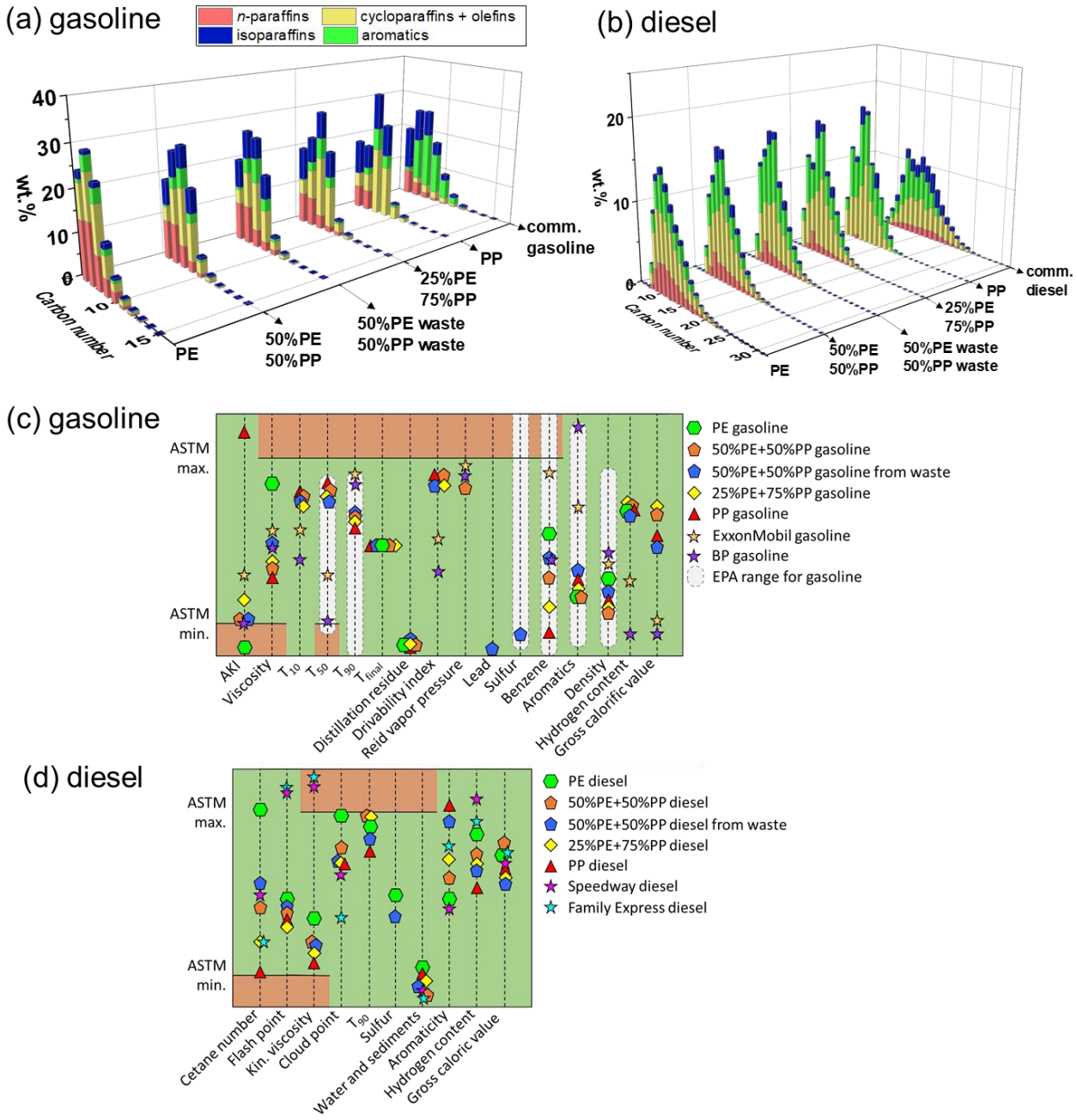

Figure 5. 6 Chemical compositions and fuel properties of the gasoline and diesel products. Chemical compositions of (a) LP-HTP gasoline and commercial gasoline and (b) LP-HTP diesel and commercial diesel. Fuel properties of (c) LP-HTP gasoline and commercial gasoline and (d) LP-HTP diesel and commercial diesel. The reported property values (y-axis) were normalized relative to the ASTM max. and ASTM min. values. The data for PE gasoline and diesel in (c) and (d) were from Jin et al.

5.3.6 Comparison of LP-HTP with other methods

The results of this study indicated the technical feasibility of using LP-HTP for producing useful products from polyolefin waste. Detailed technical and economic analyses, life-cycle analysis, and overall process optimization will be required before applying this method at an industrial scale. Preliminary findings of this study were used to provide crude estimates of energy consumption and GHG emissions of the LP-HTP method for converting polyolefin waste into clean fuels, Figure 5.7. The values are compared to those of the incineration, mechanical recycling, polyolefin synthesis methods, and the methods for producing fuels from crude oil or from pyrolysis followed by upgrading and separations in conventional refineries. It was also assumed that the LP-HTP plant was located near material recycling facilities and the transportation of polyolefin waste to the plant was neglected in the analysis. The scope of this comparison is based on the "cradle-to-gate" model (Benavides, Sun, Han, Dunn, & Wang, 2017; "Carbon emissions of different fuels - Forest Research," n.d.; Han et al., 2015; Lee et al., 2020; Rodrigues et al., 2018). For example, for producing fuels from crude oil, the mining, transporting, distillation, and refining steps are considered. For producing fuels from polyolefin waste, the feedstock collection and preparation, reaction, distillation, and any necessary upgrading steps are considered. The details can be found in Table B.10. Among all methods, the LP-HTP method has the lowest energy consumption. This method is estimated to save 92% and 13% energy compared to producing clean fuels from crude oil and from pyrolysis, respectively. Converting polyolefin waste into fuels with the LP-HTP method requires 90% less energy compared to mechanical recycling of sorted polyolefin waste into polymers.

The GHG emissions of LP-HTP are also the lowest among all the above methods, 71% lower than for producing fuels from crude oil, and 27% lower than pyrolysis, if the processing is done near a material recycling facility. The oils can be easily separated into gasoline and diesel fuels via distillation. Then there is no need for transporting them to refineries for upgrading or separation. The mechanical recycling method results in eight times higher GHG emissions compared to the LP-HTP method because of the high energy used in drying, molding, and other processes. The incineration method also has high GHG emissions because the polyolefin waste is converted to CO_2. Overall, LP-HTP is potentially more energy-efficient and environmental-friendly than incineration, mechanical recycling, producing fuels from crude oil, or from pyrolysis.

It has the potential to convert 220 million tons of global polyolefin waste into 190 million tons of clean fuels and save 1.5 billion barrels of crude-oil-equivalent energy annually.

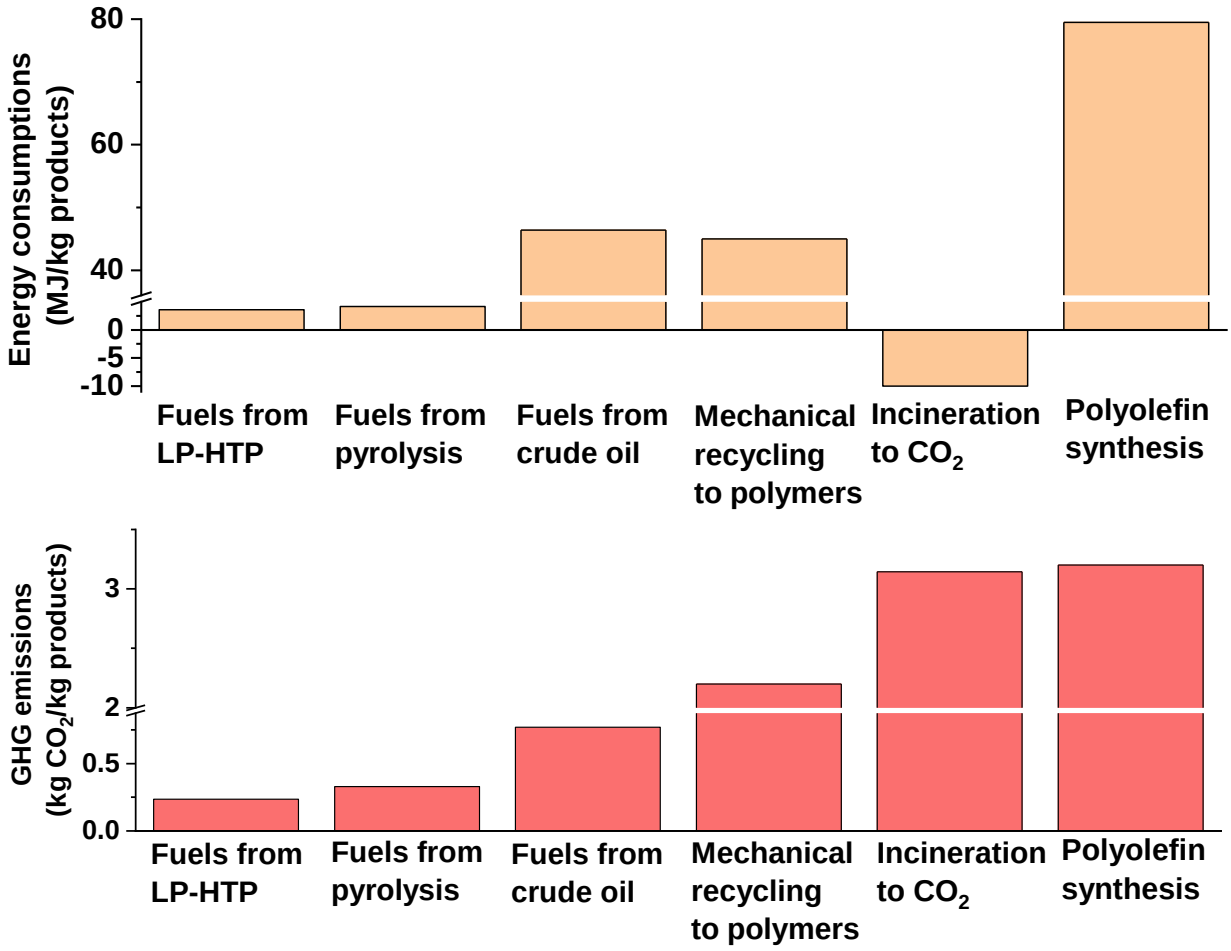

Figure 5. 7 Estimated energy consumption and GHG emissions. (a) Energy consumption and (b) GHG emissions of LP-HTP, producing fuels from pyrolysis and from crude oil, mechanical recycling, incineration, and polyolefin synthesis.

5.4 Conclusions

The new low-pressure hydrothermal processing (LP-HTP) method requires an order-of-magnitude lower pressure and less water than the SWL method for converting polyolefin waste into clean oils. This method requires 90% lower capital costs and 80% less energy compared to SWL. This study shows that LP-HTP can produce oils with C_4-C_{25} hydrocarbons with high yields (87%) and little char (<0.5%). The oils can be distilled into two fractions. The heavy fraction from PE oil was qualified as No. 1 ultra-low sulfur diesel but the light fraction as gasoline blendstock

only. The light fraction from PP oil was qualified as high-quality gasoline but the heavy fraction as marginal-quality diesel.

Although depolymerization of PE and PP in LP-HTP follows different pathways, the overall conversion rates are similar. For this reason, co-processing of PE and PP improves the fuel qualities of both fractions. For oils derived from mixtures with 50 wt% or more PP, the light fraction meets all the requirements for high-quality clean gasoline, and the heavy fraction for high cetane number, No. 1 ultra-low sulfur diesel. The energy requirements and GHG emissions of the LP-HTP method are only 8% of those for producing fuels from crude oil.

Overall, this method is a robust, flexible, energy-efficient, and environmental-friendly method for reducing the polyolefin waste accumulation in the environment. It can potentially convert 220 million tons of polyolefin waste annually to 190 million tons of fuels with energy savings equivalent to 1.5 billion barrels of crude oil. The oils can also be processed in refineries to produce monomers to help achieve a circular hydrocarbon economy, Figure 5.1. Transforming polyolefin waste into valuable, useful products will create a driving force to reduce the plastic waste accumulation, and also reduce associated risks to human health and the environment.

CHAPTER 6 CONCLUSION

6.1 Conclusions of PE conversion via SWL

HTP is a versatile upcycling method, which can convert post-consumer PE waste into fuels, waxes, gases, and monomers. In our study, we investigated multiple reaction conditions and the complete reaction pathways were developed based on detailed chemical composition analyses of reaction products at different reaction time. Optimal reaction conditions were identified and used to convert actual PE waste. Valuable products including ultra-low sulfur gasoline, or diesel fuels, and clean waxes were obtained. No char was found in any condition. The diesel fraction met all requirements for No. 1-D ultra-low sulfur diesel and the gasoline fraction can be used as a gasoline blendstock. Preliminary economic analysis indicated that HTP can be a more profitable process than pyrolysis or producing fuels from crude oil.

6.2 Conclusions of mixed polyolefin conversion via LP-HTP

Low-pressure hydrothermal processing (LP-HTP) was developed for the conversion of mixed polyolefin waste into clean fuels. It requires an order-of-magnitude lower pressure and less water than the SWL method. LP-HTP saves 90% capital costs and 80% energy compared to SWL. In this study, PE and PP were found to follow their individual reaction pathways, while the overall conversion rates are similar. Therefore, the co-processing is practical and improves the product qualities. Mixed polyolefins were converted into oils with high yields (87%) and a range between C_4-C_{25} hydrocarbons. Little char (<0.5%) was observed. Oil products were distilled into two fractions. For oils derived from polyolefin feedstock with 50 wt% or more PP, the light fraction was qualified as high-quality clean gasoline, and the heavy fraction for No. 1 ultra-low sulfur diesel with high cetane number. The evaluations also showed that LP-HTP can save 92% of energy demand and GHG emissions compared to those for producing fuels from crude oil.

LP-HTP is a robust, flexible, energy-efficient, and environmental-friendly method. It has the potential to reduce the polyolefin waste accumulation by converting the waste into clean fuels. If all annually generated polyolefin waste, 220 million tons, are converted using LP-HTP, about 1.5 billion barrels of crude oil equivalent energy can be saved, with associated GHG emissions. The oil products can also be further processed in refineries to achieve a circular economy. The

development of LP-HTP for converting polyolefin waste into useful products can help create a driving force for reducing the plastic waste accumulation and reduce risks to human health and the environment.

6.3 Recommendations

Our work so far has built a solid basis for the development of HTP. Further studies can be started from the following directions:

(1) convert the current lab-scale batch reaction mode into a larger-scale continuous reaction mode;

(2) study further mixed plastic waste such as the mixture of polyolefins and polystyrenes;

(3) improve the current life-cycle analysis and technical economic analysis using a more systematic and detailed approach and assessment.

APPENDIX A. SUPPLEMENTARY MATERIAL FOR CHAPTER 4

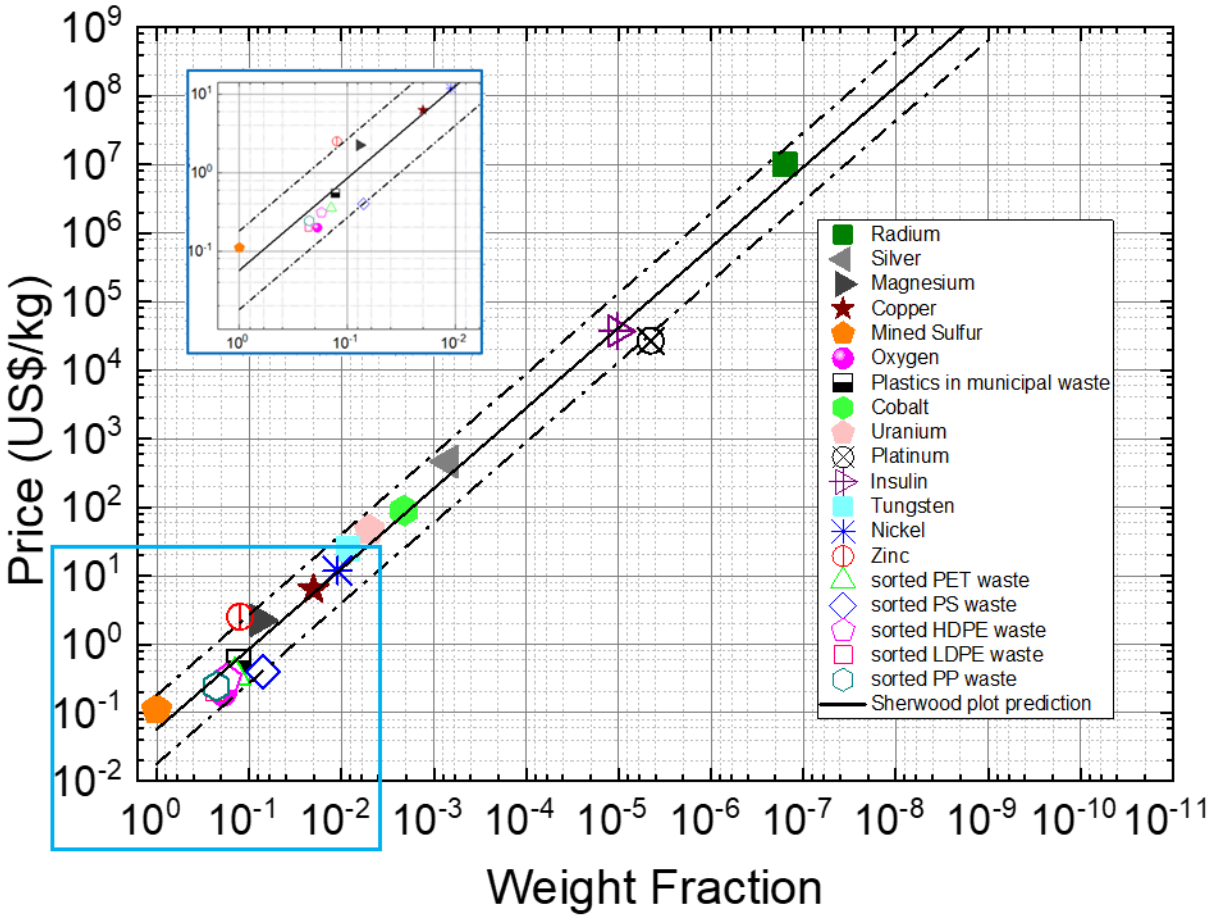

Figure A.1 Sherwood plot of current market prices of metals, sulfur, oxygen, insulin and sorted plastic waste versus their feedstock concentrations.

The market price of a product is usually related to its feedstock cost and manufacturing cost. If its feedstock cost is relatively low, its manufacturing cost is expected to be within an order of magnitude of its market price. The manufacturing cost is generally related to its concentration in the feedstock; the lower the concentration of a target material in its feedstock, the higher the manufacturing cost, and the higher the price. This relation is shown in a log-log plot, known as the Sherwood plot, which shows the relationship between the prices of well-known products (such as metals, sulfur, oxygen, and insulin) and their feedstock concentrations (wt.%) (Dahmus & Gutowski, 2007; Geyer et al., 2017b; "Home of Metals news prices ETFs |," n.d.; "Sort for Value

Online Calculator," n.d.; Sherwood, 1959). The plot is useful for estimating the manufacturing cost of producing a target product from a new feedstock. To test the Sherwood plot for predicting the processing costs for producing various sorted plastic wastes from a representative waste mixture, the current prices of the sorted plastic waste, PET, PS, HDPE, LDPE, and PP (Grübler, 1998) (Johnson, Harper, Lifset, & Graedel, 2007), are plotted versus their respective concentrations in a typical plastic waste in Fig. S1. The results indicate that the prices of the sorted plastic waste are within an order of magnitude equal to the prices predicted by the best-fit Sherwood line in Fig. S1.

The costs for retrieving a kilogram of plastic waste mixtures from a landfill, with an average concentration of plastic waste of about 14 wt. %, was estimated to be about \$0.8/kg, from Fig. S1. Processing the plastic waste into useful products will incur additional costs. Since virgin plastics are currently produced from crude oil at a lower cost, it would not be economical to retrieve plastic waste from landfills.

The oceans are expected to have more plastics than fish by 2050 (PlasticsEurope, 2AD). Once the waste gets into the oceans, it is irreversible because the cost of cleaning the oceans is enormous. The prices of the state-of-the-art separation technologies for removing microplastics and toxic chemicals from water are about \$0.003 per gallon (Mihelcic et al., 2017; Tiemann, 2010). The oceans have 3.5×10^{20} gallons of water. To restore the oceans to the pristine state would cost about $\$10^{18}$, or 10,000 times the global GDP, which is clearly unaffordable. If the current trend continues, the costs for protecting the environment from further damage by plastic pollution would become increasingly beyond reach.

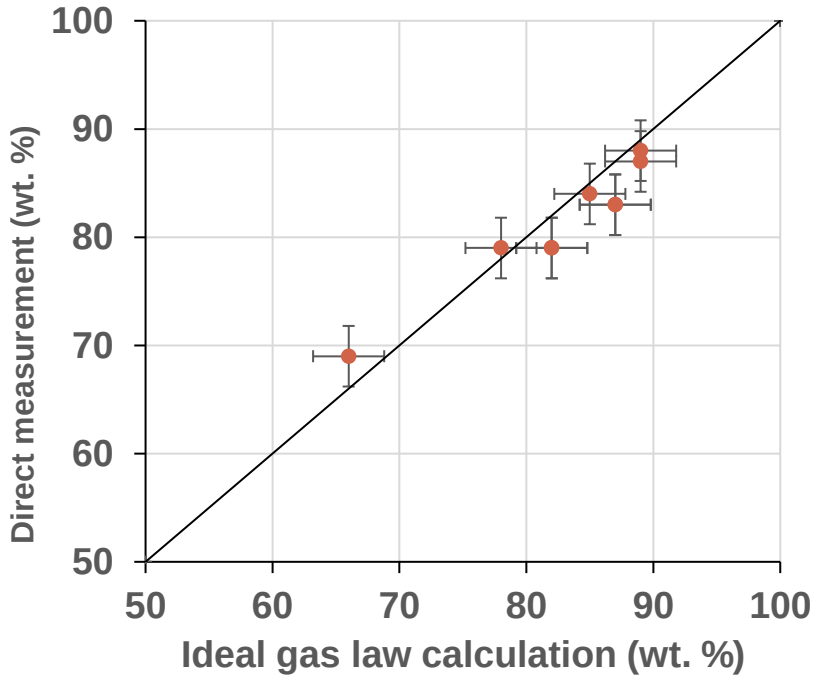

Figure A.2 Comparison of HTP oil yields obtained from two methods: (1) ideal gas law calculations, and (2) measured weights of the collected oil. The oil yields obtained from the two methods are in agreement within experimental error.

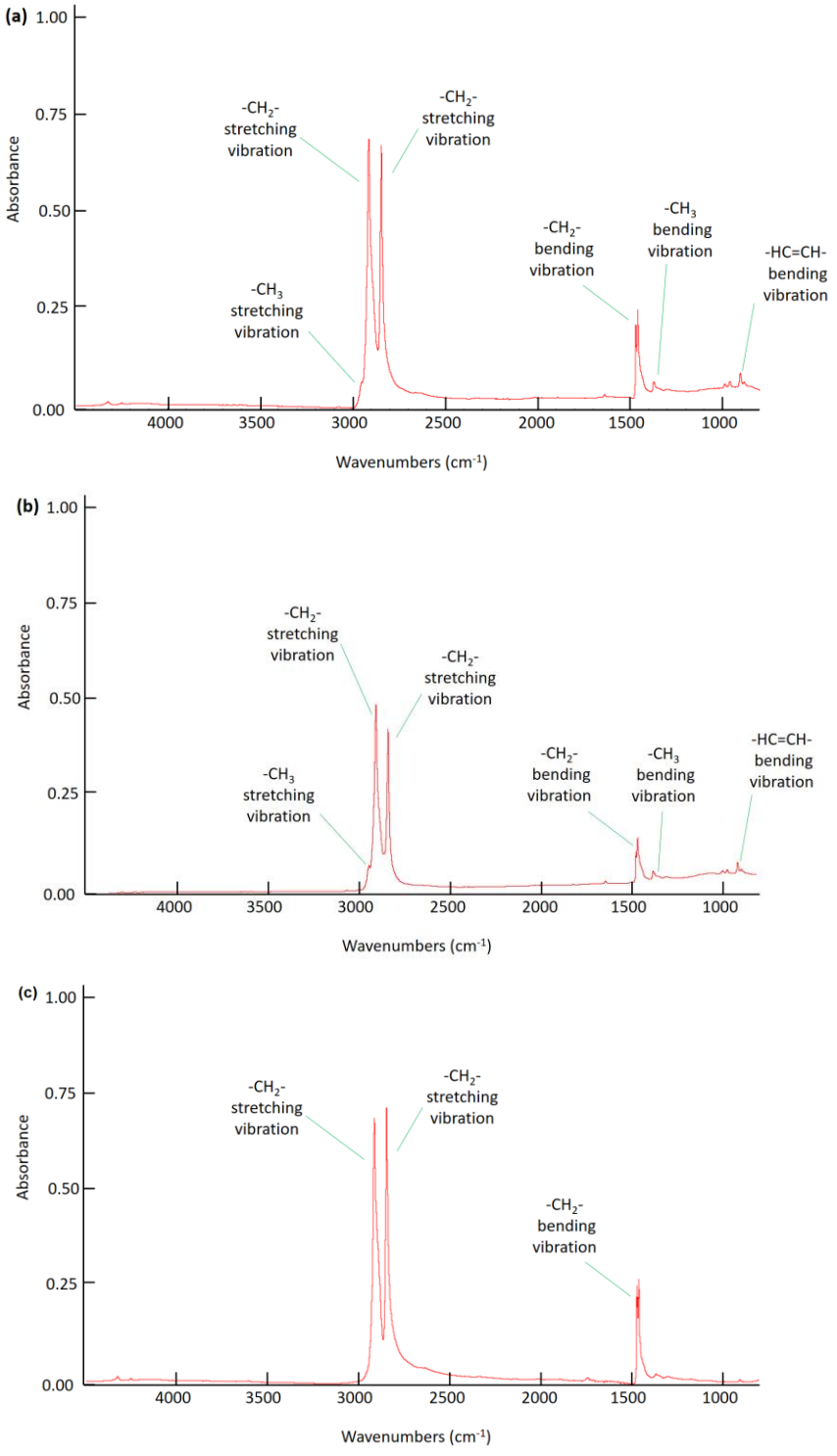

Figure A.3 FTIR analysis of (a) HTP wax produced under 425 °C and 30 min and (b) HTP wax produced under 425 °C and 40 min and (c) model HDPE.

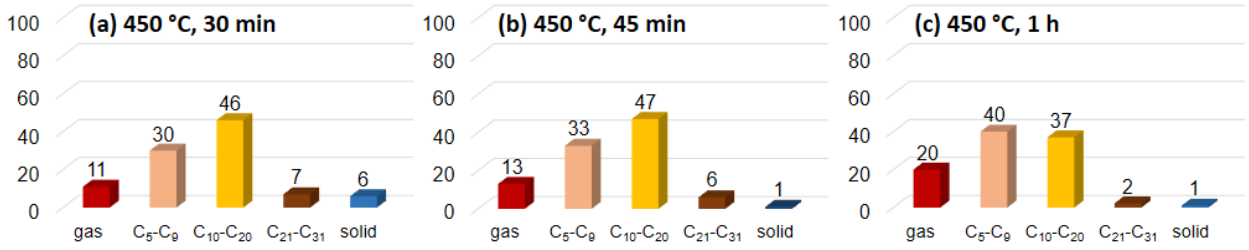

Figure A.4 HTP yields (Y-axis in wt. %) of products obtained from model HDPE at reaction temperatures of 450 °C and reaction time from 30 min to 1 h.

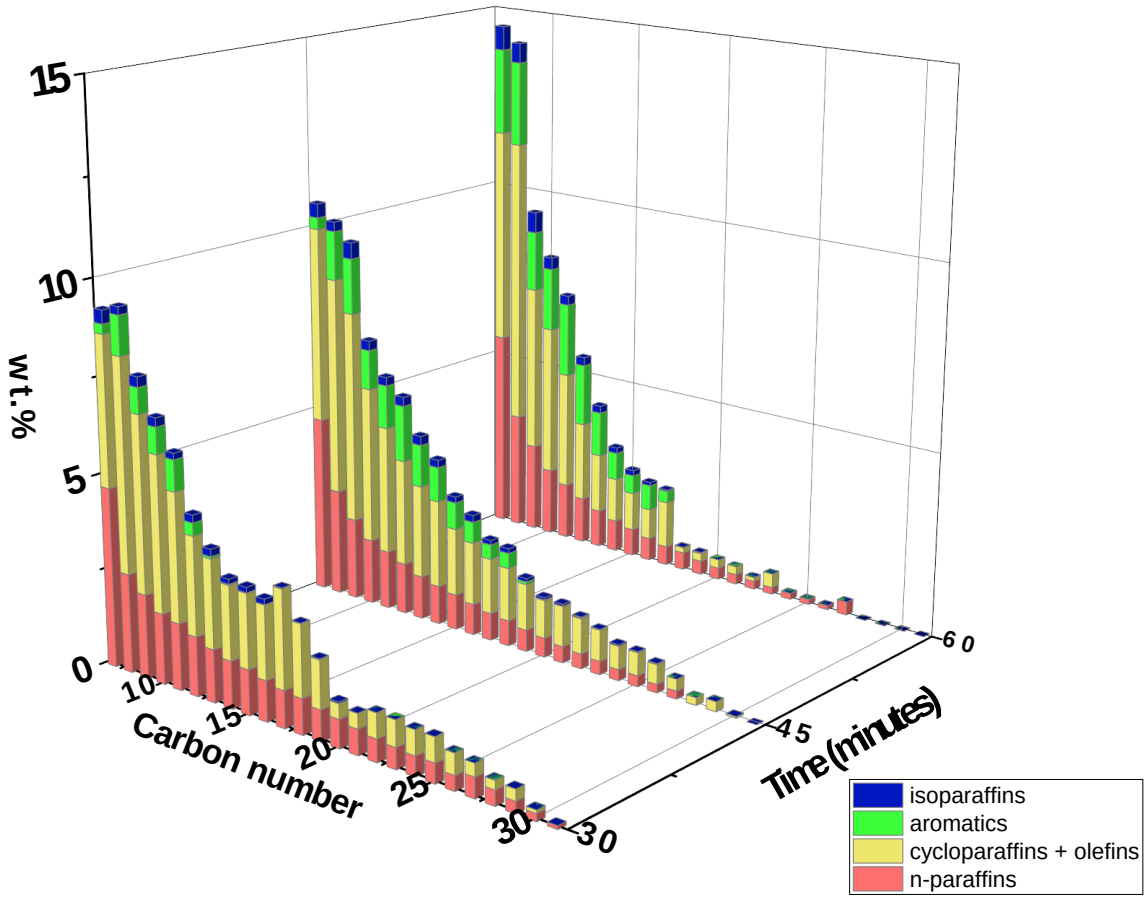

Figure A.5 Carbon number distribution of the HTP oil obtained at a reaction temperature of 450 °C.

Equation S1. Dissociation of HDPE Polymers

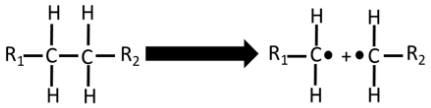

Equation S2. Hydrogen Abstraction

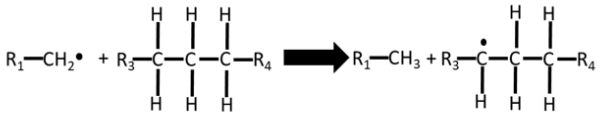

Equation S3. β-scission

Equation S4. Three Steps of Cyclization

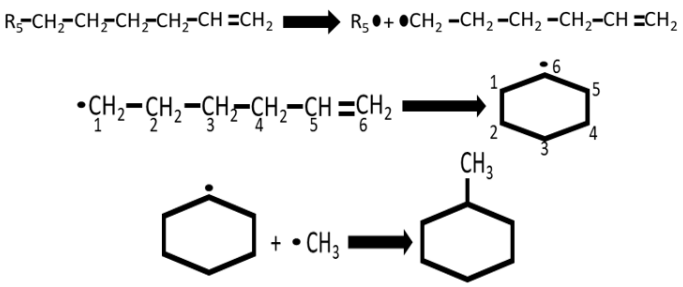

Equation S5. Dehydrogenation

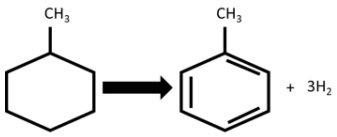

Equation S6. Isomerization

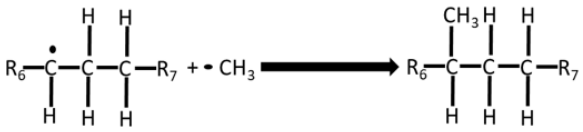

Equation S7. Gas Formations

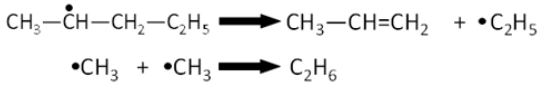

Figure A.6 Detailed reaction description.

The depolymerization of PE is initiated by free radical dissociation. In PE, the bond energy of the C-C bond, 348 kJ/mol, is lower than that of the C-H bond, 413 kJ/mol. Thus, primarily C-C bonds are broken first to generate free radicals (Equation S1). Representative hydrogen abstraction and β-scission are shown in Equation S2 and Equation S3. The produced α-olefins generate free radicals by another dissociation reaction, and the radicals can cyclize, as shown in Equation S4. Alkylbenzenes are generated from cycloparaffins by dehydrogenation, as shown in Equation S5. Multi-ring aromatics are converted from alkylbenzenes via further dehydrogenation (not shown). The small fraction of isoparaffins is produced from n-paraffin radicals, as shown in Equation S6. Gas is formed by the recombination of short free radicals, as shown in Equation S7. The term R_n represents a $(CH_2)_n$ group with n equals 1 to 7.

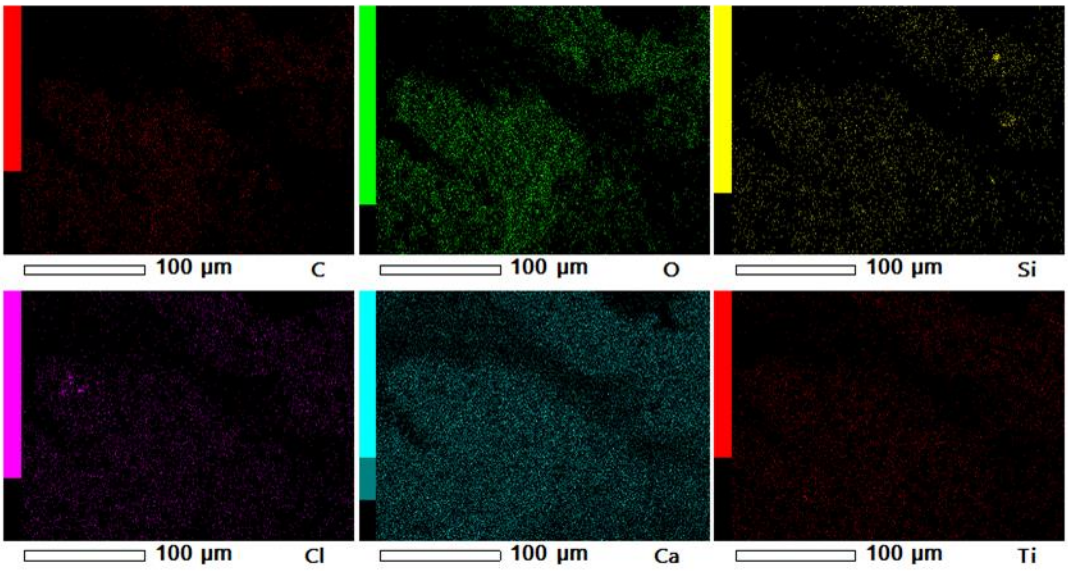

Figure A.7 SEM-EDS plots of the inorganic solid.

Table A.1 Chromatographic conditions for the analysis of HTP gas.

Parameters	Description
Analytical column	FID: Agilent GS Alumina Capillary Column (30 m × 0.53 mm) TCD: Supelco Carboxen 1000 Packed Column
Carrier gas	Helium, constant pressure of 60 kPa
Oven temperature	Linear temperature ramp from 40 °C to 190 ^{0}C at a rate of 10 °C/min, hold at 190 °C for 7 min
Detector	channel 1: flame ionization detector (detection of C_1-C_6 hydrocarbons)

Table A.2 Chromatographic conditions for GC×GC-FID.

Parameter	Description
Analytical column	Primary: DB-17ms Agilent (30 m × 0.25 mm × 0.25 μm) Secondary: DB-1ms Agilent (0.8 m × 0.25 mm × 0.25 μm)
Carrier gas	UHP helium, 1.5 mL/min
Oven temperature	Isothermal 40 °C for 0.2 min, followed by a linear gradient of 3 °C/min to a temperature 260 °C being held isothermally for 20 min
Modulation period	2.5 s with 0.42 s hot pulse time
Offsets	Secondary oven: 50 °C Modulator: 15 °C
Temperatures	Inlet: 280 °C FID: 300 °C

Table A.3 Chromatographic conditions for GC×GC-TOF/MS analyses.

Parameter	Description
Analytical column	Primary: ZB-35HT Phonomenex (60 m × 0.25 mm × 0.25 μm) Secondary: ZB-1HT Phenomenex (1.9 m × 0.25 mm × 0.25 μm)
Carrier gas	UHP helium, 1.25 mL/min
Oven temperature	Isothermal 40 °C for 0.2 min, followed by a linear gradient of 3 °C/min to a temperature 300 °C being held isothermally for 20 min
Modulation period	3.0 s with 0.50 s hot pulse time
Offsets	Secondary oven: 10 °C Modulator: 70 °C
Temperatures	Inlet: 280 °C Transfer line: 300 °C

Table A.4 Element weight fractions in the inorganic solid product from EREMA (425 °C, 2.5 h).

Element	**Weight fractions (ca. wt. %)**
O	53
Ca	31
C	10
Ti	3
Cl	2
Si	1

Table A.5 HTP gas composition for model PE at 425 °C and 2.5 h from GC-FID.

Alkanes	wt. %
C1	4.1
C2	10.7
C3	11.9
C4	3.4
C5	0.9
C6	0.0
Alkenes	wt. %
C2	5.8
C3	38.3
C4	19.3
C5	5.3
C6	0.2

Table A.6 Chemical composition of oil product obtained from HTP of EREMA pellets, HDPE grocery bags, and HDPE milk jugs under reaction temperature of 425 °C and reaction time of 2.5 h

	Model HDPE	**EREMA pellets**	**Grocery bags**	**Milk jugs**
Paraffins				
***n*-paraffins**	wt. %	wt. %	wt. %	wt. %
C5	1.60	1.06	0.90	1.98
C6	2.98	2.57	3.02	3.72
C7	3.83	3.77	5.30	3.88
C8	2.61	2.45	3.31	3.23
C9	2.19	2.10	2.74	2.71
C10	1.92	1.87	2.29	2.32
C11	1.84	1.76	2.03	2.08
C12	1.68	1.59	1.73	1.80
C13	1.47	1.41	1.47	1.45
C14	1.34	1.30	1.20	1.22
C15	1.27	1.24	1.06	1.06
C16	1.16	1.13	0.88	0.89
C17	1.05	1.03	0.74	0.74
C18	0.99	0.98	0.65	0.65
C19	0.88	0.87	0.52	0.55
C20	0.80	0.82	0.46	0.48
C21	0.73	0.75	0.36	0.36
C22	0.65	0.68	0.32	0.37
C23	0.60	0.60	0.26	0.35
C24	0.55	0.60	0.25	0.33
C25	0.55	0.58	0.21	0.34
C26	0.45	0.46	0.19	0.29
C27	0.40	0.41	0.15	0.27
C28	0.41	0.42	0.16	0.29
C29	0.39	0.35	0.14	0.27
C30	0.36	0.37	0.16	0.24
C31	0.29	0.23	0.08	0.18
total *n*-paraffins	**32.96**	**31.44**	**30.58**	**32.05**
Isoparaffins	wt. %	wt. %	wt. %	wt. %
C5	0.45	0.12	0.08	0.41
C6	0.31	0.33	0.27	0.50
C7	1.54	1.61	1.83	2.12
C8	0.00	0.16	0.00	0.00
C9	0.32	0.32	0.55	0.38
C10	0.23	0.32	0.40	0.34
C11	0.26	0.25	0.33	0.28
C12	0.27	0.28	0.33	0.28
C13	0.26	0.28	0.30	0.25
C14	0.25	0.31	0.31	0.24

C15	0.21	0.25	0.23	0.18
C16	0.26	0.27	0.22	0.18
C17	0.18	0.23	0.16	0.13
C18	0.18	0.22	0.13	0.12
C19	0.16	0.17	0.09	0.08
C20	0.15	0.19	0.12	0.10
C21	0.11	0.20	0.07	0.07
C22	0.07	0.12	0.05	0.03
C23	0.08	0.13	0.04	0.05
C24	0.39	0.60	0.18	0.29
total isoparaffins	**5.67**	**6.37**	**5.70**	**6.02**

Cycloparaffins				
Monocycloparaffins	wt. %	wt. %	wt. %	wt. %
C7	2.88	2.91	4.03	5.40
C8	1.23	1.52	2.34	1.90
C9	2.38	2.57	3.61	3.10
C10	2.37	2.43	3.26	3.00
C11	1.97	1.96	2.62	2.47
C12	2.03	2.10	2.48	2.27
C13	1.49	1.58	1.69	1.80
C14	1.85	1.47	1.83	1.57
C15	1.46	1.62	1.55	1.41
C16	1.01	1.52	1.36	1.24
C17	0.92	1.16	0.70	0.66
C18	1.31	1.74	1.15	1.25
C19	1.11	1.11	0.83	0.87
C20	1.36	1.56	1.04	0.92
C21	1.29	1.35	0.68	0.76
C22	1.09	1.10	0.62	0.80
C23	1.14	0.87	0.44	0.64
C24	1.09	1.08	0.59	0.67
C25	1.12	1.02	0.53	0.74
C26	1.09	1.10	0.45	0.81
C27	0.91	0.74	0.31	0.63
C28	1.03	0.63	0.37	0.60
C29	0.97	1.19	0.43	0.82
C30	0.62	0.58	0.21	0.52
total monocycloparaffins	**33.72**	**34.91**	**33.12**	**34.84**

Dicycloparaffins	wt. %	wt. %	wt. %	wt. %
C8	2.76	2.77	3.68	3.63
C9	3.09	3.17	4.67	4.28
C10	1.21	1.28	1.85	1.55
C11	1.23	1.39	1.70	1.40
C12	0.81	0.81	1.16	0.99

C13	1.18	1.07	1.51	1.06
C14	0.75	1.07	1.06	1.06
C15	0.82	0.57	0.74	0.64
C16	1.05	0.55	0.67	0.53
C17	1.03	0.59	0.93	0.72
C18	0.68	0.27	0.39	0.24
C19	0.83	0.42	0.40	0.30
C20	0.28	0.25	0.16	0.22
C21	0.33	0.21	0.27	0.23
C22	0.51	0.29	0.24	0.22
total dicycloparaffins	**16.59**	**14.72**	**19.41**	**17.07**
Tricycloparaffins	wt. %	wt. %	wt. %	wt. %
C10	0.04	0.03	0.05	0.05
C11	0.07	0.05	0.10	0.09
C12	0.03	0.03	0.07	0.05
C13	0.01	0.01	0.04	0.03
C14	0.02	0.02	0.02	0.02
C15	0.02	0.02	0.01	0.02
C16	0.04	0.00	0.00	0.00
C17	0.01	0.01	0.01	0.01
total tricycloparaffins	**0.23**	**0.19**	**0.31**	**0.27**
total cycloparaffins	**50.53**	**49.81**	**52.84**	**52.17**
Aromatics				
Alkylbenzenes	wt. %	wt. %	wt. %	wt. %
C6/benzene	0.12	0.13	0.15	0.15
C7/toluene	0.77	0.73	1.01	1.02
C8	1.08	1.10	1.35	1.34
C9	0.72	0.85	0.94	0.86
C10	0.40	0.51	0.59	0.45
C11	0.18	0.15	0.23	0.20
C12	0.16	0.19	0.20	0.19
C13	0.09	0.11	0.10	0.09
C14	0.08	0.10	0.08	0.07
C15	0.08	0.09	0.06	0.06
C16	0.05	0.06	0.04	0.04
C17	0.06	0.07	0.04	0.04
C18	0.06	0.05	0.04	0.03
C19	0.01	0.00	0.00	0.01
C20	0.03	0.03	0.01	0.02
C21	0.26	0.33	0.06	0.14
total alkylbenzenes	**4.14**	**4.50**	**4.90**	**4.70**
Cycloaromatics	wt. %	wt. %	wt. %	wt. %
C9	0.06	0.06	0.08	0.07

C10	0.44	0.44	0.48	0.50
C11	0.79	0.98	0.86	0.78
C12	0.66	0.86	0.61	0.66
C13	0.49	0.63	0.44	0.48
C14	0.38	0.54	0.39	0.35
C15	0.26	0.45	0.20	0.23
C16	0.12	0.22	0.08	0.08
C17	0.08	0.22	0.06	0.06
C18	0.08	0.10	0.02	0.04
C19+	0.31	0.59	0.10	0.13
total cycloaromatics	**3.67**	**5.09**	**3.32**	**3.39**

Naphthalenes	wt. %	wt. %	wt. %	wt. %
C10	0.03	0.03	0.05	0.03
C11	0.10	0.11	0.16	0.09
C12	0.15	0.14	0.14	0.12
C13	0.12	0.16	0.17	0.12
C14	0.20	0.16	0.17	0.13
C15	0.25	0.22	0.20	0.17
C16	0.19	0.25	0.11	0.17
C17	0.06	0.10	0.03	0.05
C18	0.11	0.14	0.02	0.06
total naphthalenes	**1.21**	**1.32**	**1.05**	**0.94**

Biphenyls	wt. %	wt. %	wt. %	wt. %
C12	0.00	0.00	0.00	0.00
C13	0.02	0.03	0.03	0.01
C14	0.07	0.06	0.08	0.04
C15	0.17	0.10	0.17	0.07
C16	0.19	0.13	0.29	0.11
C17	0.38	0.26	0.35	0.13
C18	0.49	0.34	0.26	0.27
total biphenyls	**1.32**	**0.92**	**1.18**	**0.64**

Anthracenes and Phenanthrenes	wt. %	wt. %	wt. %	wt. %
C14	0.00	0.00	0.00	0.00
C15	0.01	0.01	0.01	0.00
C16	0.03	0.03	0.05	0.02
C17	0.39	0.41	0.22	0.05
total anthra and phena	**0.43**	**0.45**	**0.28**	**0.07**

Pyrenes	wt. %	wt. %	wt. %	wt. %
C16	0.01	0.01	0.02	0.01
C17	0.04	0.02	0.05	0.01
C18	0.02	0.07	0.06	0.00
total pyrenes	**0.07**	**0.10**	**0.14**	**0.01**

total aromatics	**10.83**	**12.38**	**10.88**	**9.75**

Table A.7 Chemical composition of commercial gasoline samples (ExxonMobil, GoLo, Shell) and HTP gasoline obtained at 425 °C and 2.5 h.

	HTP gasoline	**ExxonMobil**	**GoLo**	**Shell**
***n*-paraffins**	wt. %	wt. %	wt. %	wt. %
C5	2.42	17.85	21.10	12.94
C6	7.44	5.71	6.23	5.13
C7	11.42	3.53	2.80	1.94
C8	8.47	1.24	1.23	1.42
C9	5.06	0.54	0.40	0.70
C10	2.69	0.21	0.17	0.38
C11	1.48	0.10	0.09	0.21
C12	0.80	0.06	0.05	0.05
C13	0.42	0.04	0.02	0.02
C14	0.23	0.02	0.01	0.00
C15	0.13	0.01	0.00	0.00
C16	0.08	0.00	0.00	0.00
C17	0.04	0.00	0.00	0.00
C18	0.03	0.00	0.00	0.00
C19	0.01	0.00	0.00	0.00
C20	0.01	0.00	0.00	0.00
total *n*-paraffins	**40.75**	**29.29**	**32.11**	**22.80**
Isoparaffins	wt. %	wt. %	wt. %	wt. %
C5	0.36	1.11	3.58	9.37
C6	1.04	11.89	11.43	9.84
C7	4.81	8.26	6.72	5.18
C8	1.85	6.21	4.88	3.02
C9	1.55	2.41	2.05	2.73
C10	0.72	1.26	1.03	1.64
C11	0.46	0.69	0.69	1.05
C12	0.22	0.56	0.39	0.43
C13	0.13	0.21	0.13	0.13
C14	0.11	0.11	0.05	0.03
C15	0.05	0.02	0.01	0.00
C16	0.03	0.01	0.00	0.00
C17	0.01	0.00	0.00	0.00
C18	0.01	0.00	0.00	0.00
total isoparaffins	**11.35**	**32.73**	**30.94**	**33.42**
Cycloparaffins				
Monocycloparaffins	wt. %	wt. %	wt. %	wt. %
C7	9.13	2.15	1.90	1.99
C8	5.49	1.15	1.16	1.15

C9	4.72	0.86	0.94	1.57
C10	3.05	0.62	0.57	1.11
C11	1.53	0.30	0.28	0.62
C12	0.89	0.14	0.11	0.18
C13	0.48	0.07	0.03	0.03
C14	0.28	0.01	0.00	0.00
C15	0.14	0.00	0.00	0.00
C16	0.08	0.00	0.00	0.00
C17	0.04	0.00	0.00	0.00
C18	0.02	0.00	0.00	0.00
C19	0.01	0.00	0.00	0.00
total monocycloparaffins	**25.85**	**5.31**	**5.00**	**6.64**
Dicycloparaffins	wt. %	wt. %	wt. %	wt. %
C8	4.39	0.18	0.18	0.07
C9	5.35	0.43	0.40	0.66
C10	0.82	0.08	0.12	0.27
C11	0.50	0.05	0.07	0.20
C12	0.21	0.02	0.01	0.04
C13	0.11	0.00	0.00	0.00
C14	0.05	0.00	0.00	0.00
C15	0.02	0.00	0.00	0.00
C16	0.01	0.00	0.00	0.00
total dicycloparaffins	**11.46**	**0.76**	**0.78**	**1.23**
Tricycloparaffins	wt. %	wt. %	wt. %	wt. %
C10	0.01	0.01	0.01	0.00
C11	0.01	0.00	0.00	0.00
total tricycloparaffins	**0.02**	**0.01**	**0.01**	**0.00**
total cycloparaffins	**37.34**	**6.08**	**5.79**	**7.86**
Aromatics				
Alkylbenzenes	wt. %	wt. %	wt. %	wt. %
C6/benzene	0.41	0.91	0.56	0.53
C7/toluene	2.76	6.95	6.85	7.22
C8	3.27	8.84	9.64	10.39
C9	1.68	7.34	7.18	8.85
C10	0.66	2.75	2.66	3.52
C11	0.17	0.80	0.68	0.83
C12	0.12	0.24	0.15	0.18
C13	0.03	0.04	0.02	0.02
C14	0.02	0.00	0.00	0.00
C15	0.01	0.00	0.00	0.00
total alkylbenzenes	**9.12**	**27.88**	**27.73**	**31.54**
Cycloaromatics	wt. %	wt. %	wt. %	wt. %

C9	0.08	0.31	0.28	0.35
C10	0.32	1.49	0.98	1.74
C11	0.48	0.95	1.18	1.15
C12	0.22	0.28	0.16	0.19
C13	0.11	0.03	0.02	0.02
C14	0.05	0.00	0.00	0.00
C15	0.01	0.00	0.00	0.00
total cycloaromatics	**1.28**	**3.06**	**2.63**	**3.46**

Naphthalenes	wt. %	wt. %	wt. %	wt. %
C10	0.02	0.28	0.22	0.24
C11	0.05	0.44	0.29	0.35
C12	0.04	0.14	0.14	0.17
C13	0.02	0.04	0.05	0.06
C14	0.01	0.01	0.01	0.02
total naphthalenes	**0.14**	**0.91**	**0.73**	**0.85**

Biphenyls	wt. %	wt. %	wt. %	wt. %
C12	0.00	0.00	0.00	0.00
C13	0.00	0.01	0.01	0.02
C14	0.01	0.01	0.02	0.03
C15	0.01	0.01	0.02	0.02
total biphenyls	**0.02**	**0.04**	**0.06**	**0.07**
total aromatics	**10.55**	**31.89**	**31.15**	**35.92**

Table A.8 Chemical composition of commercial diesel samples (Family Express – 2 samples, Meijer, Marathon, Speedway), HTP diesel, a mixture of Speedway diesel with 10 vol. % of HTP diesel (HTP-10D), and a mixture of Speedway diesel with 50 vol. % of HTP diesel (HTP-50D).

	HTP diesel	**Fam. Exp. #1**	**Meijer**	**Fam. Exp. #2**	**Marathon**	**Speedway**
Paraffins						
***n*-paraffins**	wt. %	wt. %	wt. %	wt. %	wt. %	wt. %
C7	0.25	0.10	0.12	0.08	0.17	0.13
C8	1.18	0.14	0.16	0.10	0.35	0.22
C9	2.66	0.54	0.18	0.55	0.56	0.30
C10	3.59	0.69	0.28	0.77	0.91	0.61
C11	4.06	0.86	0.58	0.90	1.51	1.12
C12	4.05	0.90	0.88	0.87	1.59	1.34
C13	3.68	1.02	1.08	0.93	1.72	1.43
C14	3.16	1.26	1.16	1.01	1.68	1.25
C15	2.70	1.40	1.38	1.34	1.94	1.40
C16	2.08	1.24	1.12	1.33	1.77	1.31
C17	1.53	1.24	1.77	1.39	1.57	1.27
C18	1.23	0.98	1.53	1.23	1.48	1.14
C19	0.77	0.90	1.35	0.84	1.10	0.91
C20	0.54	0.54	0.91	0.57	0.80	0.71
C21	0.36	0.38	0.83	0.43	0.60	0.63
C22	0.25	0.19	0.52	0.21	0.31	0.36
C23	0.15	0.08	0.29	0.10	0.15	0.22
C24	0.11	0.04	0.12	0.04	0.07	0.11
C25	0.07	0.02	0.05	0.01	0.03	0.04
C26	0.05	0.00	0.01	0.00	0.01	0.02
C27	0.03	0.00	0.00	0.00	0.00	0.00
C28	0.02	0.00	0.00	0.00	0.00	0.00
C29	0.01	0.00	0.00	0.00	0.00	0.00
total	**32.55**	**12.53**	**14.32**	**12.71**	**18.31**	**14.53**
Isoparaffins	wt. %	wt. %	wt. %	wt. %	wt. %	wt. %
C7	0.12	0.11	0.13	0.09	0.14	0.13
C8	0.18	0.12	0.13	0.08	0.25	0.18
C9	0.68	0.60	0.43	0.57	0.72	0.54
C10	0.66	0.83	0.49	0.90	1.14	0.81
C11	0.79	0.89	0.87	0.97	1.78	1.17
C12	0.90	0.90	1.12	0.91	2.18	1.59
C13	0.95	1.37	1.86	1.25	2.89	2.42
C14	0.96	1.36	2.10	1.25	2.82	2.09

C15	0.73	2.00	2.04	1.89	3.22	2.39
C16	0.63	1.85	2.24	1.99	3.56	2.64
C17	0.48	2.59	3.21	2.59	4.14	2.98
C18	0.31	2.39	3.06	2.54	3.31	2.61
C19	0.19	2.11	3.49	2.40	3.24	2.64
C20	0.12	1.37	3.00	1.63	3.22	2.35
C21	0.07	0.74	1.87	0.79	1.45	1.32
C22	0.02	0.31	1.01	0.41	0.99	0.95
C23	0.00	0.09	0.85	0.12	0.33	0.64
C24	0.00	0.00	0.29	0.00	0.06	0.23
total	**7.79**	**19.65**	**28.22**	**20.38**	**35.42**	**27.67**

Cycloparaffins						
Mono-	wt. %	wt. %	wt. %	wt. %	wt. %	wt. %
C7	0.29	0.14	0.19	0.10	0.21	0.20
C8	1.49	0.25	0.29	0.18	0.41	0.35
C9	2.92	0.56	0.59	0.56	0.68	0.63
C10	4.02	1.01	1.10	1.05	1.48	1.32
C11	4.26	1.33	1.68	1.33	2.24	2.20
C12	4.25	1.71	2.07	1.49	2.64	2.80
C13	4.12	1.52	2.33	1.49	2.90	3.00
C14	3.25	2.35	2.44	2.26	2.85	3.50
C15	2.82	2.69	3.03	2.56	3.19	2.65
C16	2.24	1.86	2.48	2.04	1.88	2.48
C17	1.63	2.67	3.56	3.04	2.20	3.04
C18	1.40	2.19	3.76	2.43	2.06	2.80
C19	0.77	2.17	2.63	2.06	1.60	2.20
C20	0.36	1.70	2.80	1.80	0.93	2.38
C21	0.27	0.79	1.64	0.83	0.74	1.06
C22	0.06	0.16	1.10	0.37	0.18	0.59
C23	0.04	0.00	0.45	0.02	0.03	0.30
C24	0.03	0.00	0.09	0.00	0.00	0.03
total	**34.20**	**23.08**	**32.23**	**23.63**	**26.24**	**31.52**

Di- + Tri-	wt. %	wt. %	wt. %	wt. %	wt. %	wt. %
C8	0.17	0.00	0.00	0.00	0.00	0.00
C9	1.41	0.06	0.07	0.05	0.12	0.08
C10	1.15	0.30	0.38	0.19	0.32	0.38
C11	1.30	1.43	0.95	0.86	0.80	1.03
C12	1.03	2.30	1.00	1.66	0.91	1.37
C13	0.70	2.22	0.81	1.65	0.70	1.00

C14	0.96	1.47	0.37	0.76	0.37	0.64
C15	0.42	0.54	0.19	0.20	0.14	0.27
C16	0.15	0.18	0.12	0.12	0.06	0.11
C17	0.08	0.00	0.00	0.00	0.00	0.00
C18	0.00	0.00	0.00	0.00	0.00	0.00
C19	0.01	0.00	0.00	0.00	0.00	0.00
C20	0.00	0.00	0.00	0.00	0.00	0.00
C21	0.03	0.00	0.00	0.00	0.00	0.00
total	**7.40**	**9.51**	**3.89**	**5.50**	**3.42**	**4.87**
total cycloparaffins	**41.60**	**32.59**	**36.12**	**29.13**	**29.66**	**36.39**

Aromatics						
Alkylbenzenes	wt. %	wt. %	wt. %	wt. %	wt. %	wt. %
C6/benzene	0.00	0.00	0.01	0.00	0.00	0.01
C7/toluene	0.16	0.06	0.11	0.05	0.09	0.10
C8	1.11	0.33	0.39	0.27	0.34	0.37
C9	1.64	0.84	0.84	0.78	0.79	0.90
C10	1.24	0.86	1.07	0.82	0.70	0.93
C11	0.97	0.80	1.26	0.81	0.74	0.96
C12	0.75	1.12	1.69	1.09	0.77	1.27
C13	0.38	0.65	0.99	0.73	0.45	0.71
C14	0.36	0.47	0.58	0.38	0.32	0.55
C15	0.19	0.12	0.29	0.14	0.18	0.22
C16	0.11	0.05	0.21	0.11	0.15	0.17
C17	0.04	0.02	0.20	0.05	0.04	0.10
C18	0.04	0.04	0.08	0.02	0.05	0.07
C19	0.00	0.00	0.04	0.00	0.01	0.02
C20	0.00	0.00	0.01	0.00	0.00	0.04
total	**6.99**	**5.36**	**7.78**	**5.25**	**4.61**	**6.42**

Cycloaromatics	wt. %	wt. %	wt. %	wt. %	wt. %	wt. %
C9	0.14	0.06	0.13	0.06	0.03	0.06
C10	1.04	0.86	1.47	0.78	0.67	0.92
C11	2.16	2.41	2.65	2.32	1.40	1.98
C12	2.16	4.73	2.19	4.35	1.95	2.25
C13	1.69	3.94	1.44	4.38	1.80	2.05
C14	1.16	3.52	1.07	3.49	1.81	1.58
C15	0.58	2.42	1.05	2.95	1.43	1.58
C16	0.03	0.74	0.73	0.82	0.77	0.91
C17	0.03	0.10	0.49	0.13	0.32	0.59
C18	0.00	0.01	0.11	0.00	0.05	0.05

total	**8.99**	**18.80**	**11.31**	**19.27**	**10.23**	**11.97**
Naphthalenes	wt. %	wt. %	wt. %	wt. %	wt. %	wt. %
C10	0.12	0.02	0.04	0.02	0.01	0.02
C11	0.42	0.20	0.15	0.18	0.05	0.10
C12	0.43	0.74	0.28	0.78	0.16	0.28
C13	0.37	1.19	0.16	1.19	0.22	0.31
C14	0.18	1.33	0.20	1.54	0.20	0.26
C15	0.12	1.34	0.18	1.31	0.18	0.29
C16	0.00	0.92	0.01	0.78	0.07	0.06
C17	0.00	0.01	0.00	0.07	0.00	0.01
total	**1.64**	**5.76**	**1.03**	**5.87**	**0.89**	**1.32**
Biphenyls	wt. %	wt. %	wt. %	wt. %	wt. %	wt. %
C12	0.00	0.02	0.03	0.02	0.02	0.02
C13	0.04	0.09	0.11	0.09	0.06	0.06
C14	0.11	0.18	0.22	0.26	0.10	0.15
C15	0.16	0.98	0.40	1.20	0.25	0.39
C16	0.04	1.09	0.23	1.37	0.24	0.42
C17	0.00	1.51	0.08	1.62	0.14	0.37
C18	0.00	0.30	0.00	0.56	0.00	0.01
total	**0.34**	**4.17**	**1.07**	**5.12**	**0.81**	**1.42**
Anthracenes and Phenanthrenes	wt. %	wt. %	wt. %	wt. %	wt. %	wt. %
C14	0.00	0.02	0.00	0.02	0.00	0.00
C15	0.00	0.19	0.00	0.29	0.01	0.03
C16	0.00	0.57	0.00	0.59	0.01	0.05
C17+	0.00	0.47	0.00	0.60	0.00	0.03
total	**0.00**	**1.25**	**0.00**	**1.50**	**0.02**	**0.11**
Pyrenes	wt. %	wt. %	wt. %	wt. %	wt. %	wt. %
C16	0.00	0.15	0.03	0.12	0.00	0.02
C17	0.00	0.08	0.05	0.17	0.00	0.02
C18	0.00	0.00	0.00	0.04	0.00	0.00
total	**0.00**	**0.23**	**0.08**	**0.33**	**0.00**	**0.04**
total aromatics	**17.97**	**35.57**	**21.27**	**37.34**	**16.55**	**21.29**

Table A.9 GC×GC-TOF/MS results for HTP wax obtained at 425 °C and 40 min.

	peak area		
	n-paraffin	α-olefin	ratio
C12	221143	97564	2.27
C13	1095734	255220	4.29
C14	1451632	601304	2.41
C15	1313529	459367	2.86
C16	1092166	337083	3.24
C17	818415	231070	3.54
C18	611822	170184	3.60
C19	563599	106587	5.29
C20	460794	105465	4.37
C21	826707	224581	3.68
C22	1331093	297512	4.47
C23	1335026	307541	4.34
C24	1227574	328294	3.74
C25	1189172	277816	4.28
C26	1038271	226422	4.59
C27	947216	183738	5.16
C28	774361	176012	4.40
C29	640728	166012	3.86
C30	490391	157184	3.12
C31	365964	110205	3.32
C32	267137	97955	2.73
C33	172217	51253	3.36
C34	109369		

The content of olefins (20 wt.%) was determined from GC×GC-TOF/MS equipped with high-temperature columns. The mass spectra yield approximate quantitative results because each compound has a different response factor. For this reason, the α-olefins to *n*-paraffins mass ratios for each carbon number were estimated from the peak area ratios.

Table A.10 Energy ratios and GHG emissions of PE HTP, mechanical recycling of plastic, pyrolysis of plastic, biomass HTP, and incineration.

	PE HTP	Mechanical recycling	Pyrolysis	Biomass HTP	Incineration
Products	Fuels/Wax	PE	Oils	Fuels	Energy
Process energy input (MJ/kg feedstock)	3.2[1]	1.9[4]	3.6[7]	8.9[10]	-
Energy output (MJ/kg feedstock)	37[2]	42[5]	36[8]	39[11]	-
Energy ratio	11.6	21.7	10.0	4.4	3.7[13]
GHG emission (kg CO_2/kg feedstock)	0.25[3]	0.24[6]	0.7[9]	0.4[12]	3.2[14]

(1) 2.8 MJ/kg for HTP, adapted from ref. (Olivares et al., 2014) and 0.4 MJ/kg for distillation, calculated based on the boiling point and heat capacity of the oil.
(2) The heating value of 45 MJ/kg and oil yield of 82 wt. %.
(3) 0.20 kg CO_2 for HTP, adapted from ref. (Tzanetis, Posada, & Ramirez, 2017) and 0.05 kg CO_2 for distillation, calculated using 0.448 kg CO_2/kWh for the electricity used for supporting distillation.
(4) Calculated using 0.448 kg CO_2/kWh for the electricity used for process.
(5) 42 MJ/kg of PE polymers.
(6) Adapted from ref. (Kreiger, Mulder, Glover, & Pearce, 2014).
(7) Adapted from ref. (Sharma, Moser, Vermillion, Doll, & Rajagopalan, 2014), where a pyrolysis pilot plant aims to convert 1-2 tons of plastics into fuels per day. The reaction temperature was 450 °C. Energy consumed for washing and drying of plastic was excluded.
(8) Assuming 45 MJ/kg for the oil, and 80 wt. % oil yield.
(9) Adapted from ref. (Opatokun, Strezov, & Kan, 2015).
(10) Including HTP and hydrotreating for biomass, adapted from ref. [1].
(11) Adapted from ref. (Sivaramakrishnan & Ravikumar, 2011).
(12) Adapted from ref. (Tzanetis et al., 2017).
(13) Modified from ref. (Nabavi-Pelesaraei, Bayat, Hosseinzadeh-Bandbafha, Afrasyabi, & Chau, 2017).
(14) It was assumed that 1kg PE was combusted completely.

Table A.11 Costs, revenues, and profits for plastic HTP, mechanical recycling, catalytic pyrolysis, diesel refinery, and biomass HTP.

($/ton of feedstock treated)	PE-HTP		Mechanical Recycling[5]	Catalytic pyrolysis[7]	Diesel from crude oil[8]	Biomass-HTP[9]
Scale	100 ton/day		-	100 ton/day	-	2,000 ton/day
(1) Capital cost	141[1]		-	-	-	85
(2) Feedstock cost	-				450	7
(3) Processing cost	110[2]				162	90
(4) Total cost = (1) +(2)+(3)	251		480	370	612	252
	Fuels	Wax				Fuels
(5) Revenue	583[3]	970[4]	810[6]	445	690	207[10]
Profit = (5)-(4)	332	719	330	75	78	-45

(1) Instruments included size reduction treatment, HTL reactor system, and distillation unit. Data was modified from ref. (Zhu et al., 2014) and "0.6 rule" was used for scale change from 2,000 ton/day to 100 ton/day.
(2) Processing costs included energy consumption, waste disposal, labor, and maintenance. Data was modified from ref. (Zhu et al., 2014).
(3) Revenue included the selling of HTP gasoline, HTP diesel, and heavy oil (as base oil), as $500/ton, $690/ton, and $800 /ton, respectively.
(4) The wax yield was 97 wt.%. The wax unit price is $1,000/ton, data obtained from http://paraffinwaxco.com/paraffin-wax-price-list/.
(5) Data updated from ref. (Plinke et al., 2020).
(6) Data obtained from https://www.alibaba.com/showroom/recycled-polyethylene.html.
(7) Data obtained from Boston Consulting Group, https://www.bcg.com/publications/2019/plastic-waste-circular-solution.aspx.
(8) Data obtained from Energy Information Administration, https://www.eia.gov/petroleum/gasdiesel/;and http://www.voltaoil.com/what-makes-up-retail-price-for-gasoline/
(9) Data modified from ref. (Zhu et al., 2014).
(10) Based on a 30 wt. % diesel yield of biomass-HTP (Zhu et al., 2014), and a diesel price of $690/ton.

APPENDIX B. SUPPLEMENTARY MATERIAL FOR CHAPTER 5

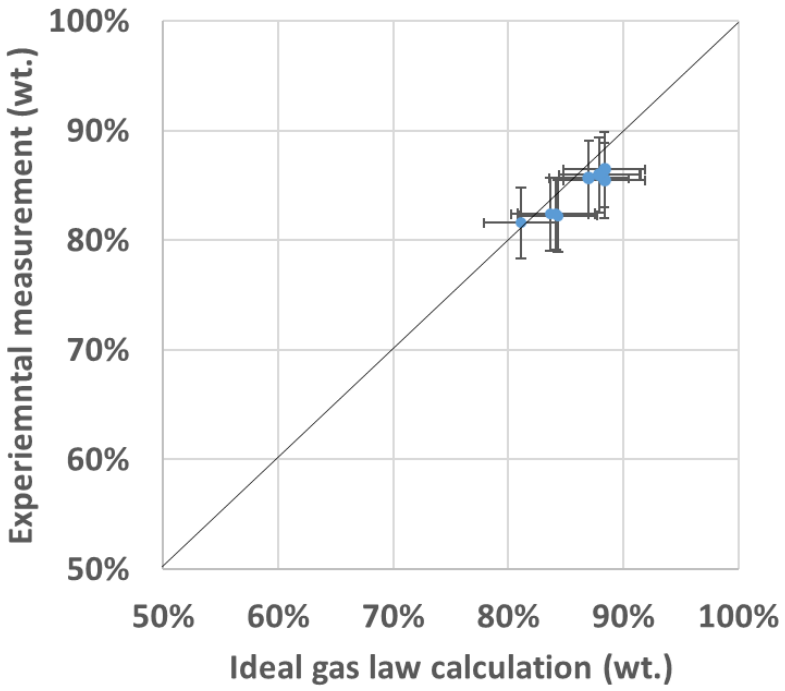

Figure B.**1** Comparison of oil yields obtained from two methods: (1) ideal gas law calculations, and (2) measured weights of the collected oils. The oil yields obtained from the two methods agreed within experimental error.

Table B.1 Parameters for GC-FID analysis of gas products.

Parameter	Description
Column	J&W GS-CarbonPLOT GC Column, 30 m, 0.32 mm, 3.00 µm, 7 inch cage (FID: Front Detector, 20 Hz Data Rate, 0.01 min Minimum Peak Width)
Gas Flow Rates	2.5 mL/min He (12.03 psi, 40 cm/s avg. velocity), 45.0 mL/min H_2, 400 mL/min Air
Oven Temperature	Hold at 50 °C for 1 min, ramp from 50 °C to 350 °C at rate of 10 °C/min, hold at 350 °C for 5 min
Temperatures	Inlet: 275 °C; Detector: 275 °C
Pressure & Split Ratio	Inlet: constant pressure of 12.0 psi, 107 mL/min total flow (Split Ratio of 19.2, Split Flow of 99.2 mL/min)
Sample Injections (Manual Injection)	C_1-C_6 Paraffins (1000 molar ppm each, in He): 1 mL C_2-C_6 Olefins (100 molar ppm each, in He): 2 mL Gas samples: 1 mL

Table B.2 Comparison of capital costs and energy consumptions for LP-HTP and SWL.

	LP-HTP	SWL	Savings of LP-HTP compared to SWL
Reaction temperature (°C)	450	450	-
Reaction pressure (MPa)	1.55	23	-
Scale (ton of feedstock/day)	24	24	-
Capital cost for reactor ($/ton of feedstock)	11[1]	111[2]	90%
Energy consumption (MJ/kg of feedstock)	1.46[3]	7.04[4]	84%

*1. Data adapted from Fivga et al. 2018 (Fivga & Dimitriou, 2018).
2. Data adapted from Galera et al. 2014 (Galera & Ortiz, 2015).
3. Calculated as 1.3 MJ/kg for the polyolefin conversion and 0.16 MJ/kg for heating up water (5 wt%) (NIST, n.d.).
4. Calculated as 1.3 MJ/kg for the polyolefin conversion and 5.74 MJ/kg for heating up water (64 wt%) (NIST, n.d.).

Table B.3 Chemical compositions of oil products converted from model PE at 450 °C, 1 hr, and different pressures.

Pressures	23MPa	10.25 MPa	3.75 MPa	1.55 MPa	0.25 MPa
Light Hydrocarbons (C5-)	5.65	5.24	6.51	7.45	9.11
Paraffins					
n-paraffins					
C6	4.56	4.71	5.18	4.98	5.29
C7	5.21	5.43	5.53	5.52	5.60
C8	2.88	3.17	2.93	3.22	3.20
C9	2.26	2.50	2.39	2.62	2.55
C10	1.71	2.07	1.91	3.10	2.99
C11	1.42	1.73	1.59	1.70	1.63
C12	1.17	1.45	1.37	1.44	1.33
C13	0.95	1.20	1.08	1.14	1.07
C14	0.78	0.99	0.88	0.92	0.86
C15	0.67	0.85	0.75	0.77	0.71
C16	0.55	0.69	0.61	0.61	0.56
C17	0.46	0.57	0.50	0.49	0.45
C18	0.40	0.49	0.43	0.41	0.37
C19	0.32	0.39	0.34	0.32	0.29
C20	0.26	0.32	0.28	0.24	0.22
C21	0.22	0.25	0.22	0.19	0.17
C22	0.18	0.22	0.18	0.16	0.13
C23	0.16	0.18	0.15	0.12	0.11
C24	0.13	0.14	0.13	0.10	0.09
C25	0.13	0.13	0.12	0.09	0.08
C26	0.08	0.08	0.08	0.05	0.05
C27	0.07	0.07	0.07	0.04	0.04
C28	0.07	0.06	0.06	0.03	0.03
C29	0.06	0.05	0.05	0.03	0.03
C30	0.04	0.04	0.05	0.03	0.03
C31	0.04	0.03	0.04	0.02	0.02
Total *n*-paraffins	**24.78**	**27.77**	**26.90**	**28.36**	**27.92**
Isoparaffins					
C6	0.72	0.61	0.67	0.71	0.76
C7	0.40	0.35	0.36	0.38	0.39
C8	0.45	0.44	0.32	0.36	0.44
C9	0.46	0.42	0.37	0.47	0.47
C10	0.33	0.34	0.31	0.36	0.36
C11	0.27	0.29	0.35	0.30	0.30
C12	0.28	0.32	0.28	0.34	0.31
C13	0.27	0.32	0.28	0.31	0.31
C14	0.22	0.28	0.36	0.27	0.26
C15	0.18	0.22	0.18	0.21	0.20
C16	0.16	0.20	0.18	0.19	0.18

C17	0.12	0.16	0.16	0.15	0.13
C18	0.08	0.11	0.09	0.11	0.05
C19	0.04	0.05	0.10	0.09	0.01
C20	0.06	0.06	0.08	0.09	0.03
C21	0.05	0.05	0.05	0.05	0.01
C22	0.03	0.06	0.06	0.06	0.01
C23	0.03	0.04	0.03	0.04	0.01
C24	0.03	0.05	0.03	0.03	0.03
C25	0.04	0.05	0.05	0.04	0.02
C26	0.02	0.02	0.04	0.02	0.01
C27	0.01	0.01	0.01	0.01	0.00
C28	0.01	0.00	0.01	0.01	0.00
C29	0.00	0.00	0.00	0.01	0.00
C30	0.00	0.00	0.01	0.00	0.00
C31	0.00	0.00	0.00	0.00	0.00
Total Isoparaffins	**4.26**	**4.47**	**4.38**	**4.59**	**4.29**
Cycloparaffins and olefins					
Monocycloparaffins and olefins					
C6	3.57	3.29	3.46	3.50	3.67
C7	4.85	4.11	5.07	4.87	4.24
C8	3.75	3.88	4.09	4.07	3.63
C9	2.94	3.21	3.55	2.93	2.64
C10	2.71	2.54	2.62	1.69	1.65
C11	2.14	2.32	2.37	2.18	2.16
C12	1.73	1.71	1.80	1.82	1.37
C13	0.79	0.82	0.87	1.18	0.74
C14	1.28	1.34	1.36	1.34	1.02
C15	1.10	1.27	1.15	1.11	1.04
C16	0.94	1.09	0.96	1.02	0.86
C17	0.85	0.97	0.84	0.83	0.68
C18	0.79	0.83	0.80	0.76	0.64
C19	0.69	0.93	0.62	0.64	0.64
C20	0.45	0.52	0.51	0.45	0.40
C21	0.52	0.62	0.54	0.48	0.48
C22	0.44	0.46	0.36	0.33	0.30
C23	0.30	0.38	0.32	0.26	0.24
C24	0.50	0.50	0.46	0.37	0.29
C25	0.21	0.20	0.19	0.15	0.15
C26	0.17	0.21	0.17	0.13	0.12
C27	0.23	0.19	0.17	0.15	0.09
C28	0.11	0.13	0.13	0.10	0.11
C29	0.07	0.04	0.16	0.09	0.03
C30	0.00	0.00	0.00	0.00	0.00
Total Monocycloparaffins And Olefins	**31.09**	**31.58**	**32.55**	**30.46**	**27.18**

Dicycloparaffins and olefins					
C8	2.46	2.76	2.01	1.74	2.72
C9	1.28	1.54	1.55	1.27	1.46
C10	1.43	1.55	1.60	1.41	1.47
C11	1.02	0.98	0.82	1.01	0.79
C12	0.91	1.16	0.97	0.78	1.26
C13	1.45	1.68	1.52	1.14	1.59
C14	0.54	0.63	0.58	0.56	0.69
C15	0.46	0.56	0.48	0.42	0.48
C16	0.29	0.27	0.34	0.24	0.17
C17	0.14	0.20	0.19	0.14	0.30
C18	0.11	0.14	0.09	0.08	0.16
C19	0.06	0.05	0.06	0.04	0.05
C20+	0.24	0.19	0.15	0.07	0.24
Total Dicycloparaffins And Olefins	**10.38**	**11.70**	**10.35**	**8.90**	**11.38**
Tricycloparaffins and olefins					
C10	0.07	0.06	0.05	0.06	0.06
C11	0.08	0.10	0.08	0.06	0.08
C12	0.01	0.01	0.01	0.01	0.01
C13	0.03	0.03	0.00	0.00	0.03
C14	0.00	0.00	0.00	0.00	0.00
C15	0.01	0.01	0.01	0.01	0.02
C16+	0.12	0.12	0.10	0.06	0.10
Total Tricycloparaffins And Olefins	**0.32**	**0.33**	**0.25**	**0.19**	**0.29**
Total Cycloparaffins And Olefins	**41.79**	**43.61**	**43.15**	**39.55**	**38.86**
Aromatics					
Alkylbenzenes					
C6/benzene	0.44	0.34	0.38	0.36	0.39
C7/toluene	2.00	1.48	1.53	1.57	1.60
C8	2.39	1.82	1.85	1.96	1.96
C9	1.61	1.30	1.29	1.39	1.47
C10	0.94	0.79	0.76	0.99	0.87
C11	0.68	0.55	0.62	0.66	0.51
C12	0.41	0.38	0.36	0.38	0.32
C13	0.19	0.13	0.17	0.19	0.12
C14	0.08	0.06	0.07	0.07	0.07
C15	0.06	0.07	0.09	0.10	0.07
C16	0.04	0.05	0.05	0.05	0.04

C17	0.03	0.04	0.05	0.05	0.03
C18	0.05	0.05	0.05	0.05	0.03
C19	0.01	0.01	0.04	0.04	0.00
C20+	0.01	0.01	0.03	0.03	0.00
Total Alkylbenzenes	**8.95**	**7.07**	**7.35**	**7.88**	**7.48**
Cycloaromatics					
C9	0.16	0.13	0.14	0.14	0.30
C10	0.81	0.58	0.60	0.45	0.45
C11	1.33	0.81	1.01	1.05	0.86
C12	0.71	0.50	0.58	0.70	0.54
C13	0.39	0.32	0.35	0.36	0.33
C14	0.17	0.11	0.15	0.18	0.09
C15	0.07	0.07	0.08	0.11	0.05
C16	0.04	0.04	0.03	0.04	0.02
C17	0.01	0.01	0.01	0.01	0.01
C18+	0.09	0.12	0.04	0.04	0.11
Total Cycloaromatics	**3.77**	**2.69**	**2.99**	**3.09**	**2.76**
Diaromatics					
C10	0.12	0.10	0.11	0.11	0.12
C11	0.52	0.46	0.37	0.38	0.60
C12	0.75	0.70	0.59	0.52	0.91
C13	0.92	0.67	0.58	0.59	0.63
C14	1.20	0.96	0.91	0.98	1.03
C15	1.33	1.15	1.09	1.19	1.28
C16	1.09	0.80	0.95	0.94	0.85
C17	0.71	0.57	0.73	0.85	0.28
C18	0.10	0.11	0.20	0.20	0.07
C19	0.01	0.03	0.01	0.01	0.01
C20+	0.00	0.00	0.00	0.00	0.00
Total Diaromatics	**6.76**	**5.56**	**5.55**	**5.78**	**5.79**
Triaromatics					
C14	0.06	0.08	0.02	0.02	0.14
C15	0.08	0.10	0.08	0.08	0.13
C16	0.78	0.67	0.48	0.44	0.99
C17	1.16	1.06	1.06	1.22	0.97
C18	0.98	0.78	0.70	0.70	0.80
C19+	0.82	0.74	0.64	0.71	0.69
Total Triaromatics	**3.88**	**3.43**	**2.99**	**3.17**	**3.71**
Total Aromatics	**23.36**	**18.74**	**18.88**	**19.91**	**19.75**

Table B.**4** Chemical compositions of oil products converted from model PP at 450 °C, 1 hr, and different pressures.

Pressures	23MPa	10.25 MPa	3.75 MPa	1.55 MPa	0.25 MPa
Light Hydrocarbons (C5-)	13.26	14.37	13.61	15.10	16.44
Paraffins					
n-paraffins					
C6	2.26	2.88	3.55	3.72	2.51
C7	3.13	3.21	2.94	3.01	3.09
C8	0.00	0.00	0.00	0.00	0.00
C9	0.00	0.00	0.00	0.00	0.00
C10	0.02	0.24	0.25	0.33	0.23
C11	0.00	0.02	0.00	0.02	0.02
C12	0.01	0.03	0.01	0.01	0.05
C13	0.00	0.00	0.00	0.00	0.01
C14	0.01	0.02	0.02	0.02	0.03
C15	0.00	0.00	0.00	0.00	0.01
C16	0.00	0.00	0.00	0.00	0.01
C17	0.00	0.00	0.00	0.00	0.00
C18	0.00	0.00	0.00	0.00	0.00
C19	0.00	0.00	0.00	0.00	0.00
C20	0.00	0.00	0.00	0.00	0.00
C21	0.00	0.00	0.00	0.00	0.00
C22	0.00	0.00	0.00	0.00	0.00
C23	0.00	0.00	0.00	0.00	0.00
C24	0.00	0.00	0.00	0.00	0.00
C25	0.00	0.00	0.00	0.00	0.00
C26	0.00	0.00	0.00	0.00	0.00
C27	0.00	0.00	0.00	0.00	0.00
C28	0.00	0.00	0.00	0.00	0.00
C29	0.00	0.00	0.00	0.00	0.00
C30	0.00	0.00	0.00	0.00	0.00
C31	0.00	0.00	0.00	0.00	0.00
Total *n*-paraffins	**5.43**	**6.41**	**6.78**	**7.11**	**5.99**
Isoparaffins					
C6	3.85	3.70	3.37	3.55	3.85
C7	3.19	3.13	3.01	3.09	3.00
C8	3.79	3.97	3.93	2.79	3.91
C9	4.13	5.10	4.21	4.15	4.37
C10	0.28	0.85	0.28	0.25	0.31
C11	0.56	0.84	1.06	1.00	0.72
C12	0.09	0.22	0.24	0.22	0.12
C13	0.04	0.05	0.07	0.08	0.04
C14	0.31	0.48	0.92	0.83	0.31
C15	0.04	0.04	0.07	0.07	0.03
C16	0.02	0.02	0.04	0.04	0.02

C17	0.09	0.12	0.26	0.22	0.08
C18	0.01	0.01	0.01	0.01	0.01
C19	0.05	0.04	0.13	0.13	0.03
C20	0.02	0.03	0.05	0.04	0.02
C21	0.00	0.00	0.01	0.01	0.00
C22	0.02	0.01	0.05	0.05	0.01
C23	0.01	0.01	0.02	0.02	0.01
C24	0.00	0.00	0.01	0.02	0.00
C25	0.01	0.00	0.03	0.02	0.00
C26	0.01	0.00	0.01	0.01	0.00
C27	0.00	0.00	0.00	0.00	0.00
C28	0.00	0.00	0.00	0.00	0.00
C29	0.00	0.00	0.00	0.00	0.01
C30	0.00	0.00	0.01	0.00	0.02
C31	0.00	0.00	0.00	0.00	0.00
Total Isoparaffins	**16.51**	**18.63**	**17.79**	**16.61**	**16.84**
Cycloparaffins and olefins					
Monocycloparaffins and olefins					
C6	2.56	2.37	2.36	2.47	2.45
C7	2.77	2.88	2.69	3.47	2.71
C8	6.55	6.78	9.58	8.75	6.45
C9	6.71	6.96	7.06	7.11	6.84
C10	3.08	2.77	2.64	2.51	3.17
C11	2.23	2.09	2.18	2.00	2.11
C12	2.27	2.23	2.17	2.02	2.09
C13	0.40	0.39	0.33	0.34	0.53
C14	0.19	0.31	0.17	0.30	0.32
C15	0.06	0.09	0.09	0.03	0.18
C16	0.00	0.00	0.00	0.00	0.01
C17	0.00	0.00	0.00	0.00	0.01
C18	0.00	0.00	0.00	0.00	0.00
C19	0.00	0.00	0.00	0.00	0.00
C20	0.00	0.00	0.00	0.00	0.00
C21	0.00	0.00	0.00	0.00	0.00
C22	0.00	0.00	0.00	0.00	0.00
C23	0.00	0.00	0.00	0.00	0.00
C24	0.00	0.00	0.00	0.00	0.00
C25	0.00	0.00	0.00	0.00	0.00
C26	0.00	0.00	0.00	0.00	0.00
C27	0.00	0.00	0.00	0.01	0.00
C28	0.00	0.01	0.01	0.01	0.04
C29	0.01	0.01	0.03	0.01	0.03
C30	0.00	0.00	0.00	0.00	0.00
Total Monocycloparaffins And Olefins	**26.83**	**26.88**	**29.32**	**29.05**	**26.93**

Dicycloparaffins and olefins					
C8	1.10	1.20	1.27	2.24	1.11
C9	0.93	0.84	1.14	1.17	1.02
C10	0.94	1.03	1.04	1.04	0.92
C11	0.57	0.74	0.69	0.70	0.81
C12	0.63	0.88	0.86	0.90	0.86
C13	1.05	1.29	1.27	1.31	1.04
C14	0.59	0.68	0.67	0.58	0.66
C15	0.56	0.88	0.76	0.60	0.82
C16	0.00	0.04	0.00	0.00	0.09
C17	0.00	0.00	0.00	0.00	0.00
C18	0.00	0.00	0.00	0.00	0.00
C19	0.00	0.00	0.00	0.00	0.00
C20+	0.00	0.00	0.00	0.00	0.00
Total Dicycloparaffins And Olefins	**6.38**	**7.60**	**7.70**	**8.54**	**7.32**
Tricycloparaffins and olefins					
C10	0.01	0.01	0.01	0.02	0.01
C11	0.01	0.01	0.01	0.01	0.01
C12	0.00	0.00	0.00	0.00	0.00
C13	0.00	0.00	0.00	0.00	0.00
C14	0.00	0.00	0.00	0.00	0.00
C15	0.00	0.00	0.00	0.02	0.00
C16+	0.00	0.00	0.00	0.00	0.00
Total Tricycloparaffins And Olefins	**0.02**	**0.02**	**0.03**	**0.05**	**0.02**
Total Cycloparaffins And Olefins	**33.23**	**34.50**	**37.04**	**37.65**	**34.28**
Aromatics					
Alkylbenzenes					
C6/benzene	0.11	0.10	0.09	0.09	0.10
C7/toluene	1.34	1.18	1.07	1.09	1.24
C8	4.54	3.79	3.56	3.53	4.00
C9	5.09	3.92	3.77	3.95	4.04
C10	1.79	1.53	1.45	1.09	1.55
C11	1.17	1.01	0.88	0.85	1.00
C12	0.68	0.59	0.56	0.36	0.58
C13	0.17	0.20	0.12	0.10	0.18
C14	0.02	0.02	0.03	0.02	0.02
C15	0.00	0.00	0.00	0.00	0.00
C16	0.00	0.00	0.00	0.00	0.00

C17	0.00	0.00	0.00	0.00	0.00
C18	0.00	0.00	0.00	0.00	0.00
C19	0.00	0.00	0.00	0.00	0.00
C20+	0.00	0.00	0.00	0.00	0.00
Total Alkylbenzenes	**14.90**	**12.35**	**11.54**	**11.08**	**12.72**
Cycloaromatics					
C9	0.04	0.03	0.03	0.10	0.03
C10	0.46	0.27	0.27	0.25	0.34
C11	1.52	1.14	1.12	1.16	1.15
C12	1.33	0.97	0.88	0.64	0.93
C13	0.80	0.61	0.56	0.45	0.71
C14	0.28	0.30	0.19	0.09	0.28
C15	0.12	0.14	0.10	0.06	0.12
C16	0.01	0.02	0.01	0.00	0.01
C17	0.00	0.00	0.00	0.00	0.00
C18+	0.00	0.00	0.00	0.00	0.00
Total Cycloaromatics	**4.55**	**3.47**	**3.15**	**2.76**	**3.57**
Diaromatics					
C10	0.03	0.03	0.02	0.02	0.03
C11	0.24	0.22	0.25	0.33	0.24
C12	0.98	0.87	0.78	0.97	0.87
C13	0.96	0.82	0.80	0.84	0.80
C14	1.29	1.05	1.13	1.11	1.03
C15	1.59	1.43	1.43	1.54	1.43
C16	1.28	1.14	1.09	0.95	1.12
C17	1.05	1.02	0.69	0.28	0.96
C18	0.04	0.12	0.08	0.02	0.10
C19	0.00	0.00	0.00	0.00	0.00
C20+	0.00	0.00	0.00	0.00	0.00
Total Diaromatics	**7.47**	**6.68**	**6.29**	**6.06**	**6.59**
Triaromatics					
C14	0.08	0.00	0.08	0.07	0.04
C15	0.09	0.06	0.09	0.18	0.08
C16	1.00	0.68	0.75	0.99	0.66
C17	1.34	1.24	1.09	0.95	1.25
C18	0.98	0.82	0.78	0.79	0.74
C19+	0.91	0.78	0.72	0.65	0.78
Total Triaromatics	**4.39**	**3.57**	**3.51**	**3.63**	**3.56**
Total Aromatics	**31.32**	**26.09**	**24.49**	**23.54**	**26.44**

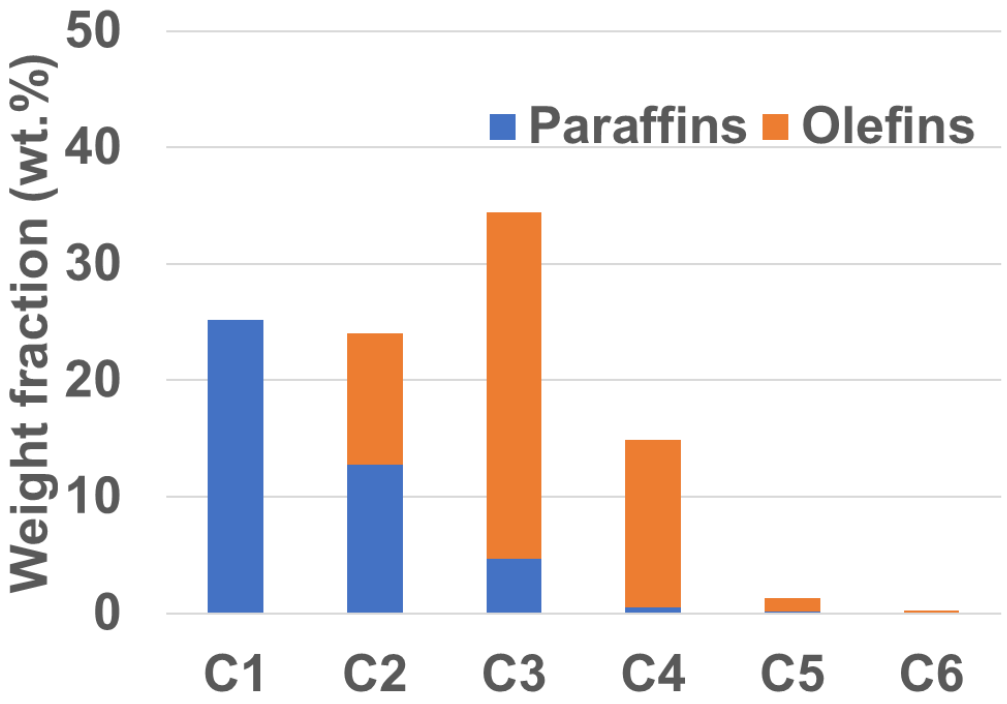

Figure B.**2** Chemical compositions of gases converted at 450 °C, 45 min, and 1.55 MPa, from mixed polyolefins at a PE/PP ratio of 1:1.

Table B.**5** Element weight fractions of inorganic solid from actual polyolefin waste acquired from SEM-EDS analysis.

Element	Weight fractions (ca. wt%)
O	48
Ca	24
C	11
N	9
Ti	4
Fe	1
Cl	1
Si	1
Al	0.5
Mg	0.5

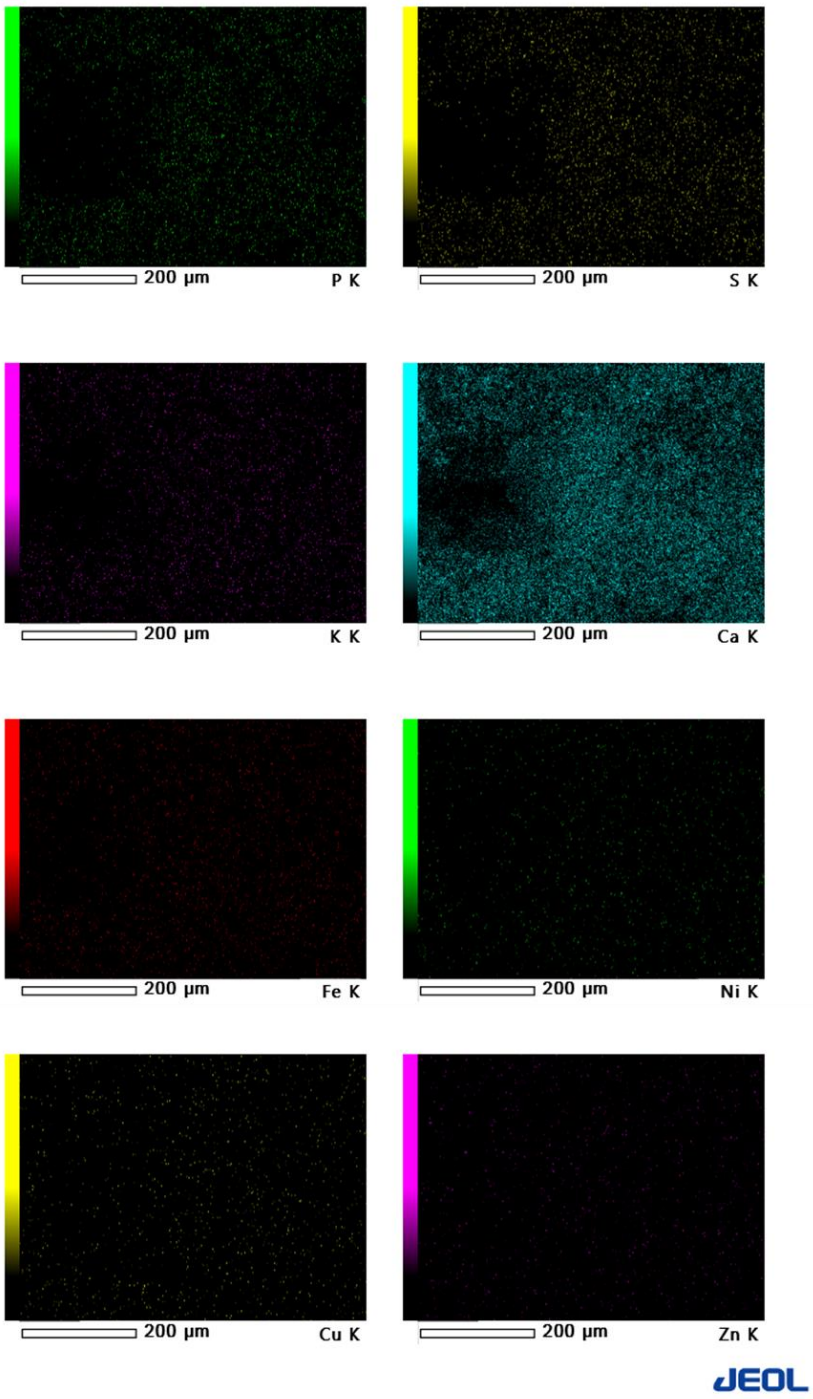

Fig**ure** B.**3** SEM-EDS plots of inorganic solid from actual polyolefin waste.

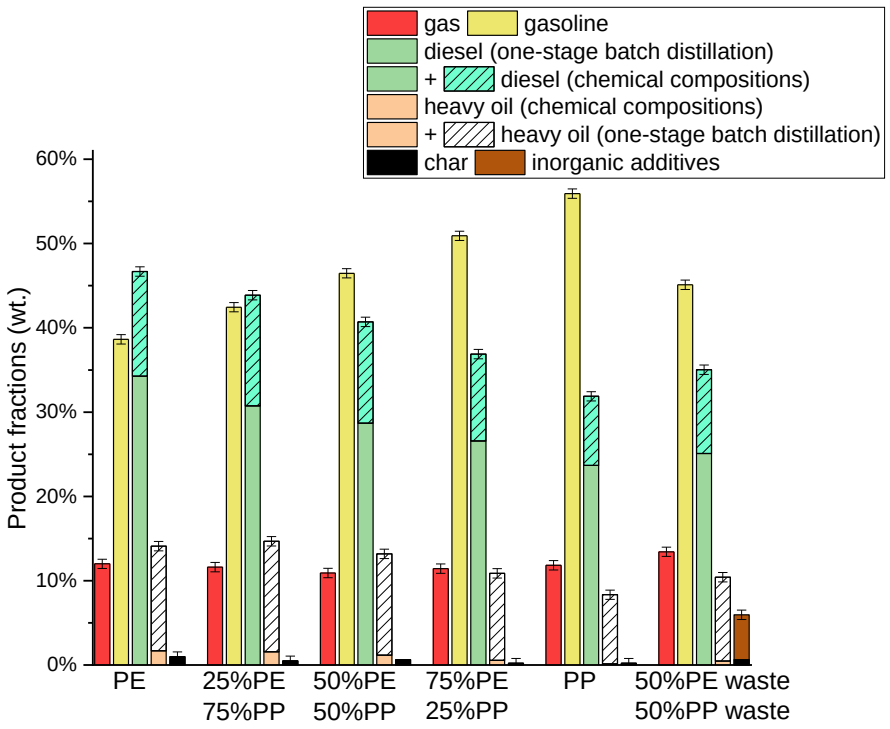

Figure B.**4** Yields of gas, oil (gasoline, diesel, and heavy oil), char, and inorganic additives of PE, PP, and PE/PP mixtures at 450 °C, 45 min, 1.55 MPa. The yields were calculated based on the weight of the plastic feedstock used in each test.

Table B.**6** Chemical compositions of the gasoline fractions derived from PP and mixed polyolefins compared to those of commercial gasoline.

C#	50% PE + 50%PP	50% PE waste + 50% PP waste	25% PE + 75% PP	PP	comm. gasoline
Light Hydrocarbons (C5-)	17.69	19.33	21.32	20.63	24.01
Paraffins					
n-paraffins					
C6	7.59	7.42	5.98	4.61	4.97
C7	7.67	7.42	5.66	4.15	1.95
C8	4.26	3.39	2.70	0.00	1.21
C9	2.11	1.75	1.10	0.00	0.54
C10	0.73	1.00	0.76	0.01	0.23
C11	0.18	0.15	0.07	0.00	0.15
C12	0.06	0.05	0.02	0.00	0.07
C13	0.02	0.02	0.01	0.00	0.01
C14	0.01	0.01	0.00	0.00	0.00
C15	0.00	0.00	0.00	0.00	0.00
C16	0.00	0.00	0.00	0.00	0.00
C17	0.00	0.00	0.00	0.00	0.00
C18	0.00	0.00	0.00	0.00	0.00
C19	0.00	0.00	0.00	0.00	0.00
C20	0.00	0.00	0.00	0.00	0.00
C21	0.00	0.00	0.00	0.00	0.00
C22	0.00	0.00	0.00	0.00	0.00
C23	0.00	0.00	0.00	0.00	0.00
C24	0.00	0.00	0.00	0.00	0.00
C25	0.00	0.00	0.00	0.00	0.00
C26	0.00	0.00	0.00	0.00	0.00
C27	0.00	0.00	0.00	0.00	0.00
C28	0.00	0.00	0.00	0.00	0.00
C29	0.00	0.00	0.00	0.00	0.00
C30	0.00	0.00	0.00	0.00	0.00
C31	0.00	0.00	0.00	0.00	0.00
Total *n*-paraffins	22.61	21.22	16.31	8.77	9.12
Isoparaffins					
C6	4.87	5.51	6.41	7.02	8.31
C7	5.01	5.34	5.03	4.88	3.43
C8	4.26	3.96	5.18	7.40	2.92
C9	4.67	4.61	5.13	6.50	2.91
C10	0.51	0.46	0.41	0.37	1.32
C11	0.26	0.21	0.23	0.32	0.68
C12	0.05	0.04	0.02	0.03	0.32

C13	0.01	0.01	0.00	0.00	0.09
C14	0.01	0.01	0.00	0.01	0.00
C15	0.00	0.00	0.00	0.00	0.00
C16	0.00	0.00	0.00	0.00	0.00
C17	0.00	0.00	0.00	0.00	0.00
C18	0.00	0.00	0.00	0.00	0.00
C19	0.00	0.00	0.00	0.00	0.00
C20	0.00	0.00	0.00	0.00	0.00
C21	0.00	0.00	0.00	0.00	0.00
C22	0.00	0.00	0.00	0.00	0.00
C23	0.00	0.00	0.00	0.00	0.00
C24	0.00	0.00	0.00	0.00	0.00
C25	0.00	0.00	0.00	0.00	0.00
C26	0.00	0.00	0.00	0.00	0.00
C27	0.00	0.00	0.00	0.00	0.00
C28	0.00	0.00	0.00	0.00	0.00
C29	0.00	0.00	0.00	0.00	0.00
C30	0.00	0.00	0.00	0.00	0.00
C31	0.00	0.00	0.00	0.00	0.00
Total Isoparaffins	19.63	20.15	22.42	26.52	19.96
Cycloparaffins and olefins					
Monocycloparaffins and olefins					
C6	2.82	2.82	2.93	2.96	0.11
C7	6.98	6.88	5.82	3.81	1.60
C8	9.48	7.95	10.72	13.10	1.73
C9	6.24	5.42	7.19	9.45	1.54
C10	1.60	1.04	1.10	2.05	1.24
C11	0.58	0.51	0.51	0.58	0.61
C12	0.15	0.14	0.13	0.20	0.18
C13	0.01	0.01	0.00	0.00	0.00
C14	0.00	0.00	0.00	0.00	0.00
C15	0.00	0.00	0.00	0.00	0.00
C16	0.00	0.00	0.00	0.00	0.00
C17	0.00	0.00	0.00	0.00	0.00
C18	0.00	0.00	0.00	0.00	0.00
C19	0.00	0.00	0.00	0.00	0.00
C20	0.00	0.00	0.00	0.00	0.00
C21	0.00	0.00	0.00	0.00	0.00
C22	0.00	0.00	0.00	0.00	0.00
C23	0.00	0.00	0.00	0.00	0.00
C24	0.00	0.00	0.00	0.00	0.00
C25	0.00	0.00	0.00	0.00	0.00
C26	0.00	0.00	0.00	0.00	0.00
C27	0.00	0.00	0.00	0.00	0.00
C28	0.00	0.00	0.00	0.00	0.00
C29	0.00	0.00	0.00	0.00	0.00

C30	0.00	0.00	0.00	0.00	0.00
Total Monocycloparaffins And Olefins	**27.86**	**24.78**	**28.40**	**32.16**	**7.02**
Dicycloparaffins and olefins					
C8	1.71	1.61	1.26	0.88	0.02
C9	1.17	0.86	0.98	1.02	0.23
C10	0.66	0.60	0.58	0.45	0.22
C11	0.09	0.10	0.06	0.14	0.15
C12	0.03	0.03	0.04	0.06	0.01
C13	0.00	0.00	0.00	0.00	0.00
C14	0.00	0.00	0.00	0.00	0.00
C15	0.00	0.00	0.00	0.00	0.00
C16	0.00	0.00	0.00	0.00	0.00
C17	0.00	0.00	0.00	0.00	0.00
C18	0.00	0.00	0.00	0.00	0.00
C19	0.00	0.00	0.00	0.00	0.00
C20+	0.00	0.00	0.00	0.00	0.00
Total Dicycloparaffins And Olefins	**3.66**	**3.20**	**2.92**	**2.55**	**0.63**
Tricycloparaffins and olefins					
C10	0.00	0.00	0.00	0.00	0.01
C11	0.00	0.00	0.00	0.00	0.00
C12	0.00	0.00	0.00	0.00	0.00
C13	0.00	0.00	0.00	0.00	0.00
C14	0.00	0.00	0.00	0.00	0.00
C15	0.00	0.00	0.00	0.00	0.00
C16+	0.00	0.00	0.00	0.00	0.00
Total Tricycloparaffins And Olefins	**0.00**	**0.00**	**0.00**	**0.00**	**0.01**
Total Cycloparaffins And Olefins	**31.51**	**27.98**	**31.32**	**34.71**	**7.66**
Aromatics					
Alkylbenzenes					
C6/benzene	0.34	0.51	0.21	0.10	0.48
C7/toluene	2.13	2.88	1.80	1.36	9.98
C8	3.66	4.75	4.05	4.49	13.41
C9	1.74	2.31	2.03	2.64	9.04
C10	0.36	0.46	0.34	0.41	3.42
C11	0.10	0.12	0.07	0.10	0.75
C12	0.01	0.02	0.01	0.02	0.08

C13	0.00	0.00	0.00	0.00	0.00
C14	0.00	0.00	0.00	0.00	0.00
C15	0.00	0.00	0.00	0.00	0.00
C16	0.00	0.00	0.00	0.00	0.00
C17	0.00	0.00	0.00	0.00	0.00
C18	0.00	0.00	0.00	0.00	0.00
C19	0.00	0.00	0.00	0.00	0.00
C20+	0.00	0.00	0.00	0.00	0.00
Total Alkylbenzenes	**8.35**	**11.06**	**8.51**	**9.12**	**37.15**
Cycloaromatics					
C9	0.03	0.04	0.02	0.01	0.35
C10	0.07	0.09	0.05	0.04	0.76
C11	0.06	0.08	0.04	0.04	0.37
C12	0.01	0.02	0.01	0.02	0.06
C13	0.00	0.00	0.00	0.00	0.00
C14	0.00	0.00	0.00	0.00	0.00
C15	0.00	0.00	0.00	0.00	0.00
C16	0.00	0.00	0.00	0.00	0.00
C17	0.00	0.00	0.00	0.00	0.00
C18+	0.00	0.00	0.00	0.00	0.00
Total Cycloaromatics	**0.18**	**0.23**	**0.11**	**0.11**	**1.55**
Diaromatics					
C10	0.01	0.01	0.00	0.00	0.19
C11	0.01	0.02	0.01	0.01	0.23
C12	0.01	0.01	0.00	0.01	0.06
C13	0.00	0.00	0.00	0.00	0.04
C14	0.00	0.00	0.00	0.00	0.02
C15	0.00	0.00	0.00	0.00	0.01
C16	0.00	0.00	0.00	0.00	0.00
C17	0.00	0.00	0.00	0.00	0.00
C18	0.00	0.00	0.00	0.00	0.00
C19	0.00	0.00	0.00	0.00	0.00
C20+	0.00	0.00	0.00	0.00	0.00
Total Diaromatics	**0.03**	**0.04**	**0.01**	**0.02**	**0.55**
Triaromatics					
C14	0.00	0.00	0.00	0.00	0.00
C15	0.00	0.00	0.00	0.00	0.00
C16	0.00	0.00	0.00	0.00	0.00
C17	0.00	0.00	0.00	0.00	0.00
C18	0.00	0.00	0.00	0.00	0.00
C19+	0.00	0.00	0.00	0.00	0.00
Total Triaromatics	**0.00**	**0.00**	**0.00**	**0.00**	**0.00**
Total Aromatics	**8.56**	**11.33**	**8.63**	**9.25**	**39.25**

Table B.7 Fuel properties of the gasoline fractions derived from PP and mixed polyolefins compared to those of commercial gasoline.

Properties	50% PE + 50% PP	50% PE waste + 50% PP waste	25% PE + 75% PP	PP	BP gasoline	Exxon Mobil gasoline	Requirements
Anti-knocking index (AKI)	87	87	88	98	87	90	≥87
Kinematic Viscosity (mm^2/s)	0.563	0.596	0.564	0.553	0.585	0.614	0.40-0.88
T_{10} (°C)	59	57	56	60	49	54	≤65
T_{50} (°C)	112	108	109	113	77	86	77-118
T_{90} (°C)	160	161	159	157	176	181	≤190
T_{final} (°C)	170	170	170	170	-	-	≤225
Distillation residue (wt%)	0	0	0	0	-	-	≤2
Drivability index (DI(°C))	585	569	569	585	481	520	≤591
Reid vapor pressure (psi)	9.42	-	-	-	9.63	9.71	≤10
Lead (ppm)	-	0.4	-	-	-	-	≤17
Sulfur (ppm)	-	7.7	-	-	-	-	≤80
Benzene (wt%)	0.34	0.51	0.21	0.10	0.48	0.94	≤1
Aromatics (wt%)	8.56	11.33	8.63	9.25	39.25	29.55	-
Density (g/cm^3)	0.722	0.735	0.725	0.726	0.753	0.747	-
Hydrogen content (wt%)	15.04	14.91	15.06	14.95	13.49	14.18	-
Gross calorific value (MJ/kg)	45.13	44.22	45.18	44.78	44.47	44.99	-

*Density and viscosity were measured at 15 °C.

Table B.**8** Chemical compositions of the diesel fractions derived from PP and mixed polyolefins compared to those of commercial diesel.

C#	50% PE + 50% PP	50% PE waste + 50% PP waste	25% PE + 75% PP	PP	comm. diesel
Paraffins					
n-paraffins					
C6	0.03	0.03	0.03	0.02	0.02
C7	0.05	0.04	0.04	0.02	0.01
C8	0.28	0.24	0.15	0.00	0.09
C9	1.28	1.25	0.79	0.00	0.50
C10	3.36	3.07	2.71	0.55	0.72
C11	2.24	1.77	1.20	0.09	0.83
C12	2.09	1.55	1.04	0.10	0.78
C13	1.71	1.20	0.86	0.02	0.81
C14	1.42	0.95	0.71	0.10	0.89
C15	1.12	0.70	0.54	0.02	1.05
C16	0.74	0.45	0.37	0.01	1.08
C17	0.49	0.28	0.24	0.01	1.21
C18	0.31	0.18	0.16	0.00	1.05
C19	0.18	0.09	0.09	0.00	0.72
C20	0.10	0.05	0.04	0.00	0.48
C21	0.05	0.03	0.03	0.00	0.32
C22	0.03	0.02	0.02	0.00	0.18
C23	0.01	0.01	0.01	0.00	0.09
C24	0.01	0.00	0.00	0.00	0.05
C25	0.00	0.00	0.00	0.00	0.03
C26	0.00	0.00	0.00	0.00	0.02
C27	0.00	0.00	0.00	0.00	0.01
C28	0.00	0.00	0.00	0.00	0.00
C29	0.00	0.00	0.00	0.00	0.00
C30	0.00	0.00	0.00	0.00	0.00
C31	0.00	0.00	0.00	0.00	0.00
Total *n*-paraffins	**15.56**	**11.96**	**9.10**	**1.01**	**10.99**
Isoparaffins					
C6	0.02	0.02	0.03	0.03	0.02
C7	0.01	0.01	0.01	0.01	0.01
C8	0.18	0.15	0.19	0.21	0.16
C9	0.32	0.48	0.32	0.24	0.41
C10	0.84	0.93	0.87	0.71	0.90
C11	1.83	1.68	2.29	2.39	0.95
C12	1.18	0.90	0.95	0.52	0.95
C13	0.91	0.73	0.60	0.28	1.18
C14	1.45	1.14	1.38	2.02	1.25
C15	0.64	0.50	0.41	0.15	1.76
C16	0.55	0.37	0.36	0.04	2.05

C17	0.39	0.30	0.37	0.37	2.54
C18	0.10	0.10	0.07	0.02	2.30
C19	0.07	0.04	0.07	0.10	1.10
C20	0.06	0.03	0.03	0.03	0.70
C21	0.04	0.02	0.02	0.00	0.41
C22	0.02	0.01	0.01	0.02	0.26
C23	0.01	0.00	0.00	0.00	0.12
C24	0.00	0.00	0.00	0.00	0.12
C25	0.00	0.00	0.00	0.00	0.02
C26	0.00	0.00	0.00	0.00	0.01
C27	0.00	0.00	0.00	0.00	0.00
C28	0.00	0.00	0.00	0.00	0.00
C29	0.00	0.00	0.00	0.00	0.00
C30	0.00	0.00	0.00	0.00	0.00
C31	0.00	0.00	0.00	0.00	0.00
Total Isoparaffins	**8.62**	**7.41**	**7.99**	**7.15**	**17.25**
Cycloparaffins and olefins					
Monocycloparaffins and olefins					
C6	0.04	0.03	0.05	0.04	0.06
C7	0.02	0.02	0.02	0.02	0.00
C8	1.57	0.83	3.10	3.29	0.17
C9	4.26	4.56	4.76	5.19	0.67
C10	3.08	3.62	2.87	4.14	1.01
C11	5.09	4.62	6.04	6.51	1.21
C12	6.00	5.24	6.18	8.25	1.24
C13	2.92	2.62	2.49	2.86	1.20
C14	3.57	2.77	3.14	2.61	2.32
C15	2.80	2.01	2.49	1.38	2.90
C16	1.89	1.18	1.40	0.06	2.69
C17	1.35	0.82	0.98	0.03	3.20
C18	0.92	0.48	0.64	0.00	2.20
C19	0.56	0.29	0.36	0.00	3.01
C20	0.21	0.11	0.14	0.00	2.03
C21	0.17	0.06	0.08	0.00	1.48
C22	0.04	0.02	0.01	0.00	0.85
C23	0.01	0.00	0.00	0.00	0.42
C24	0.00	0.00	0.00	0.00	0.37
C25	0.00	0.00	0.00	0.00	0.08
C26	0.00	0.00	0.00	0.00	0.04
C27	0.00	0.00	0.00	0.00	0.00
C28	0.00	0.02	0.00	0.00	0.00
C29	0.00	0.02	0.00	0.00	0.00
C30	0.00	0.00	0.00	0.00	0.00
Total Monocycloparaffins And Olefins	**34.50**	**29.30**	**34.75**	**34.37**	**27.17**

Dicycloparaffins and olefins					
C8	0.42	0.27	0.33	0.28	0.01
C9	0.85	0.69	0.75	0.53	0.08
C10	1.79	1.43	1.52	1.07	0.22
C11	1.39	1.56	1.04	1.01	0.92
C12	1.74	1.76	2.84	2.31	1.82
C13	3.21	2.32	3.48	3.04	2.29
C14	1.06	1.06	1.37	1.44	0.85
C15	0.67	0.48	0.52	1.64	0.85
C16	0.29	0.29	0.29	1.39	0.14
C17	0.11	0.08	0.12	0.54	0.00
C18	0.05	0.02	0.05	0.03	0.00
C19	0.02	0.00	0.01	0.00	0.00
C20+	0.02	0.00	0.04	0.00	0.01
Total Dicycloparaffins And Olefins	**11.62**	**9.97**	**12.36**	**13.28**	**7.17**
Tricycloparaffins and olefins					
C10	0.02	0.02	0.02	0.02	0.02
C11	0.03	0.02	0.02	0.01	0.01
C12	0.00	0.01	0.00	0.00	0.06
C13	0.00	0.00	0.00	0.00	0.13
C14	0.00	0.00	0.00	0.00	0.20
C15	0.00	0.01	0.00	0.00	0.08
C16+	0.00	0.00	0.00	0.02	0.03
Total Tricycloparaffins And Olefins	**0.05**	**0.06**	**0.04**	**0.04**	**0.52**
Total Cycloparaffins And Olefins	**46.17**	**39.33**	**47.15**	**47.69**	**34.85**
Aromatics					
Alkylbenzenes					
C6/benzene	0.00	0.00	0.00	0.00	0.00
C7/toluene	0.05	0.07	0.04	0.09	0.04
C8	1.13	1.91	1.47	1.51	0.28
C9	3.49	5.77	5.96	6.35	0.82
C10	2.62	4.43	2.74	4.20	1.06
C11	2.52	2.95	2.58	3.49	0.99
C12	1.41	2.15	1.72	1.70	1.28
C13	0.57	0.65	0.56	0.56	0.60
C14	0.22	0.21	0.15	0.17	0.24
C15	0.16	0.13	0.12	0.01	0.23
C16	0.07	0.08	0.03	0.00	0.16

C17	0.04	0.03	0.02	0.00	0.05
C18	0.03	0.02	0.01	0.00	0.07
C19	0.00	0.00	0.00	0.00	0.00
C20+	0.00	0.00	0.00	0.00	0.00
Total Alkylbenzenes	**12.31**	**18.40**	**15.40**	**18.08**	**5.82**
Cycloaromatics					
C9	0.12	0.17	0.10	0.21	0.05
C10	0.93	0.96	0.94	0.60	0.51
C11	2.48	3.28	3.30	3.78	1.96
C12	2.01	3.39	2.22	2.74	3.90
C13	1.14	1.69	1.54	2.04	2.53
C14	0.29	0.56	0.45	0.62	1.46
C15	0.29	0.32	0.30	0.40	1.07
C16	0.08	0.09	0.08	0.07	0.47
C17	0.01	0.00	0.00	0.00	0.26
C18+	0.03	0.01	0.02	0.00	0.39
Total Cycloaromatics	**7.37**	**10.47**	**8.94**	**10.47**	**12.59**
Diaromatics					
C10	0.19	0.32	0.14	0.07	0.02
C11	0.88	1.33	0.99	0.98	0.32
C12	1.87	2.22	2.19	2.17	2.30
C13	1.52	2.07	1.72	2.26	1.59
C14	2.00	2.33	2.14	2.84	2.61
C15	1.73	1.80	2.01	3.02	3.43
C16	0.88	1.15	1.00	1.58	2.95
C17	0.26	0.49	0.31	0.60	1.45
C18	0.03	0.02	0.02	0.04	0.05
C19	0.00	0.00	0.00	0.00	0.00
C20+	0.00	0.00	0.00	0.00	0.00
Total Diaromatics	**9.35**	**11.73**	**10.50**	**13.55**	**14.72**
Triaromatics					
C14	0.06	0.07	0.08	0.09	0.30
C15	0.05	0.07	0.06	0.16	0.45
C16	0.29	0.26	0.30	0.65	1.81
C17	0.19	0.24	0.20	0.53	0.71
C18	0.02	0.06	0.03	0.30	0.37
C19+	0.00	0.00	0.00	0.14	0.14
Total Triaromatics	**0.62**	**0.70**	**0.67**	**1.86**	**3.78**
Total Aromatics	**29.64**	**41.29**	**35.51**	**43.96**	**36.91**

Table B.**9** Fuel properties of the diesel fractions derived from PP and mixed polyolefins compared to those of commercial diesel.

Properties	50% PE + 50% PP	50% PE waste + 50% PP waste	25% PE + 75% PP	PP	Speedway diesel	Family Express diesel	ASTM requirements for No. 1 diesel
Cetane number	47	52	44	40	52	49	≥40
Flash point (°C)	45	45	43	44	58	59	≥38
Kinematic viscosity (mm^2/s)	0.823	0.833	0.830	0.845	0.828	0.848	1.3-2.4
Cloud point (°C)	-10	-8	-8	-8	-11	-18	≤-7
T_{90} (°C)	288	284	288	282	-	-	≤288
Sulfur (ppm)	-	6.5	-	-	-	-	≤15
Water and sediments (ppm)	57	72	80	89	61	42	≤500
Aromatics (wt%)	29.64	41.29	35.51	43.96	22.93	36.91	-
Hydrogen content (wt%)	13.06	12.49	12.49	12.19	13.89	13.42	-
Gross heating value (MJ/kg)	46.09	44.90	45.13	45.38	45.57	45.93	-

*Density and viscosity were measured at 40 °C.

Table B.**10** Comparison of energy consumption and GHG emissions for LP-HTP, pyrolysis, producing fuels from crude oil, mechanical recycling, incineration, and polyolefin synthesis.

	Energy consumption (MJ/kg feed)	GHG emission (kg CO_2/kg feed)
LP-HTP	3.61[a]	0.24[f]
Pyrolysis	4.16[b]	0.33[g]
Producing fuels from crude oil	46.39[c]	0.77[h]
Mechanical recycling	45[d]	2.2[d]
Incineration	-10[e]	3.14[i]
Polyolefin synthesis	79.5[d]	3.2[d]

*a. Calculated based on the energy consumed for LP-HTP reaction and distillation.
b. Calculated as 3.86 MJ/kg from Benavides et al. 2017 for pyrolysis conversion, and 0.3 MJ/kg for the transportation from pyrolysis plants into refineries (Benavides et al., 2017).
c. Obtained from Rodrigues et al. 2018 (Rodrigues et al., 2018).
d. Obtained from Franklin Associates 2011 (Associates, 2011).
e. Obtained from Lee et al. 2020 (Lee et al., 2020). Incineration can generate 10 MJ/kg of plastic feedstock.
f. Calculated based on assuming combusting propane for energy consumption.
g. Calculated as 0.31 kg CO_2/kg for conversion from Benavides et al. 2017, and 0.02 kg CO_2/kg for transportation (Benavides et al., 2017).
h. Adapted from Han et al. 2015 (Han et al., 2015).
i. Calculated based on CO_2 generation from the combustion of PE and PP.

APPENDIX C. PERMISSIONS FOR REPRINTING

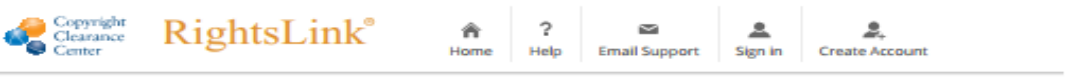

Conversion of polyethylene waste into clean fuels and waxes via hydrothermal processing (HTP)

Author: Kai Jin,Petr Vozka,Gozdem Kilaz,Wan-Ting Chen,Nien-Hwa Linda Wang

Publication: Fuel

Publisher: Elsevier

Date: 1 August 2020

Please note that, as the author of this Elsevier article, you retain the right to include it in a thesis or dissertation, provided it is not published commercially. Permission is not required, but please ensure that you reference the journal as the original source. For more information on this and on your other retained rights, please visit: https://www.elsevier.com/about/our-business/policies/copyright#Author-rights

BACK CLOSE WINDOW

Low-pressure hydrothermal processing of mixed polyolefin wastes into clean fuels

Author: Kai Jin,Petr Vozka,Clayton Gentilcore,Gozdem Kilaz,Nien-Hwa Linda Wang

Publication: Fuel
Publisher: Elsevier
Date: 15 June 2021

LIST OF REFERENCES

Adyel, T. M. (2020). Accumulation of plastic waste during COVID-19. *Science (New York, N.Y.)*, *369*(6509), 1314–1315. https://doi.org/10.1126/science.abd9925

Ahmed, I. I., Nipattummakul, N., & Gupta, A. K. (2011). Characteristics of syngas from co-gasification of polyethylene and woodchips. *Applied Energy*, *88*(1), 165–174.

Akiya, N., & Savage, P. E. (2002). Roles of Water for Chemical Reactions in High-Temperature Water. *Chemical Reviews*, *102*(8), 2725–2750. https://doi.org/10.1021/cr000668w

Akubo, K., Nahil, M. A., & Williams, P. T. (2019). Aromatic fuel oils produced from the pyrolysis-catalysis of polyethylene plastic with metal-impregnated zeolite catalysts. *Journal of the Energy Institute*, *92*(1), 195–202.

Andrady, A. L. (2017). The plastic in microplastics: A review. *Marine Pollution Bulletin*, *119*(1), 12–22.

Anuar Sharuddin, S. D., Abnisa, F., Wan Daud, W. M. A., & Aroua, M. K. (2016). A review on pyrolysis of plastic wastes. *Energy Conversion and Management*, *115*, 308–326. https://doi.org/10.1016/j.enconman.2016.02.037

Associates, F. (2011). *Cradle-to-gate life cycle inventory of nine plastic resins and four polyurethane precursors*. Eastern Research Group, INC. Prairie Village, KS, USA.

Bai, B., Jin, H., Fan, C., Cao, C., Wei, W., & Cao, W. (2019). Experimental investigation on liquefaction of plastic waste to oil in supercritical water. *Waste Management*, *89*, 247–253. https://doi.org/10.1016/j.wasman.2019.04.017

Bai, B., Wang, W., & Jin, H. (2020). Experimental study on gasification performance of polypropylene (PP) plastics in supercritical water. *Energy*, *191*, 116527.

Baytekin, B., Baytekin, H. T., & Grzybowski, B. A. (2013). Retrieving and converting energy from polymers: Deployable technologies and emerging concepts. *Energy and Environmental Science*, *6*(12), 3467–3482. https://doi.org/10.1039/c3ee41360h

Benavides, P. T., Sun, P., Han, J., Dunn, J. B., & Wang, M. (2017). Life-cycle analysis of fuels from post-use non-recycled plastics. *Fuel*, *203*, 11–22. https://doi.org/10.1016/j.fuel.2017.04.070

Bergmann, M., Mützel, S., Primpke, S., Tekman, M. B., Trachsel, J., & Gerdts, G. (2019). White and wonderful? Microplastics prevail in snow from the Alps to the Arctic. *Science Advances*, *5*(8), eaax1157. https://doi.org/10.1126/sciadv.aax1157

Brown, T. M., Duan, P., & Savage, P. E. (2010). Hydrothermal liquefaction and gasification of Nannochloropsis sp. *Energy and Fuels*, *24*(6), 3639–3646. https://doi.org/10.1021/ef100203u

Carbon emissions of different fuels - Forest Research. (n.d.). Retrieved November 5, 2020, from https://www.forestresearch.gov.uk/tools-and-resources/biomass-energy-resources/reference-biomass/facts-figures/carbon-emissions-of-different-fuels/

Chen, W. T., Jin, K., & Linda Wang, N. H. (2019). Use of Supercritical Water for the Liquefaction of Polypropylene into Oil [Research-article]. *ACS Sustainable Chemistry and Engineering*, *7*(4), 3749–3758. https://doi.org/10.1021/acssuschemeng.8b03841

Chen, W. T., Tang, L., Qian, W., Scheppe, K., Nair, K., Wu, Z., … Zhang, Y. (2016). Extract Nitrogen-Containing Compounds in Biocrude Oil Converted from Wet Biowaste via Hydrothermal Liquefaction. *ACS Sustainable Chemistry and Engineering*, *4*(4), 2182–2190. https://doi.org/10.1021/acssuschemeng.5b01645

Chiba, S., Saito, H., Fletcher, R., Yogi, T., Kayo, M., Miyagi, S., … Fujikura, K. (2018a). Human footprint in the abyss: 30 year records of deep-sea plastic debris. *Marine Policy*, *96*(August 2017), 204–212. https://doi.org/10.1016/j.marpol.2018.03.022

Chiba, S., Saito, H., Fletcher, R., Yogi, T., Kayo, M., Miyagi, S., … Fujikura, K. (2018b). Human footprint in the abyss: 30 year records of deep-sea plastic debris. *Marine Policy*, *96*(August 2017), 204–212. https://doi.org/10.1016/j.marpol.2018.03.022

Choy, C. A., Robison, B. H., Gagne, T. O., Erwin, B., Firl, E., Halden, R. U., … Rolsky, C. (2019). The vertical distribution and biological transport of marine microplastics across the epipelagic and mesopelagic water column. *Scientific Reports*, *9*(1), 1–9.

Cole, M., Lindeque, P., Halsband, C., & Galloway, T. S. (2011). Microplastics as contaminants in the marine environment: A review. *Marine Pollution Bulletin*, *62*(12), 2588–2597. https://doi.org/10.1016/j.marpolbul.2011.09.025

Copeland, C., & Tiemann, M. (2013). Water infrastructure needs and investment: Review and analysis of key issues? *Water Infrastructure: Needs and Financing Options*, 1–51. Retrieved from https://www.scopus.com/inward/record.uri?eid=2-s2.0-84946913111&partnerID=40&md5=2beacf48d79470c6cd3b610969936129

Cox, K. D., Covernton, G. A., Davies, H. L., Dower, J. F., Juanes, F., & Dudas, S. E. (2019). Human consumption of microplastics. *Environmental Science & Technology*, *53*(12), 7068–7074.

Dahmus, J. B., & Gutowski, T. G. (2007). What Gets Recycled: An Information Theory Based Model for Product Recycling. *Environmental Science & Technology*, *41*(21), 7543–7550. https://doi.org/10.1021/es062254b

Das, P., & Tiwari, P. (2018). Valorization of packaging plastic waste by slow pyrolysis. *Resources, Conservation and Recycling*, *128*, 69–77.

Eco.cycle. (2011). *Why incineration is bad for our economy, environment and community September 2011 www.ecocycle.org/zerowaste 1* |. (September).

Environmental Protection Agency, U. (2020). *Advancing Sustainable Materials Management: 2018 Fact Sheet Assessing Trends in Materials Generation and Management in the United States*.

Eralytics. (n.d.). Spectral fuel analysis in seconds. Retrieved September 22, 2019, from https://eralytics.com/wp-content/uploads/eraspec_bro_EN_web.pdf

ERASPEC Fuel analyzer - Spectral Fuel Analysis in Seconds. (n.d.). Retrieved December 28, 2020, from https://eralytics.com/instruments/eraspec-fuel-analyzer/

Eriksson, O., & Finnveden, G. (2017). Energy recovery from waste incineration - The importance of technology data and system boundaries on CO2 emissions. *Energies*, *10*(4). https://doi.org/10.3390/en10040539

Fivga, A., & Dimitriou, I. (2018). Pyrolysis of plastic waste for production of heavy fuel substitute: A techno-economic assessment. *Energy*, *149*, 865–874.

Funazukuri, T. (2015). Hydrothermal Depolymerization of Polyesters and Polycarbonate in the Presence of Ammonia and Amines. In *Recycling Materials Based on Environmentally Friendly Techniques*. https://doi.org/10.5772/59198

Galera, S., & Ortiz, F. J. G. (2015). Techno-economic assessment of hydrogen and power production from supercritical water reforming of glycerol. *Fuel*, *144*, 307–316.

Garcia, J. M., & Robertson, M. L. (2017). The future of plastics recycling. *Science*, *358*(6365), 870–872. https://doi.org/10.1126/science.aaq0324

Geyer, R., Jambeck, J. R., & Law, K. L. (2017a). Production, use, and fate of all plastics ever made. *Science Advances*, *3*(7), e1700782. https://doi.org/10.1126/sciadv.1700782

Geyer, R., Jambeck, J. R., & Law, K. L. (2017b). Production, uses, and fate of all plastics ever made. *Science Advances*, *3*(7), 5. https://doi.org/10.1126/sciadv.1700782

Gracida-Alvarez, U. R., Winjobi, O., Sacramento-Rivero, J. C., & Shonnard, D. R. (2019). System analyses of high-value chemicals and fuels from a waste high-density polyethylene refinery. Part 1: Conceptual design and techno-economic assessment. *ACS Sustainable Chemistry & Engineering*, *7*(22), 18254–18266.

Great Pacific Garbage Patch | National Geographic Society. (n.d.). Retrieved February 25, 2020, from https://www.nationalgeographic.org/encyclopedia/great-pacific-garbage-patch/

Grübler, A. (1998). *Technology and Global Change*. Retrieved from https://books.google.com/books?hl=en&lr=&id=MqIQUV3nJrAC&oi=fnd&pg=PR9&dq=Grübler+A.+Technology+and+Global+Change.+Cambridge+University+Press%3B+1998&ots=qmqsjBi0QI&sig=6bCg8JESbND8LSwJMlGoyET2jTw#v=onepage&q=Grübler A. Technology and Global Change. Cam

Guern, C. Le. (2018). WHEN THE MERMAIDS CRY: THE GREAT PLASTIC TIDE. Retrieved from http://coastalcare.org/2009/11/plastic-pollution/

Han, J., Forman, G. S., Elgowainy, A., Cai, H., Wang, M., & DiVita, V. B. (2015). A comparative assessment of resource efficiency in petroleum refining. *Fuel*, *157*, 292–298.

Hatakeyama, K., Kojima, T., & Funazukuri, T. (2014). Chemical recycling of polycarbonate in dilute aqueous ammonia solution under hydrothermal conditions. *Journal of Material Cycles and Waste Management*, *16*(1), 124–130. https://doi.org/10.1007/s10163-013-0151-8

Home of Metals news prices etfs |. (n.d.). Retrieved February 25, 2020, from https://mineralprices.com/

Hopewell, J., Dvorak, R., & Kosior, E. (2009). Plastics recycling: Challenges and opportunities. *Philosophical Transactions of the Royal Society B: Biological Sciences*, *364*(1526), 2115–2126. https://doi.org/10.1098/rstb.2008.0311

Horton, A. A., Walton, A., Spurgeon, D. J., Lahive, E., & Svendsen, C. (2017). Microplastics in freshwater and terrestrial environments: Evaluating the current understanding to identify the knowledge gaps and future research priorities. *Science of the Total Environment*, *586*, 127–141. https://doi.org/10.1016/j.scitotenv.2017.01.190

International, A. (2020). ASTM D4814 - 20a Standard Specification for Automotive Spark-Ignition Engine Fuel. *West Conshohocken, PA; ASTM International*.

International, ASTM. (2016). ASTM D56 - 16a Standard Test Method for Flash Point by Tag Closed Cup Tester. *West Conshohocken, PA; ASTM International*.

International, ASTM. (2018). ASTM D93 - 18 Standard Test Methods for Flash Point by Pensky-Martens Closed Cup Tester. *West Conshohocken, PA; ASTM International*.

International, ASTM. (2019). ASTM D975 - 19b Standard Specification for Diesel Fuel. *West Conshohocken, PA; ASTM International*.

International, ASTM. (2020). ASTM D975 - 20b Standard Specification for Diesel Fuel. *West Conshohocken, PA; ASTM International*.

Janajreh, I., Adeyemi, I., & Elagroudy, S. (2020). Gasification feasibility of polyethylene, polypropylene, polystyrene waste and their mixture: Experimental studies and modeling. *Sustainable Energy Technologies and Assessments*, *39*, 100684.

Jin, K., Vozka, P., Gentilcore, C., Kilaz, G., & Wang, N.-H. L. (2021). Low-pressure hydrothermal processing of mixed polyolefin wastes into clean fuels. *Fuel*, *294*, 120505.

Jin, K., Vozka, P., Kilaz, G., Chen, W. T., & Wang, N.-H. L. (2020). Conversion of polyethylene waste into clean fuels and waxes via hydrothermal processing (HTP). *Fuel*, *273*(117726). https://doi.org/https://doi.org/10.1016/j.fuel.2020.117726

Johnson, J., Harper, E. M., Lifset, R., & Graedel, T. E. (2007). Dining at the periodic table: Metals concentrations as they relate to recycling. *Environmental Science and Technology*, *41*(5), 1759–1765. https://doi.org/10.1021/es060736h

Kannan, P., Al Shoaibi, A., & Srinivasakannan, C. (2013). Energy recovery from co-gasification of waste polyethylene and polyethylene terephthalate blends. *Computers & Fluids*, *88*, 38–42.

Karbalaei, S., Hanachi, P., Walker, T. R., & Cole, M. (2018). Occurrence, sources, human health impacts and mitigation of microplastic pollution. *Environmental Science and Pollution Research*, *25*(36), 36046–36063.

Kassargy, C., Awad, S., Burnens, G., Kahine, K., & Tazerout, M. (2017). Experimental study of catalytic pyrolysis of polyethylene and polypropylene over USY zeolite and separation to gasoline and diesel-like fuels. *Journal of Analytical and Applied Pyrolysis*, *127*, 31–37.

Kassargy, C., Awad, S., Burnens, G., Kahine, K., & Tazerout, M. (2018). Gasoline and diesel-like fuel production by continuous catalytic pyrolysis of waste polyethylene and polypropylene mixtures over USY zeolite. *Fuel*, *224*, 764–773.

Klemeš, J. J., Van Fan, Y., Tan, R. R., & Jiang, P. (2020). Minimising the present and future plastic waste, energy and environmental footprints related to COVID-19. *Renewable and Sustainable Energy Reviews*, *127*, 109883.

Kreiger, M. A., Mulder, M. L., Glover, A. G., & Pearce, J. M. (2014). Life cycle analysis of distributed recycling of post-consumer high density polyethylene for 3-D printing filament. *Journal of Cleaner Production*, *70*, 90–96. https://doi.org/10.1016/j.jclepro.2014.02.009

Lavers, J. L., & Bond, A. L. (2017). Exceptional and rapid accumulation of anthropogenic debris on one of the world's most remote and pristine islands. *Proceedings of the National Academy of Sciences*, *114*(23), 6052–6055. https://doi.org/10.1073/pnas.1619818114

Laville, S., & Taylor, M. (2017). *A million bottles a minute: world's plastic binge "as dangerous as climate change."* Retrieved from http://www.ecologiapolitica.org/wordpress/wp-content/uploads/2017/08/04-Guardian.pdf

Lebreton, L., Egger, M., & Slat, B. (2019). A global mass budget for positively buoyant macroplastic debris in the ocean. *Scientific Reports*, *9*(1), 1–10.

Lebreton, L., Slat, B., Ferrari, F., Sainte-Rose, B., Aitken, J., Marthouse, R., … Levivier, A. (2018). Evidence that the Great Pacific Garbage Patch is rapidly accumulating plastic. *Scientific Reports*, *8*(1), 1–15.

Lee, U., Benavides, P. T., & Wang, M. (2020). Life cycle analysis of waste-to-energy pathways. In *Waste-to-Energy* (pp. 213–233). Elsevier.

Li, L., Luo, Y., Li, R., Zhou, Q., Peijnenburg, W. J. G. M., Yin, N., … Zhang, Y. (2020). Effective uptake of submicrometre plastics by crop plants via a crack-entry mode. *Nature Sustainability*, *3*(11), 929–937.

MacArthur, E., Beyond plastic waste. In American Association for the Advancement of Science: 2017. (n.d.).

MacArthur, D. E. (2017). Beyond plastic waste. *Science*, *358*(6365), 843. https://doi.org/10.1126/science.aao6749

Marcilla, A., Beltrán, M. I., & Navarro, R. (2009). Thermal and catalytic pyrolysis of polyethylene over HZSM5 and HUSY zeolites in a batch reactor under dynamic conditions. *Applied Catalysis B: Environmental*, *86*(1–2), 78–86.

Mihelcic, J. R., Jason Ren, Z., Cornejo, P. K., Fisher, A., Simon, A. J., Snyder, S. W., … Turgeon, J. (2017). *Accelerating Innovation that Enhances Resource Recovery in the Wastewater Sector: Advancing a National Testbed Network*. https://doi.org/10.1021/acs.est.6b05917

MIL-DTL-5624W. (2016). Detailed Specification Turbine Fuel, Aviation, Grades JP-4 and JP-5. *AFPA/PTPT*.

Mitrano, D. M., & Wohlleben, W. (2020). Microplastic regulation should be more precise to incentivize both innovation and environmental safety. *Nature Communications*, *11*(1), 1–12.

Moriya, T., & Enomoto, H. (1999). Characteristics of polyethylene cracking in supercritical water compared to thermal cracking. *Polymer Degradation and Stability*, *65*(3), 373–386. https://doi.org/10.1016/S0141-3910(99)00026-9

Nabavi-Pelesaraei, A., Bayat, R., Hosseinzadeh-Bandbafha, H., Afrasyabi, H., & Chau, K. wing. (2017). Modeling of energy consumption and environmental life cycle assessment for incineration and landfill systems of municipal solid waste management - A case study in Tehran Metropolis of Iran. *Journal of Cleaner Production*, *148*, 427–440. https://doi.org/10.1016/j.jclepro.2017.01.172

Naqvi, S. R., Bibi, A., Naqvi, M., Noor, T., Nizami, A.-S., Rehan, M., & Ayoub, M. (2018). New trends in improving gasoline quality and octane through naphtha isomerization: a short review. *Applied Petrochemical Research*, *8*(3), 131–139. https://doi.org/10.1007/s13203-018-0204-y

Ni, H.-G., Lu, S.-Y., Mo, T., & Zeng, H. (2016). Brominated flame retardant emissions from the open burning of five plastic wastes and implications for environmental exposure in China. *Environmental Pollution*, *214*, 70–76. https://doi.org/https://doi.org/10.1016/j.envpol.2016.03.049

NIST. (n.d.). Thermophysical Properties of Fluid Systems. Retrieved from https://webbook.nist.gov/chemistry/fluid/

Olivares, J. A., Baxter, I., Brown, J., Carleton, M., Cattolico, R. A., Taraka, D., … Skaggs, R. (2014). *National Alliance for Advanced Biofuels and Bio-Products Final Technical Report*. https://doi.org/10.2172/1166710

Onwudili, J. A., Insura, N., & Williams, P. T. (2009). Composition of products from the pyrolysis of polyethylene and polystyrene in a closed batch reactor: Effects of temperature and residence time. *Journal of Analytical and Applied Pyrolysis*, *86*(2), 293–303.

Opatokun, S. A., Strezov, V., & Kan, T. (2015). Product based evaluation of pyrolysis of food waste and its digestate. *Energy*, *92*, 349–354. https://doi.org/10.1016/j.energy.2015.02.098

Pabortsava, K., & Lampitt, R. S. (2020). High concentrations of plastic hidden beneath the surface of the Atlantic Ocean. *Nature Communications*, *11*(1), 1–11.

Park, K.-B., Jeong, Y.-S., & Kim, J.-S. (2019). Activator-assisted pyrolysis of polypropylene. *Applied Energy*, *253*, 113558.

Pedersen, T. H., Grigoras, I. F., Hoffmann, J., Toor, S. S., Daraban, I. M., Jensen, C. U., … Rosendahl, L. A. (2016). Continuous hydrothermal co-liquefaction of aspen wood and glycerol with water phase recirculation. *Applied Energy*, *162*, 1034–1041. https://doi.org/10.1016/j.apenergy.2015.10.165

Peterson, A. A., Vogel, F., Lachance, R. P., Fröling, M., Antal, M. J., & Tester, J. W. (2008). Thermochemical biofuel production in hydrothermal media: A review of sub- and supercritical water technologies. *Energy and Environmental Science*, *1*(1), 32–65. https://doi.org/10.1039/b810100k

PlasticsEurope. (2AD). *WEF_The_New_Plastics_Economy.pdf*. (January), 1–36. https://doi.org/10.1103/Physrevb.74.035409

Plinke, E., Wenk, N., Wloff, G., Castiglione, D., & Palmark, M. (2020). *Mechanical Recycling of PVC Waste, Study for DG XI of the European Commission (B4-3040/98/000821/MAR/E3)*. Retrieved from https://ec.europa.eu/environment/waste/studies/pvc/mech_recylce.pdf

Prata, J. C., da Costa, J. P., Lopes, I., Duarte, A. C., & Rocha-Santos, T. (2020). Environmental exposure to microplastics: An overview on possible human health effects. *Science of the Total Environment*, *702*, 134455.

Ragaert, K., Delva, L., & Van Geem, K. (2017). Mechanical and chemical recycling of solid plastic waste. *Waste Management*, *69*, 24–58. https://doi.org/10.1016/j.wasman.2017.07.044

Ragusa, A., Svelato, A., Santacroce, C., Catalano, P., Notarstefano, V., Carnevali, O., … Draghi, S. (n.d.). Plasticenta: First evidence of microplastics in human placenta. *Environment International*, *146*, 106274. https://doi.org/https://doi.org/10.1016/j.envint.2020.106274

Rochman, C. M., Browne, M. A., Halpern, B. S., Hentschel, B. T., Hoh, E., Karapanagioti, H. K., … Thompson, R. C. (2013). Policy: Classify plastic waste as hazardous. *Nature*, *494*(7436), 169–170. https://doi.org/10.1038/494169a

Rochman, C. M., & Hoellein, T. (2020). The global odyssey of plastic pollution. *Science*, *368*(6496), 1184–1185. https://doi.org/10.1126/science.abc4428

Rodrigues, V., Martins, A. A., Nunes, M. I., Quintas, A., Mata, T. M., & Caetano, N. S. (2018). LCA of constructing an industrial building: focus on embodied carbon and energy. *Energy Procedia*, *153*, 420–425.

Santos, B. P. S., Almeida, D., Maria de Fatima, V. M., & Henriques, C. A. (2018). Petrochemical feedstock from pyrolysis of waste polyethylene and polypropylene using different catalysts. *Fuel*, *215*, 515–521.

Savage, P. E. (1999). Organic chemical reactions in supercritical water. *Chemical Reviews*, *99*(2), 603–622.

Savage, P. E. (2000). Mechanisms and kinetics models for hydrocarbon pyrolysis. *Journal of Analytical and Applied Pyrolysis*, *54*(1), 109–126. https://doi.org/10.1016/S0165-2370(99)00084-4

Savage, P. E., Gopalan, S., Mizan, T. I., Martino, C. J., & Brock, E. E. (1995). Reactions at supercritical conditions: Applications and fundamentals. *AIChE Journal*, *41*(7), 1723–1778. https://doi.org/10.1002/aic.690410712

Schemme, S., Samsun, R. C., Peters, R., & Stolten, D. (2017, October 1). Power-to-fuel as a key to sustainable transport systems – An analysis of diesel fuels produced from CO2 and renewable electricity. *Fuel*, Vol. 205, pp. 198–221. https://doi.org/10.1016/j.fuel.2017.05.061

Schwabl, P., Koppel, S., Konigshofer, P., Bucsics, T., Trauner, M., Reiberger, T., & Liebmann, B. (2019). Detection of various microplastics in human stool: A prospective case series. *Annals of Internal Medicine*, *171*(7), 453–457. https://doi.org/10.7326/M19-0618

Schyns, Z. O. G., & Shaver, M. P. (2020). Mechanical Recycling of Packaging Plastics: A Review. *Macromolecular Rapid Communications*, 2000415.

Seshasayee, M. S., & Savage, P. E. (2020). Oil from plastic via hydrothermal liquefaction: Production and characterization. *Applied Energy*, *278*, 115673.

Sharma, B. K., Moser, B. R., Vermillion, K. E., Doll, K. M., & Rajagopalan, N. (2014). Production, characterization and fuel properties of alternative diesel fuel from pyrolysis of waste plastic grocery bags ☆. *Fuel Processing Technology*, *122*, 79–90. https://doi.org/10.1016/j.fuproc.2014.01.019

Sherwood, T. K. (1959). *Mass transfer between phases*. Pennsylvania State University.

Silva, A. L. P., Prata, J. C., Walker, T. R., Campos, D., Duarte, A. C., Soares, A. M. V. M., … Rocha-Santos, T. (2020). Rethinking and optimising plastic waste management under COVID-19 pandemic: Policy solutions based on redesign and reduction of single-use plastics and personal protective equipment. *Science of the Total Environment*, *742*, 140565.

Singh, P., Déparrois, N., Burra, K. G., Bhattacharya, S., & Gupta, A. K. (2019). Energy recovery from cross-linked polyethylene wastes using pyrolysis and CO2 assisted gasification. *Applied Energy*, *254*, 113722.

Sivaramakrishnan, K., & Ravikumar, P. (2011). Determination of Higher Heating Value of Biodiesels. *International Journal of Engineering Science and Technology*, *3*(11), 7981–7987.

Smith, M., Love, D. C., Rochman, C. M., & Neff, R. A. (2018). Microplastics in Seafood and the Implications for Human Health. *Current Environmental Health Reports*, *5*(3), 375–386. https://doi.org/10.1007/s40572-018-0206-z

Sort for Value Online Calculator. (n.d.). Retrieved November 16, 2019, from https://plasticsrecycling.org/markets/sort-for-value-online-calculator

Souza Machado, A. A., Lau, C. W., Kloas, W., Bergmann, J., Bachelier, J. B., Faltin, E., … Rillig, M. C. (2019). Microplastics Can Change Soil Properties and Affect Plant Performance. *Environmental Science & Technology*. https://doi.org/10.1021/acs.est.9b01339

Su, L., Wu, X., Liu, X., Chen, L., Chen, K., & Hong, S. (2005). Investigation on polypropylene degradation in supercritical water adding benzoyl peroxide. *Chinese Journal of Chemical Engineering*, Vol. 13, pp. 845–848.

Su, X., Zhao, Y., Zhang, R., & Bi, J. (2004). Investigation on degradation of polyethylene to oils in supercritical water. *Fuel Processing Technology*, *85*(8–10), 1249–1258. https://doi.org/10.1016/j.fuproc.2003.11.044

Tiemann, M. (2010). *CRS Report for Congress Water Infrastructure Needs and Investment: Review and Analysis of Key Issues Claudia Copeland Specialist in Resources and Environmental Policy*. Retrieved from www.crs.gov

Tyskeng, S., & Finnveden, G. (2010). Comparing Energy Use and Environmental Impacts of Recycling and Waste Incineration. *Journal of Environmental Engineering*, *136*(8), 744–748. https://doi.org/10.1061/(ASCE)EE.1943-7870.0000206

Tzanetis, K. F., Posada, J. A., & Ramirez, A. (2017). Analysis of biomass hydrothermal liquefaction and biocrude-oil upgrading for renewable jet fuel production: The impact of reaction conditions on production costs and GHG emissions performance. *Renewable Energy*, *113*, 1388–1398. https://doi.org/10.1016/j.renene.2017.06.104

Ügdüler, S., Van Geem, K. M., Denolf, R., Roosen, M., Mys, N., Ragaert, K., & De Meester, S. (2020). Towards closed-loop recycling of multilayer and coloured PET plastic waste by alkaline hydrolysis. *Green Chemistry*, *22*(16), 5376–5394.

Vozka, P., Mo, H., Šimáček, P., & Kilaz, G. (2018). Middle distillates hydrogen content via GC×GC-FID. *Talanta*, *186*. https://doi.org/10.1016/j.talanta.2018.04.059

Vozka, Petr, & Kilaz, G. (2019b). How to obtain a detailed chemical composition for middle distillates via GC × GC-FID without the need of GC × GC-TOF/MS. *Fuel*, *247*, 368–377. https://doi.org/10.1016/j.fuel.2019.03.009

Wang, Y., & Zhang, F. S. (2012). Degradation of brominated flame retardant in computer housing plastic by supercritical fluids. *Journal of Hazardous Materials*, *205–206*, 156–163. https://doi.org/10.1016/j.jhazmat.2011.12.055

Watanabe, M., Hirakoso, H., Sawamoto, S., Tadafumi Adschiri, & Arai, K. (1998). Polyethylene conversion in supercritical water. *Journal of Supercritical Fluids*, *13*(1–3), 247–252. https://doi.org/10.1016/S0896-8446(98)00058-8

Williams, P. T., & Slaney, E. (2007). Analysis of products from the pyrolysis and liquefaction of single plastics and waste plastic mixtures. *Resources, Conservation and Recycling*, *51*(4), 754–769. https://doi.org/10.1016/j.resconrec.2006.12.002

Wright, S. L., & Kelly, F. J. (2017). Plastic and Human Health: A Micro Issue? *Environmental Science and Technology*, *51*(12), 6634–6647. https://doi.org/10.1021/acs.est.7b00423

Zhao, P., Yuan, Z., Zhang, J., Song, X., Wang, C., Guo, Q., & Ragauskas, A. J. (2021). Supercritical water co-liquefaction of LLDPE and PP into oil: properties and synergy. *Sustainable Energy & Fuels*, *5*(2), 575–583.

Zhao, X., Zhan, L., Xie, B., & Gao, B. (2018). Products derived from waste plastics (PC, HIPS, ABS, PP and PA6) via hydrothermal treatment: Characterization and potential applications. *Chemosphere*, *207*, 742–752. https://doi.org/10.1016/j.chemosphere.2018.05.156

Zhu, Y., Biddy, M. J., Jones, S. B., Elliott, D. C., & Schmidt, A. J. (2014). Techno-economic analysis of liquid fuel production from woody biomass via hydrothermal liquefaction (HTL) and upgrading. *Applied Energy*, *129*, 384–394. https://doi.org/10.1016/j.apenergy.2014.03.053